

Sl. No.	<p style="text-align: center;">IIT Ropar List of Recent Publications with Abstract Coverage: June-August, 2023</p>
1.	<p>4D potential energy surface of NCCN–H₂ collision: Rotational dynamics by <i>p</i>-H₂ and <i>o</i>-H₂ at interstellar temperatures A Kushwaha, TJ Dhilip Kumar - The Journal of Chemical Physics, 2023</p> <p>Abstract The rotational excitation rates of NCCN species are studied for its collision with hydrogen (H₂) in temperatures ranging from 1 to 100 K. Such collisions can occur in the interstellar medium with H₂ in either <i>para</i> (<i>p</i>-) or <i>ortho</i> (<i>o</i>-) state, of which the <i>p</i>-H₂ state can be approximated via its collision with He (using a scaling factor) or with a reduced rigid rotor-H₂ surface (by averaging over various orientations of H₂). In the current work, a four-dimensional (4D) <i>ab initio</i> potential energy surface (PES) is considered to study the collision dynamics of H₂ in both <i>p</i>- and <i>o</i>-states and the results are compared with previous approximations. The 4D surface is constructed using the explicitly correlated coupled-cluster method CCSD(T)-F12b with the augmented triple zeta basis AVTZ and then fitted into an artificial neural networks (NN) model to augment the surface and account for missing data points. The radial coefficients are obtained from this NN fitted 4D PES via a least square fit over two spherical harmonics functions. The cross sections (σ) are computed using the close-coupling (CC) method (until 230 cm⁻¹) for both <i>p</i>- and <i>o</i>-H₂ collisions, and the rates are obtained by Boltzmann distribution over the translational energy of H₂ until 100 K. The <i>o</i>-H₂ rates are found to be higher by 25%–30% and 10%–20% compared to the <i>p</i>-H₂ rates for $\Delta j = 2$ and higher order transitions, respectively. The coupled-state/centrifugal sudden approximated rates are also computed and found to have deviations as large as 40% when compared to CC rates, thus making quantitative descriptions unreliable.</p>
2.	<p>A combined 3D-atomic/nanoscale comprehension and <i>ab initio</i> computation of iron carbide structures tailored in Q&P steels via Si alloying S Ghosh, K Rakha, AAS Devi ... - Nanoscale, 2023</p> <p>Abstract The essences of the quenching and partitioning (Q&P) process are to stabilize the finely divided retained austenite (RA) via carbon (C) partitioning from supersaturated martensite during partitioning. Competitive reactions, i.e., transition carbide precipitation, C segregation, and decomposition of austenite, might take place concurrently during partitioning. In order to maintain the high volume fraction of RA, it is crucial to suppress the carbide precipitation sufficiently. Since silicon (Si) in the cementite θ (Fe₃C) is insoluble, alloying Si in adequate concentrations prolongs its precipitation during the partitioning step. Consequently, C partitioning facilitates the desired chemical stabilization of RA. To elucidate the mechanisms of formation of transition η (Fe₂C) carbides as well as cementite, θ (Fe₃C), besides the transformation of transition carbides to more stable θ during the quenching and partitioning (Q&P) process, samples of 0.4 wt% C steels tailored with different Si contents were extensively characterized for microstructural evolution at different partitioning temperatures (T_p) using high resolution transmission electron microscopy (HR-TEM) and three-dimensional atom probe tomography (3D-APT). While 1.5 wt% Si in the steel allowed only the formation of η carbides even at a high T_p of 300 °C, reduction in Si content to 0.75 wt% only partially stabilized η carbides, allowing limited $\eta \rightarrow \theta$ transformation. With 0.25 wt% Si, only θ was present in the microstructure, suggesting a $\eta \rightarrow \theta$ transition during the early partitioning stage, followed by coarsening due to enhanced growth kinetics at 300 °C. Although η carbides precipitated in martensite under paraequilibrium conditions at 200 °C, θ carbides precipitated under negligible partitioning local equilibrium conditions at 300 °C. Competition with the formation of</p>

	<p>orthorhombic η and θ precipitation further examined via ab initio (density functional theory, DFT) computation and a similar probability of formation/thermodynamic stability were obtained. With an increase in Si concentration, the cohesive energy decreased when Si atoms occupied C positions, indicating decreasing stability. Overall, the thermodynamic prediction was in accord with the HR-TEM and 3D-APT results.</p>
3.	<p>A Comparative review of different methods used for studying the efficacy of functional electrical stimulation for foot drop patients B Basumatary, I Kundu, S Ghosh...A Sahani... - IETE Technical Review, 2023</p> <p>Abstract Foot drop is a neurological disorder in which the person cannot lift the upper part of the foot from the ground. Functional electrical stimulation (FES) is utilized for treating foot drop. Gait speed is associated with the clinical study of the FES system to study its effectiveness. The review paper compares the various methods used to evaluate the effectiveness of FES treatment, including gait analysis, Timed-Up-and-Go (TUG) test, 10-meter walk (10MW) test, 6-min walk (6MW) test and clinical assessments scales. By examining the strengths and limitations of each method, on the basis of recent research studies that have used these methods to evaluate the effectiveness of FES treatment, this paper aims to provide a comprehensive understanding of the different methods used to study the effectiveness of FES for treating Foot Drop patients and to identify the most effective and reliable methods for future studies.</p>
4.	<p>A Coupled-dipolar plasmonic antenna for enhanced and directional emission from a single NV center at the generalized Kerker condition FA Inam, RV Nair - Advanced Quantum Technologies, 2023</p> <p>Abstract Plasmonic antennas are widely used to achieve substantial emission rate enhancement. These antennas suffer from significant absorption losses that preclude the observation of Kerker conditions in such systems. The perfect balancing of the Mie-scattering moments in an antenna at the generalized Kerker condition provides radiation directionality to its far-field scattering pattern and zero absorption losses, a situation not achievable for a plasmonic system. Here, using both theoretical and computational approaches, the superposition of Mie-scattering moments induced by coupling two individual silver (Ag) cylinders in a coupled-dipolar plasmonic antenna is discussed. This results in the balancing of multipolar moments to a large extent with unidirectional scattering and hence the generalized Kerker condition in a plasmonic system. By placing a nanodiamond-based single NV- center in the plasmonic gap-cavity formed between the two Ag cylinders, >300 times Purcell enhancement is achieved with improved emission directionality leading to 80% collection efficiency. The proposed coupled-dipolar plasmonic antenna is well suited for generating bright single photon emissions with a GHz emission rate, which is helpful for quantum photonic applications.</p>
5.	<p>A Deep learning-based system for detecting anemia from eye conjunctiva images taken from a smartphone Pallavi, B Basumatary, R Shukla... B Das, AK Sahani - IETE Technical Review, 2023</p> <p>Abstract Anemia is a severe health condition commonly prevalent among women of reproductive age and children below five years. Screening patients before the condition becomes critical and can save many lives. World Health Organization (WHO) has set the “Global nutrition target 2025-anemia,” aiming to reduce 50% of anemia cases among women of reproductive age. This target can be achieved through a time-efficient, cost-effective, and easy-to-use tool. Traditional testing methods require specific chemicals, machines, and equipment that are not available everywhere. It also requires the presence of nurses, laboratory workers, and doctors. These methods are</p>

	<p>costly, time-consuming, and produce biohazard waste, thus polluting the environment. We developed an Artificial Intelligence (AI)-based bot that can be used for screening people for anemia. The bot service is based on two models: a segmentation model to segment the Region of Interest (ROI) and a classification model to classify anemic cases from normal ones. To train the model, we have collected data from 160 anemic and 140 non-anemic persons. In this paper, we have explained the architecture of the models, all the training parameters, and their deployment on cloud services using the REAN chatbot service. We manage to reach an Intersection Over Union (IOU) score of 0.922 for the segmentation model; validation recall of 0.95 and validation accuracy of 0.9699 for the classification model. This system is easy to use and does not depend on the availability of comprehensive laboratory infrastructure or trained personnel and thus can enable screening of anemia in low-resource settings.</p>
6.	<p>A linear stability analysis of instabilities with reactive flows in porous medium V Sharma, C-Y Chen, M Mishra - Physics of Fluids, 2023</p> <p>Abstract Convection, diffusion, and reaction dynamics of radial displacement of reactive fluids undergoing second-order chemical reaction in a porous medium are modeled and understood numerically. In the case of iso-viscous reactants and products, reaction dynamics are examined to understand the effect of reaction rate after solving a system of convection–diffusion–reaction equations using a method of lines. Various temporal scalings for reaction characteristics like the total amount of product and width of reaction front are obtained in terms of the Damköhler number (Da) for the first time in this work. The generation of the product having different viscosity than the reactants results in a hydrodynamic instability called viscous fingering. The numerical technique based on hybrids of compact finite difference and pseudo-spectral methods is utilized, for the first time, for the linear stability analysis (LSA) of miscible viscous fingering induced by chemical reaction. The onset time of instability (t_{on}) is found to depend on the reaction rate, and we obtain a stable zone sandwiched between two unstable zones in the Mc, t_{on} plane for a fixed Péclet number and Damköhler number, where Mc is the log-mobility ratio. The results agree with existing numerical studies validating the novel LSA technique utilized.</p>
7.	<p>A linear-time algorithm for semitotal domination in strongly chordal graphs V Tripathi, A Pandey, A Maheshwari - Discrete Applied Mathematics, 2023</p> <p>Abstract In a graph, $G=(V,E)$ without an isolated vertex, a dominating set $D \subseteq V$, is called a semitotal dominating set if for every vertex $u \in D$ there is another vertex $v \in D$ such that distance between u and v is at most two in G. Given a graph $G=(V,E)$ without an isolated vertex, the MINIMUM SEMITOTAL DOMINATION problem is to find a minimum cardinality semitotal dominating set of G. The semitotal domination number, denoted by $\gamma_{t2}(G)$, is the minimum cardinality of a semitotal dominating set of G. It is known that the decision version of the problem remains NP-complete even when restricted to chordal graphs, chordal bipartite graphs, and planar graphs. Galby et al. (2020) proved that the problem can be solved in polynomial time for bounded MIM-width graphs, which include many well known graph classes, but left the complexity of the problem in strongly chordal graphs unresolved. Henning and Pandey (2019) also asked to resolve the complexity status of the problem in strongly chordal graphs. In this paper, we resolve the complexity of the problem in strongly chordal graphs by designing a linear-time algorithm for the problem.</p>
8.	<p>A Low power differential delay cell without cross-coupled latch for ring VCO MK Singh, P Singh, DM Das...M Sakare - 18th International Conference on Ph.D Research in Microelectronics and Electronics, Proceedings, 2023</p> <p>Abstract A differential delay cell without a cross-coupled latch is proposed for a two-stage ring voltage-</p>

	<p>controlled oscillator (RVCO). In the proposed delay cell (PDC), an RC network is used in place of a cross-coupled latch to exhibit a negative conductance. It reduces the power consumption in the RVCO significantly. Two paths from the output node for discharging current are added in the PDC. It reduces the discharging time of the output node which enhances the operating frequency by almost 50%. The PDC utilizes an RC network to reduce the peak-to-peak jitter of the RVCO by making the noise current sharp, similar to an impulse function. This design approach effectively minimizes the root mean square (RMS) value of the impulse sensitivity function, resulting in stable output with reduced jitter. The post-layout simulations are performed in 65 nm CMOS technology using 1V supply voltage. At a frequency of 1.6 GHz, the proposed RVCO (PDC-RVCO) shows excellent performance with a phase noise of -100.4dBc/Hz at an offset frequency of 1 MHz. The power dissipation in the PDC-RVCO is reduced by 86.4% as compared to conventional RVCO. The peak-to-peak jitter is improved significantly by 29.7% and the Figure of merit (FOM) is improved by 11dB in the PDC-RVCO than conventional RVCO with a minor increment in area. The PDC-RVCO has the lowest (FOM)(the lower, the better) compared to other RVCO architectures in the literature.</p>
9.	<p>A multi-method bibliometric review of value co-creation research S Saxena, Amritesh, SC Mishra... - Management Research Review, 2023</p> <p>Abstract</p> <p>Purpose This paper aims to examine the origins of value co-creation (VCC) knowledge streams, vis-a-vis their progression over the past 18 years. The study explores how knowledge of this discipline emerged across the tripartite strategic paradigms of business transformation.</p> <p>Design/methodology/approach Co-citation analysis (CCA) and co-word analysis (CWA) are used as bibliometric techniques, for which, a group of articles is retrieved using Scopus's usual keyword-based search. The initial collection consists of 3,431 research articles published in business and management publications. By explaining the article clusters generated through CCA and keyword connections generated through CWA, the findings outline the origins and development of VCC research. A CWA-based chronological study adds further insights to the development of VCC research themes.</p> <p>Findings The results depict that VCC research has grown multifold in the past 18 years, whereby it has shifted its attention from a dyadic interaction approach to a multistakeholder ecosystem-based approach detailing the phenomenological instances of resource integration and institutional processes. Notably, extant research in this field has grown at a much faster rate since 2008. In fact, a stronger concentration of research emerged in the experience domain, particularly in terms of hedonic services. Development of engagement platforms has been driven by research into technologies such as IoT and artificial intelligence.</p> <p>Research limitations/implications The theoretical framework of the VCC paradigm is used to describe the aggregation of co-creation research around the three strategic pillars. This framework is useful for business strategy and to track VCC research over time.</p> <p>Practical implications This work identifies the practices and strategies of VCC at three different levels: capacity, platform and experience. The study offers insights into a variety of co-creation practices at their respective levels, incorporating micro-level dyadic interactions and macro-level processes in a service ecosystem.</p>

	<p>Originality/value</p> <p>This study uses different bibliometric methodologies to investigate the development of this scientific field over time. “Document co-citation” analysis, a more preferred bibliometric technique under CCA, is used to construct the cluster of theoretical cores of this area. The results are classified under the strategic framework of the co-creation paradigm.</p>
10.	<p>A note on homotopy perturbation approach for nonlinear coagulation equation to improve series solutions for longer times N Yadav, M Mehakpreet, S Singh ...J Kumar... - <i>Chaos, Solitons and Fractals</i>, 2023</p> <p>Abstract</p> <p>In this work, the approach presented in a recent publication by Kaur et al. (2019) is improved. The truncated series solution derived from the existing Homotopy Perturbation method (HPM) behaves peculiarly for a longer time domain and provides accurate results only for a shorter time. The Homotopy perturbation approach and the Pade approximation are coupled to estimate the nonlinear coagulation equation to tackle this problem. This significantly improves solution quality over a longer time frame by consuming fewer terms of the truncated series. The effectiveness of the new approach is tested by deriving the new analytical solutions of the number density function for a bilinear kernel with exponential initial distributions. In addition, the new solutions for physical relevant shear, Ruckenstein/Pulvermacher and Brownian kernels corresponding to exponential and gamma initial distributions are also derived. Due to the non-availability of the analytical solutions, the verification of the new results is done against the mass conserving finite volume scheme (Singh et al., 2015) for shear stress, bilinear and Brownian kernels.</p>
11.	<p>A note on semi-orthogonal (G-matrix) and semi-involutory MDS matrices T Chatterjee, A Laha - <i>Finite Fields and their Applications</i>, 2023</p> <p>Abstract</p> <p>Maximum Distance Separable (MDS) matrices are widely used in various cryptographic constructions since they provide perfect diffusion. Further, MDS matrices with easy-to-implement inverses are useful in designing diffusion layers in block ciphers. It is known that the inverse of an MDS matrix is computationally inexpensive if the matrix is either orthogonal or involutory. Generalizing the notion of orthogonal matrices, Fiedler et al. introduced semi-orthogonal property in 2012. Following this, Cheon et al. introduced semi-involutory property to generalize the involutory property in 2021. In both these cases, the aim of the authors was to construct matrices having computationally simple inverses. In this work, we show that some existing Cauchy and Vandermonde based constructions of MDS matrices satisfy semi-orthogonal properties. We give some characterization of 3×3 and 4×4 semi-involutory and semi-orthogonal matrices in light of the MDS property. We also provide some results on circulant matrices with semi-involutory and semi-orthogonal properties. Finally we give a characterization of 4×4 semi-involutory matrices which is a generalization of the 3×3 case of Cheon et al.</p>
12.	<p>A novel functional gradient hydroxyapatite coating for zirconia-based implants VS Seesala, R Rajasekaran, AK Ojha...B Das... - <i>Surface and Coatings Technology</i>, 2023</p> <p>Abstract</p> <p>The bioactivity of zirconia in osseous-implant applications has been debated widely. Acid etching, grit blasting, etc., were employed to improve the microroughness and osseointegration. Coating of calcium phosphate minerals, which are established for metals like titanium is not compatible with zirconia and suffers delamination. Here ceramic dough processing-based composite slurry having HAp and zirconia was explored to form a thin ($\sim 10 \mu\text{m}$) gradient coating on a zirconia dental screw implant. The coating has a homogeneous distribution of secondary phase without affecting the fine machined features like threads. Further, the matrix is porous with increased roughness, but a minimal compromise on strength. During the scratch test,</p>

	<p>the coating survived a normal load >70 N using a diamond indenter without any significant spalling or delamination. Given the simplicity and versatility, this approach is compatible and a promising solution for currently available bio-inert zirconia implants.</p>
13.	<p>A novel privacy protection approach with better human imperceptibility K Rana, A Pandey, P Goyal ...P Goyal - Applied Intelligence, 2023</p> <p>Abstract Our generation is quite obsessed with technology and we like to share our personal information such as photos and videos on the internet via different social networking websites i.e. Facebook, Snapchat, Instagram, etc. Therefore, it becomes easier for others to breach our privacy and harm us in a direct or indirect way. Now, computerized systems have advanced due to the improvements in Machine Learning (ML) algorithms and Artificial Intelligence (AI). These algorithms can extract sensitive information such as face attributes, text information, etc. from images or videos and can be used for privacy breaching. In this paper, we propose a novel privacy protection method by adding intelligent noise to the image while preserving image aesthetics and attributes. We determine multiple attributes for an image such as baldness, smiling, gender, etc. and we intelligently add noise to particular regions of the image that define a particular attribute using the visual explanation technique i.e. GradCam++, thereby preserving the other attributes. The addition of noise is based on the idea of Fast Gradient Sign Method (FGSM) that maximizes the gradients of the loss of an input image to create a new adversarial image. We integrate FGSM adversarial image and GradCam++ output to affect particular attributes only and hence keeping the image human imperceptible. The experiment results show that our attack outperforms the existing attacks including naive FGSM, Projected Gradient Descent (PGD), Momentum Iterative Method (MIM), Shadow Attack (SA), and Fast Minimum Norm (FMN) in terms of preserving attributes and image visual quality, when evaluated on CelebA dataset.</p>
14.	<p>A Novel two-stage partitioning based reconfiguration method for active distribution networks Y Bansal, RSodhi, S Chakrabarti... - IEEE Transactions on Power Delivery, 2023</p> <p>Abstract This paper presents a novel two-stage partitioning based network reconfiguration methodology for active distribution networks (ADNs) operating in grid-connected or islanded modes of operation. Firstly, the entire ADN is partitioned into sub-networks (SNs) using the concept of hierarchical spectral clustering (HSC) and network equivalencing. Then, the optimization of the entire network is completed in two stages. The first stage is responsible for obtaining the reconfiguration of the independent SNs. In the second stage, the entire network reconfiguration is obtained, given the switch states from the prior stage. The optimization problem is solved using modified particle swarm optimization (MPSO). Following any contingency, the ADN operates in islanded mode and the survival of the created islands is examined using the proposed adaptive load flow (ALF). Simulation results of the proposed methodology are then compared with the centralized approach. The analysis on the IEEE 33-Bus and the IEEE 118-Bus distribution network integrated with distributed generators (DGs) shows that the proposed approach significantly reduces the computation time, while the solution remains close to the one from centralized approach. The developed reconfiguration methodology is also validated in real-time using real-time digital simulator (RTDS) and dSPACE1104 (R & D controller).</p>
15.	<p>A Planar distributed receiver coil antenna array to encapsulate vertical and lateral H-Fields for drone wireless charging VK Srivastava, A Bharadwaj, A Sharma - 17th European Conference on Antennas and Propagation (EuCAP), 2023</p> <p>Abstract This paper presents a planar distributed receiver coil antenna array to harvest all the magnetic</p>

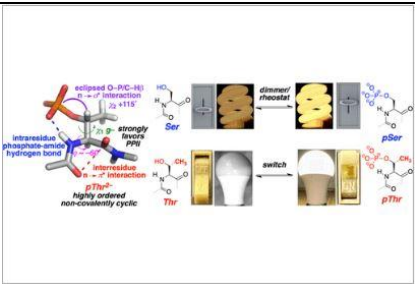
	<p>field components generated by a conventional transmitter for drone charging applications. For this purpose, four anti-parallel turn coils are placed on four arms of the drone to harvest lateral field components along with a conventional circular Rx coil that harvests vertical magnetic field. A DC combining technique is proposed for combining the output voltages induced in each receiver coil to avoid destructive superposition of responses. An EM simulator is used to analyze the potential of harvesting lateral fields by the proposed anti-parallel turn coils. Later, the anti-parallel turn coils' positions are determined based on the maximum voltage induced in these coils. The system is further verified using an experimental setup, and the results prove a significant enhancement of output voltage. Thus, proving the potential of the proposed Rx coil antenna suitable for drone charging applications.</p>
16.	<p>A Polarization insensitive circular rectenna array system for microwave power transfer and energy harvesting applications S Kumar, A Sharma - European Conference on Antennas and Propagation (EuCAP), 2023</p> <p>Abstract The power harvested by a rectenna (Rx) module is highly dependent on its relative orientation with respect to the dedicated RF transmitter (Tx) which can cause polarization mismatch. Therefore, a polarization insensitive rectenna system is proposed here to address the mentioned problem. A multipolarized circular rectenna array is designed using the conjugate impedance matching technique and a shunt dc combining topology for realizing a completely integrated design. This resulted in a low-cost, miniaturized rectenna array system making it suitable for space constraint sensor nodes utilized in IoT applications.</p>
17.	<p>A PRBS generator using merged XOR-D flip-flop as building blocks MK Singh, P Singh, U Chichhula ...M Sakare... - Circuits, Systems, and Signal Processing, 2023</p> <p>Abstract This paper presents a pseudo-random binary sequence (PRBS) generator using merged XOR-D flip-flop as building blocks. The proposed architecture uses differential cascode voltage switch logic (DCVSL)-based dynamic XOR gate. The cross-coupled architecture of the pull-up network creating positive feedback in the DCVSL XOR gate is used as a latch by adding a transistor to apply a clock signal. This arrangement reduces the requirement of one latch in a master-slave D flip-flop (MS-DFF) from each lane. It reduces the area occupied in the layout and power requirements for the PRBS generator. The post-layout simulation for the PRBS generator operating at 5 Gb/s is performed in the 65 nm CMOS technology with a 1 V supply voltage. The proposed PRBS generator requires 2.4 mW of power. The jitter is 5.6 ps for the worst-case output of the proposed PRBS generator. In the proposed merged XOR-D flip-flop, there is an improvement of 33.3%, 27.4%, 29.1%, and 31.2% in power, area, maximum operating frequency, and the number of transistors, respectively, compared to when both XOR gate and D flip-flop are used separately. The figure of merit is improved by 14.8% for the proposed PRBS generator.</p>
18.	<p>A prospective survey on trephine biopsy of bone and bone marrow: an experience with 274 Indian patients' biopsies R Nadda, R Repaka, N Mallik ...AK Sahani - European Journal of Medical Research, 2023</p> <p>Abstract Trephine bone marrow biopsy is an effective technique for diagnosing hematological malignancies in patients of different ages. During trephine biopsy, bone marrow cores are obtained for detailed morphological evaluation to look for any abnormality and arrive at a diagnosis. The primary goal of this work is to perform a survey on Indian patients of various ages for the trephine bone marrow biopsy process. In the present study, data related to 274 trephine biopsy samples from 300 patients were acquired at the Post Graduate Institute of</p>

	<p>Medical Education and Research (PGIMER) in Chandigarh, India. Pain was found to be the sole major procedure-related complication, and patients reported no/less pain in 41 BMB (14.96%) patients, moderate pain in 82 (29.92%) cases, and unbearable pain in 151 (55.1%) BMB cases. In addition, the patients were evaluated by the authors and hematologist as non-anxious for the procedure in 34 (12.4%), anxious in 92 (33.57%), and very/highly anxious in 148 (56%) cases. The bone texture of the patients significantly affected the needle bending, number of repetitions required, and size of the bone marrow sample. This demonstrates the need for improvement in the biopsy procedure. To this end, a survey was conducted to assess the numerous difficulties and diagnostic outcomes throughout the trephine biopsy process.</p>
19.	<p>A review on nickel composite coatings deposited by jet electrodeposition Jhalak, D Beniwal - Coating Materials: Computational Aspects, Applications and Challenges: Book Chapter, 2023</p> <p>Abstract Nickel-based composite coatings are used for numerous industrial applications where good corrosion resistance, wear resistance, and mechanical properties are required. The electrodeposition technique is widely used to deposit nickel-based composite coatings. Jet electrodeposition, which uses a jet to spray plating solution on the cathode surface, allows considerably higher deposition rates with lower susceptibility to corrosion as compared to the traditional electrodeposition process. However, there are shortcomings of jet electrodeposition, such as non-uniform growth and the formation of a rough surface. This can be overcome by integrating the process with various external forces. This review presents an overview of friction-assisted, pulse-assisted, magnetic-assisted, and ultrasonic-assisted jet electrodeposition techniques that have been used for the deposition of Ni-based composite coatings. The effect of various parameters (electrolyte composition, external forces, current density, temperature, jet speed, and type of reinforcing particles) on the microstructure, surface morphology, microhardness, and tribological properties of the deposited coatings has been described. The impact of these parameters on the corrosion resistance of jet-electrodeposited Ni-based coatings has also been presented.</p>
20.	<p>A thiophenoradialene-embedded polycyclic heteroterphenoquinone exhibiting dominant antiaromatic traits PK Sharma, D Mallick, S Das - Organic Letters, 2023</p> <p>Abstract A thiophenoradialene-embedded polycyclic heteroterphenoquinone (PHTPQ) derivative of diindeno[1,2-b:2',1'-d]thiophene-2,8-dione, with antiaromatic characteristics, was synthesized by dehydrogenating its fluorescent dihydro PHTPQ precursor. The antiaromatic character was evidenced by the visible absorption band with a weakly intense tail extending to 800 nm in the near-infrared region (forbidden HOMO → LUMO transition) and non-emissive and amphoteric redox properties. Single-crystal and (anti)aromaticity analyses found a non-aromatic thiophene core while suggesting antiaromaticity/paratropicity of the pentafulvene subunits dominating the overall ground state properties.</p>
21.	<p>A virtual reality based system for a more engaging indoor exercise biking experience A Cahnder, A Airan, A Sahani - IEEE International Instrumentation and Measurement Technology Conference (I2MTC), 2023</p> <p>Abstract Lack of motivation and boredom while doing indoor exercises (in gym) can lead an individual to adhere less to his daily physical exercises. Their adherence to the exercise can be enhanced by making an exercise/task more enjoyable and exciting. To make such exercises more enjoyable and exciting, the gamification of these exercises can be done. Such gamification of these exercises often includes the use of expensive equipment and sophisticated systems that are</p>

	<p>unaffordable and hard to use for many people. The current study is aimed at developing a cheap and affordable solution for the gamification of the tradition cycling exercise in the gym and testing its accuracy in counting the number of pedal rotations and rotations per minute (RPM). Minimal hardware has been used, which involves the use of smartphone placed in the user's pocket. The phone streams acceleration data wirelessly over internet to the PC running the gaming application. In the game, an avatar riding on a virtual bike in a virtual environment mimics the movement of a real user. The whole game scene is displayed on a flat screen placed in front of the user. Here, acceleration data is used to calculate the number of rotations of pedals and RPM. The percentage of expected deviation in the (RPM) calculated by the software with respect to the actual RPM is less than 2.</p>
22.	<p>Ab initio study of metal-decorated carbon and silicon prismanes as the selective CO₂ adsorbents MA Salem, A Jalali, FG Maleki ...R Sangwan... - Modern Physics Letters B, 2023</p> <p>Abstract In this paper, we conducted comprehensive analysis of the selective adsorption of CO₂ by carbon and silicon prismanes along with metal ions. The results of calculations from B3LYP/6-31G(d,p) and M06-2X/6-31G(d,p) levels of theory show that Be²⁺, Mg²⁺, Ca²⁺ and Li⁺, Na⁺, K⁺ ions are bounded strongly enough to prismanes. The Be²⁺ ion binds more strongly to the C₈H₈ cubane with binding energy 9.66eV compared to Li⁺, Na⁺, K⁺, Mg²⁺ and Ca²⁺ ions having binding energies 1.26, 0.63, 0.51, 4.60 and 3.36eV, respectively. Similar results were obtained for larger prismanes C₁₀H₁₀ and C₁₂H₁₂. Instead of binding energy, we determine the adsorption of gases on metal-ion prismane complex along with effect of temperature on different gas adsorption shows that C₈H₈_Mg²⁺ and C₈H₈_Be²⁺ are active adsorbents at temperatures above room temperature. It is also observed that in comparison to N₂ and CH₄, CO₂ interacts more strongly with all prismanes decorated with metal ions. These non-covalent interaction plots are used to study the prismane and metal-ion interaction. Comparable study of silicon prismanes with M06 2X/6-31G (d, p) basis set, in terms of binding energy, adsorption of gases on prismane along with temperature effect, also possesses similar selectivity to CO₂ molecule with even higher adsorption energies. Thus, beryllium-decorated prismanes can be considered as promising adsorbents of carbon dioxide with good selectivity and high adsorption energy.</p>
23.	<p>Accurate and efficient flux-corrected finite volume approximation for the fragmentation problem J Paul, D Ghosh, J Kumar - Journal of Mathematical Chemistry, 2023</p> <p>Abstract In this work, we introduce a weighted finite volume scheme for multiple fragmentation problems and report a convergence criterion of the scheme. It is observed that the finite volume method mentioned in Kumar and Kumar (Appl Math Comput 219(10):5140–5151, 2013) has not estimated the physical moments of clusters with satisfactory precision. Therefore, to control this deficiency, a weight function, and a correction factor are introduced in the numerical flux to approximate the conservative formulation of the multiple fragmentation equation. The proposed scheme preserves the first two physical moments with high accuracy in the cell overlapping case for newly born clusters. It is shown that the new formulation converges weakly under certain growth restrictions on the kernels. Finally, simulation results and numerical validations are presented.</p>
24.	<p>Adaptation: Blessing or curse for higher-way meta-learning A Aimen, S Sidheekh, B Ladrecha...CK Narayanan... - Journal of IEEE Transactions on Artificial Intelligence, 2023</p> <p>Abstract The prevailing literature typically assesses the effectiveness of Meta-learning (ML) approaches on tasks that involve no more than 20 classes. However, we challenge this convention by conducting a more complex and natural task setup to test the fundamental initialization, metric,</p>

	<p>and optimization approaches. In particular, we increase the number of classes in the Omniglot and tieredImagenet datasets to 200 and 90, respectively. Interestingly, we observe that as the number of classes increases, ML approaches perform in reverse order of their degree of adaptation, with ProtoNet outperforming ANIL and MAML. ProtoNet, which does not require adaptation, is marginally affected by the increase in task complexity, while ANIL and MAML are highly affected. Despite performing full feature backbone and classifier adaptation, MetaLSTM++ exhibits an intriguing behavior of performing well. To this end, we analyze the backbone learned by different algorithms and the influence of adaptation from different perspectives. We uncover that ProtoNet learns better, and MetaLSTM++ learns the worst backbone, but the generalizability to unseen data for MetaLSTM++ is compensated by powerful adaptation to the meta-test support sets, due to its learned data-driven optimizer.</p>
25.	<p>Additive twists of L^2-norm of Fourier–Jacobi coefficients of Siegel cusp forms B Kumar, B Paul - Journal of Number Theory, 2023</p> <p>Abstract Let F be a Siegel cusp form of weight k and degree $n \geq 2$ and having Fourier–Jacobi coefficients ϕ_m. We study estimates of L^2-norms of these Fourier–Jacobi coefficients and their additive twists in two ways. One of our results generalizes a result of Kohnen and Sengupta.</p>
26.	<p>Algorithmic aspects of paired disjunctive domination in graphs MA Henning, A Pandey, V Tripathi - Theoretical Computer Science, 2023</p> <p>Abstract In a graph $G=(V,E)$ without an isolated vertex, a dominating set $D \subseteq V$ is a paired dominating set if the graph $G[D]$ induced by D has a perfect matching. Further, a set $D \subseteq V$ is a disjunctive dominating set of G if for each vertex $v \in V$, either $N_G[v] \cap D \neq \emptyset$ or there are at least two vertices in D whose distance from v is two in G. We introduce the notion of paired disjunctive domination in graphs. A disjunctive dominating set $D \subseteq V$ in the graph G is a paired disjunctive dominating set if $G[D]$ has a perfect matching. The minimum cardinality of a paired disjunctive dominating set of G is the paired disjunctive domination number, denoted by $\gamma_{pr}^d(G)$. In this article, we compute the exact value of $\gamma_{pr}^d(G)$ when G is a path, cycle, cograph, chain graph, and split graph. We prove that the decision version of the problem is NP-complete for planar graphs, bipartite graphs, and chordal graphs and design a polynomial-time algorithm to compute a minimum cardinality paired disjunctive dominating set in interval graphs. Further, we obtain lower and upper bounds on the approximation ratio of the problem and proved that the problem is APX-complete for the graphs with maximum degree 4.</p>
27.	<p>Allosteric modulation for widely spread orthologous tyrosinase enzyme by short peptidyl-urea analogue: Facile syntheses of spiro compounds S Saini, K Kaur, Mayank ...N Singh... - Catalysis Letters, 2023</p> <p>Abstract The present work demonstrates the development of an efficient catalytic hybrid model (Tyr-SS2) to synthesize various spiro-oxindoles derivatives. We have designed and synthesized a functionalized dipeptide molecule (SS2) that acts as an allosteric modulator by incorporating itself into the binding cavity of the widely spread orthologous tyrosinase enzyme (Tyr). The allosterically modified Tyr-SS2 hybrid is thoroughly characterized by using various spectroscopic techniques. Its structural stability and reusability were ensured using various analytical techniques viz. Circular Dichroism (CD), Nuclear Magnetic Resonance (NMR), Fluorescence, and UV–Visible absorption spectroscopy. The Tyr-SS2 hybrid complex was used as a catalyst for the synthesis of a series of Spiro-oxindoles derivatives, and the final products obtained were characterized by NMR and High-Resolution Mass Spectrometry (HRMS) techniques. The interactions within the Tyr-SS2 complex, the catalytic mechanism, and binding</p>

	<p>interactions between the reactants and Tyr-SS2 hybrid complex were investigated extensively by molecular docking and MD-Simulation studies. Green scale parameters like Eco scale and E-factor calculations, found to be 80 and 0.096, respectively, are the key features of the current work.</p> 
28.	<p>An Efficient Electrical-Thermal Co-Design Methodology for Analysis of High-Speed PCB Interconnects S Pathania, S Khushwaha, S Kumar...R Sharma - IEEE MTT-S International Conference on Numerical Electromagnetic and Multiphysics Modeling and Optimization (NEMO), 2023</p> <p>Abstract This paper reports a novel co-design methodology for signal integrity analysis considering thermal effects. Our analysis focuses on practical high-speed interconnect topologies. To ensure reliable and efficient system design, we introduce an efficient electrical-thermal methodology (EEM) for high-speed PCB interconnects. Using our proposed EEM, we perform electrical-thermal co-simulation to ensure efficient design and performance.</p>
29.	<p>An inherent difference between serine and threonine phosphorylation: Phosphothreonine strongly prefers a highly ordered, compact, cyclic conformation AK Pandey, HK Ganguly, SK Sinha.. - ACS Chemical Biology, 2023</p> <p>Abstract Phosphorylation and dephosphorylation of proteins by kinases and phosphatases are central to cellular responses and function. The structural effects of serine and threonine phosphorylation were examined in peptides and in proteins, by circular dichroism, NMR spectroscopy, bioinformatics analysis of the PDB, small-molecule X-ray crystallography, and computational investigations. Phosphorylation of both serine and threonine residues induces substantial conformational restriction in their physiologically more important dianionic forms. Threonine exhibits a particularly strong disorder-to-order transition upon phosphorylation, with dianionic phosphothreonine preferentially adopting a cyclic conformation with restricted ϕ ($\phi \sim -60^\circ$) stabilized by three noncovalent interactions: a strong intraresidue phosphate-amide hydrogen bond, an $n \rightarrow \pi^*$ interaction between consecutive carbonyls, and an $n \rightarrow \sigma^*$ interaction between the phosphate O_γ lone pair and the antibonding orbital of $C-H\beta$ that restricts the χ_2 side-chain conformation. Proline is unique among the canonical amino acids for its covalent cyclization on the backbone. Phosphothreonine can mimic proline's backbone cyclization via noncovalent interactions. The preferred torsions of dianionic phosphothreonine are $\phi, \psi =$ polyproline II helix $> \alpha$-helix ($\phi \sim -60^\circ$); $\chi_1 = g^-$; $\chi_2 \sim +115^\circ$ (eclipsed $C-H/O-P$ bonds). This structural signature is observed in diverse proteins, including in the activation loops of protein kinases and in protein-protein interactions. In total, these results suggest a structural basis for the differential use and evolution of threonine versus serine phosphorylation sites in proteins, with serine phosphorylation typically inducing smaller, rheostat-like changes, versus threonine phosphorylation promoting larger, step function-like switches, in proteins.</p>

		
30.	<p>An ML pipeline for real-time activity detection on low computational power devices for metaverse applications A Kumar, A Chander, A Sahani - IEEE International Instrumentation and Measurement Technology Conference (I2MTC), 2023</p> <p>Abstract This paper presents our recent work on real-time human activity detection based on the mediapipe pipeline and machine learning algorithms. A single webcam was used to capture the subject images and the data was recorded in a csv file. These CSV files were used to training and testing machine learning (ML) modes. The proposed system can detect human activities including running, jumping, squatting, bending to the left or right, and standing still. An open source framework named Mediapipe has been used to identify body makers which in result used for body pose. We tried hard coded approach and machine learning based approaches. Four models including random forest (RF), K-nearest neighbor (KNN), neural networks (NN) and convolution neural network (CNN) were tested. NN and CNN perfomed best with NN obtaining maximum accuracy of 99.76% and CNN obtaining accuracy of 100% on the test data sets. The proposed solution provides a cheap and affordable solution for home based exergaming ang rehabilitation.</p>	
31.	<p>Analyzing geomorphological and topographical controls for the heterogeneous glacier mass balance in the Sikkim Himalayas S Guha, RK Tiwari - Journal of Mountain Science, 2023</p> <p>Abstract Glacier response patterns at the catchment scale are highly heterogeneous and defined by a complex interplay of various dynamics and surface factors. Previous studies have explained heterogeneous responses in qualitative ways but quantitative assessment is lacking yet where an intrazone homogeneous climate assumption can be valid. Hence, in the current study, the reason for heterogeneous mass balance has been explained in quantitative methods using a multiple linear regression model in the Sikkim Himalayan region. At first, the topographical parameters are selected from previously published studies, then the most significant topographical and geomorphological parameters are selected with backward stepwise subset selection methods. Finally, the contributions of selected parameters are calculated by least square methods. The results show that, the magnitude of mass balance lies between -0.003 ± 0.24 to -1.029 ± 0.24 m.w.e.a⁻¹ between 2000 and 2020 in the Sikkim Himalaya region. Also, the study shows that, out of the terminus type of the glacier, glacier area, debris cover, ice-mixed debris, slope, aspect, mean elevation, and snout elevation of the glaciers, only the terminus type and mean elevation of the glacier are significantly altering the glacier mass balance in the Sikkim Himalayan region. Mathematically, the mass loss is approximately 0.40 m.w.e.a⁻¹ higher in the lake-terminating glaciers compared to the land-terminating glaciers in the same elevation zone. On the other hand, a thousand meters mean elevation drop is associated with 0.179 m.w.e.a⁻¹ of mass loss despite the terminus type of the glaciers. In the current study, the model using the terminus type of the glaciers and the mean elevation of the glaciers explains 76% of fluctuation of mass balance in the Sikkim Himalayan region.</p>	

32.	<p>Apoptosis-targeted gene therapy for non-small cell lung cancer using chitosan-poly-lactic-co-glycolic acid -based nano-delivery system and CASP8 and miRs 29A-B1 and 34A S Chattopadhyay, SS Sarkar, S Saproo, S Yadav, D Antil, B Das, S Naidu - Frontiers in Bioengineering and Biotechnology, 2023</p> <p>Abstract Non-small cell lung cancer (NSCLC) is a leading cause of cancer-related deaths worldwide, with resistance to apoptosis being a major driver of therapeutic resistance and aggressive phenotype. This study aimed to develop a novel gene therapy approach for NSCLC by targeting resistance to apoptosis. Loss of function mutations of caspase 8 (CASP8) and downregulation of microRNAs (miRs) 29A-B1 and 34A were identified as key contributors to resistance to apoptosis in NSCLC. A biodegradable polymeric nano-gene delivery system composed of chitosan-poly-lactic-co-glycolic acid was formulated to deliver initiator CASP8 and miRs 29A-B1 and 34A. The nano-formulation efficiently encapsulated the therapeutic genes effectively internalized into NSCLC cells and induced significant apoptosis. Evaluation of the nano-formulation in A549 tumor spheroids showed a significant increase in apoptosis within the core of the spheroids, suggesting effective penetration into the spheroid structures. We provide a novel nano-formulation that demonstrate therapeutic potential for suicidal gene therapy in NSCLC.</p>
33.	<p>Application of machine learning to predict hydrodynamic and thermal parameters in laminar mixed convection flows through vertical pipes D Samanta, H Shelar, S Gorai - ISME Journal of Thermofluids, 2023</p> <p>Abstract The purpose of this study is to understand the hydrodynamic and thermal characteristics in the laminar regime of mixed convection flow through vertical pipe and to apply Machine Learning (ML) to predict the friction factor (f) and Nusselt number (Nu). The numerical simulations were performed to analyse the effect of Reynolds number (Re), Grashof number (Gr) and Richardson number (Ri) on fluid flow and heat transfer in both buoyancyaiding and -opposing flows. Re is varied from 100 to 2300, Gr is varied from 1000 to 1587000 and the corresponding Ri ranges from 0.1 to 0.3. Further, various ML models were applied and trained on 758 data points to predict f and Nu. Four input parameters Re, Ri, Pr and the flow orientation were used to train five different models to predict both of them. While predicting f, XGBoost regression model and for Nu, Random Forest regression model works the best.</p>
34.	<p>Area-minimizing minimal graphs over linearly accessible domains K Jaglan, A Sairam Kaliraj - Journal of Geometric Analysis, 2023</p> <p>Abstract It is well known that minimal surfaces over convex domains are always globally area-minimizing, which is not necessarily true for minimal surfaces over non-convex domains. Recently, M. Dorff, D. Halverson, and G. Lawlor proved that minimal surfaces over a bounded linearly accessible domain D of order β for some $\beta \in (0, 1)$ must be globally area-minimizing, provided a certain geometric inequality is satisfied on the boundary of D. In this article, we prove sufficient conditions for a sense-preserving harmonic function $f = h + g^-$ to be linearly accessible of order β. Then, we provide a method to construct harmonic polynomials which maps the open unit disk $z < 1$ onto a linearly accessible domain of order β. Using these harmonic polynomials, we construct one parameter families of globally area-minimizing minimal surfaces over non-convex domains.</p>
35.	<p>Association between knowledge, attitude, social contact and social distance practices with regard to the LGBT community among heterosexual individuals living in the Punjab State of India S Kharwar, P Singh - Sexuality Research and Social Policy, 2023</p>

	<p>Abstract</p> <p>Introduction Evidence of experienced discrimination by the lesbian, gay, bisexual and transgender (LGBT) individuals makes it necessary to investigate antecedents of prejudice towards them. Desired social contact (DSC) and social distancing practices towards LGBT community may be related to the knowledge about and attitudes towards the LGBT community. However, the inter-construct mechanism underlying such practices needs to be investigated. Considering this need, the present study explored the relationship between knowledge, attitude, DSC and social distance practices towards the LGBT community.</p> <p>Methods A total of 315 heterosexual participants (male—184, female—131; $M_{age} = 24.66$, $SD_{age} = 3.38$) were contacted through emails and social media between November 2021 and February 2022 and requested to fill the questionnaires.</p> <p>Results The findings indicate that the relationships between knowledge, DSC and social distancing practices are significantly mediated by attitudes towards the LGBT community. The standardized indirect effect of knowledge (via attitude) on DSC was statistically significant ($\beta = 0.47$; 95% CI, 0.54, 0.40; $p = 0.005$). Also, knowledge's standard indirect effect (via attitude) on social distancing was statistically significant ($\beta = -0.25$; 95% CI, -0.32, -0.16; $p = 0.005$).</p> <p>Conclusions The findings assert that knowledge about and attitude towards LGBT community play a crucial role in shaping social contact and social distancing practices towards them. Increased knowledge about alternative sexualities may effectively reduce negative attitudes and social distancing practices and create a more inclusive and accepting society for sexual minority groups.</p> <p>Policy Implications Policymakers should strive to enhance the knowledge of general populations concerning sexuality and homosexual attractions through awareness programs and formal teaching.</p>
36.	<p>Audio-visual automatic group affect analysis G Sharma, A Dhall, J Cai - IEEE Transactions on Affective Computing, 2023</p> <p>Abstract Affective computing has progressed well due to methods, which can identify a person's posed and spontaneous perceived affect with high accuracy. This paper focuses on group-level affect analysis on videos, which is one of the first few multimodal group-level affect analysis studies. There are many challenges on video-based group-level affect analysis as most of the work is focused on either a single person's affect recognition or image-based group affect analysis. To address this, first, we present an audio-visual perceived group affect dataset - 'Video-level Group Affect (VGAF)'. VGAF is a large-scale dataset consisting of 4,183 group videos. The videos are collected from YouTube with large variations in the keywords for collecting data across different genders, group settings, group sizes, illuminations and poses. The variety within the dataset will help the study of perception of group affect in a real environment. The data is manually annotated for three group affect classes - positive, neutral, and negative. Further, a fusion based audio-visual method is proposed to set a benchmark performance on the proposed dataset. The experimental results show the effectiveness of facial, holistic and speech features for group-level affect analysis.</p>
37.	<p>Autofocusing and self-healing of partially blocked circular Airy derivative beams A Kumari, V Dev, V Pal - Optics and Laser Technology, 2023</p> <p>Abstract We numerically and experimentally study the autofocusing and self-healing of partially blocked</p>

	<p>circular Airy derivative beams (CADB). The CADB consists of multiple rings, and partial blocking of CADB with different kinds is achieved by using symmetric and asymmetric binary amplitude apertures, enabling blocking of inner/outer rings and sectorially. The CADB blocked with different types possesses the ability to autofocus, however, the abruptness in the autofocusing varies with the amount in certain types of blocking. The abrupt autofocusing is quantified by a maximum k-value, and how fast it changes around the autofocusing distance (z_{af}). In particular, CADB blocked with inner rings (first/two/three) exhibits an abrupt autofocusing, as the k-value sharply increases [decreases] just before [after] z_{af}. The maximum k-value always occurs at z_{af}, which decreases as the number of blocked inner rings increases. For CADB blocked with outer rings, the k-value gradually changes around z_{af}, indicating a lack of abrupt autofocusing. The value of z_{af} increases with the number of blocked outer rings. This suggests that although outer rings contain low intensities, these play an important role in abrupt autofocusing. A sectorially blocked CADB possesses an abrupt autofocusing, and maximum k-value depends on the amount of blocking. The CADB blocked with different types possesses good self-healing abilities, where blocked parts reappear as a result of redistribution of intensity. The maximum self-healing occurs at z_{af}, where an overlap integral approaches a maximum value. Finally, we have compared ideal CADB and partially blocked CADB having the same radii of central dark region, and found that an ideal CADB possesses better abrupt autofocusing. We have found a good agreement between the numerical simulations and experimental results.</p>
38.	<p>Automation of seizure diary entry using mobile-based application VP Nathasha, R Shukla, S Yadav...AK Sahani - 2023 IEEE Instrumentation and Measurement Technology Conference (I2MTC), 2023</p> <p>Abstract</p> <p>Seizure diaries are a record of seizure occurrence. Since seizures may occur at unprecedented times and their frequency is unpredictable, maintaining a seizure diary can assist doctors in determining the most appropriate treatment for their epilepsy patients. To utilize the advantages of paper-based conventional seizure diaries and their electronic counterparts, we have developed a mobile-based application that assists primary healthcare workers (Accredited Social Health Activists (ASHA) in India) in scanning and uploading a custom-designed seizure diary document maintained by the patient. The seizure diary document contains a table with rows mentioning the date and four columns each for different seizure types like a focal, generalized, combination, and unknown. Each column is further divided into three columns so that at most three seizures in a day can be recorded by coloring the box. The corners of the seizure diary have a thicker border to ensure proper corner detection and a marking on one of the edges allows orientation correction. The application scans the document and, after initial preprocessing, detects the markings and text using the inbuilt image processing algorithm with an average accuracy of 99.31%. This data is sent to the cloud server and stored using the patients' unique identification number(ID). The application also allows scanning in offline mode, wherein the information is temporarily stored in local storage till synced with the cloud storage. The doctors may access and visualize the data from the cloud server to monitor the seizure and plan the treatment. This application can thus be used to digitalize seizure diary entries for patients from rural areas with limited internet connectivity and lack of digital literacy. We asked 10 ASHA workers to use the application and 8 out of 10 could record a seizure diary within 5 minutes after one session of basic training.</p>
39.	<p>Bearing capacity and liquefaction assessment of shallow foundations resting on Vibro-Stone column densified soil in Vallur oil terminal, India T Das, M Sharma, D Choudhury - Indian Geotechnical Journal, 2023</p> <p>Abstract</p>

	<p>This article includes bearing capacity and liquefaction potential analysis of shallow foundations in Vibro-stone column densified soil using Indian Standard (IS) codes and finite element methods. The efficacy of stone columns was demonstrated through a real field project in Vallur oil terminal, Chennai, India. The subsoil at the project site was majorly non-plastic silty liquefiable soil having a very soft silty clay layer at the top 2 to 3 m. The codal analysis showed the presence of a liquefiable layer at a depth of 3 to 5 m. However, the ultimate bearing capacity effectively increased by 3 to 4.5 times, and settlement reduced to 84–92% after Vibro-stone column installation. The finite element-based computer program PLAXIS 2D was used to perform numerical analyses with plane strain idealization. Primarily, all the soil layers were modeled as Mohr–Coulomb material in numerical analysis to compute bearing capacity and settlement before and after ground improvement. Then after an effective stress-based elastoplastic UBC3D-PLM material was used to model the liquefiable layer for liquefaction potential analysis in PLAXIS 2D. The numerical analyses exhibited that the stone columns improved the bearing capacity by 43%, and consequently, the settlement was reduced by 2 times. Also, it was observed that introducing stone columns resulted in a considerable reduction in excess pore water pressure. The bearing capacity and settlement values obtained from codal and numerical analyses were compared and found to be in good agreement. The calculated settlements were within the desired limit, and the estimated bearing capacity values were greater than the allowable load intensity. Hence, the installation of Vibro-stone columns can be an effective solution to improve the strength of liquefiable soil.</p>
40.	<p>Blind Image Inpainting via Omni-dimensional Gated Attention and Wavelet Queries SS Phutke, A Kulkarni, SK Vipparthi, S Murala - Proceedings of the IEEE/CVF Conference on Computer Vision and Pattern Recognition, 2023</p> <p>Abstract Blind image in painting is a crucial restoration task that does not demand additional mask in formation to restore the corrupted regions. Yet, it is a very less explored research area due to the difficulty in discriminating between corrupted and valid regions. There exist very few approaches for blind image in painting which sometimes fail at producing plausible in painted images. Since they follow a common practice of predicting the corrupted regions and then in paint them. To skip the corrupted region prediction step and obtain better results, in this work, we propose a novel end-to-end architecture for blind image in painting consisting of wavelet query multi-head attention transformer block and the omni-dimensional gated attention. The proposed wavelet query multi-head attention in the transformer block provides encoder features via processed wavelet coefficients as query to the multi-head attention. Further, the proposed omni-dimensional gated attention effectively provides all dimensional attentive features from the encoder to the respective decoder. Our proposed approach is compared numerically and visually with existing state-of-the-art methods for blind image in painting on different standard datasets. The comparative and ablation studies prove the effectiveness of the proposed approach for blind image inpainting.</p>
41.	<p>Chitosan-poly(vinyl alcohol)-ionic liquid-grafted hydrogel for treating wastewater A Singh, N Singh, N Kaur... - New Journal of Chemistry, 2023</p> <p>Abstract A chitosan-poly(vinyl alcohol)-ionic liquid-grafted hydrogel was prepared for water purification. The hydrogel was characterized using various techniques, including nuclear magnetic resonance spectroscopy, X-ray photoelectron spectroscopy, infrared spectroscopy, powder X-ray diffraction, scanning electron microscopy, and energy-dispersive spectroscopy. The swelling properties of the hydrogels were optimized by varying the solvent, pH, time, and temperature. The maximum swelling of the hydrogel was 330%. The hydrogel absorbed dye, nitrite, and Pb²⁺, with removal rates of up to 97% for dye and 88% for Pb²⁺. The hydrogel could effectively recover oil from an oil-water mixture, where the removal mechanism was predominantly</p>

	<p>attributed to electrostatic interactions between the cationic hydrogel and the dye, Pb^{2+}, and nitrite anions. The hydrogel was biodegradable, making it environmentally friendly.</p>
42.	<p>Combination of an oxindole derivative with (-)-β-Elemene alters cell death pathways in FLT3/ITD⁺ acute myeloid leukemia cells J Alanazi, O, Bender, R Dogan...JA Malik... - <i>Molecules</i>, 2023</p> <p>Abstract Acute myeloid leukemia (AML) is one of the cancers that grow most aggressively. The challenges in AML management are huge, despite many treatment options. Mutations in FLT3 tyrosine kinase receptors make the currently available therapies less responsive. Therefore, there is a need to find new lead molecules that can specifically target mutated FLT3 to block growth factor signaling and inhibit AML cell proliferation. Our previous studies on FLT3-mutated AML cells demonstrated that β-elemene and compound 5a showed strong inhibition of proliferation by blocking the mutated FLT3 receptor and altering the key apoptotic genes responsible for apoptosis. Furthermore, we hypothesized that both β-elemene and compound 5a could be therapeutically effective. Therefore, combining these drugs against mutated FLT3 cells could be promising. In this context, dose–matrix combination-based cellular inhibition analyses, cell morphology studies and profiling of 43 different apoptotic protein targets via combinatorial treatment were performed. Our studies provide strong evidence for the hypothesis that β-elemene and compound 5a combination considerably increased the therapeutic potential of both compounds by enhancing the activation of several key targets implicated in AML cell death.</p>
43.	<p>Computational prediction of two-dimensional o-Al₂N₂ under applied strain for boosting the photocatalytic hydrogen evolution reaction performance I Bouziani, I Essaoudi, R Ahuja... - <i>International Journal of Hydrogen Energy</i>, 2023</p> <p>Abstract Photocatalytic water splitting for clean hydrogen fuel production provides a promising approach to solve the energy and environmental issues. Recently, two-dimensional (2D) photocatalysts have attracted growing interest owing to their short carrier diffusion path, abundant active sites and large surface area. This study explores the photocatalytic performance of 2D orthorhombic dialuminum dinitride (o-Al₂N₂) using density functional theory. The computational results show that the o-Al₂N₂ monolayer has a semiconductor character with indirect and moderate bandgap. Moreover, this system exhibits high light absorption in the visible region, referring to its high capacity for harvesting sunlight. Meanwhile, under neutral pH, the band edge positions are suitable to straddle water redox potentials and the hydrogen evolution reaction is energetically favorable to allow hydrogen production on the surface of 2D o-Al₂N₂ compound. More importantly, the photocatalytic activity of o-Al₂N₂ monolayer is significantly improved under slight biaxial compressive strain. Therefore, our findings suggest that the o-Al₂N₂ nanomaterial is a highly efficient 2D photocatalyst for hydrogen production via water splitting under neutral pH. © 2023 Hydrogen Energy Publications LLC.</p>
44.	<p>Concept of integrating geothermal energy for enhancing the performance of solar stills S Verma, R Das, NK Mishra - <i>Desalination</i>, 2023</p> <p>Abstract Solar stills have been coupled to several preheating systems to increase their productivity, but never before to a borehole exchanger. In this work, a coaxial type borehole exchanger has been integrated with a single basin solar still. Transient and steady-state heat transfer models are presented to assess the behaviour of the combined system for a four-month winter period corresponding to the Urmia Lake region in Iran. Because ground serves as a heat source during winters and a heat sink during summer, integration with a ground exchanger is seen to increase the solar still's productivity for the winter months, by about 126 % for the considered values of</p>

	<p>parameters. It is also seen that the steady model over calculates the total distillate collected, by about 7 % for ground exchanger integrated still and underestimates it by about 0.2 % for an independent still, respectively. It is observed that larger inner and smaller outer radius of the ground exchanger are desirable. Further, the water mass flow rate is seen to possess an optimal value at which the still's output gets maximized. This work is proposed to be a first step in analysing the usefulness of extracting geothermal energy via a borehole exchanger for desalination application via a solar still.</p>
45.	<p>Confocal mapping of stable room-temperature emission centers in gadolinium doped vacancy-ordered double halide perovskite, Gd:Cs₂SnCl₆ AA Bhat, N Singh, RV Nair... - Optical Materials, 2023</p> <p>Abstract The recent advancement in bandgap engineering through controlled doping has widen the prospect of vacancy ordered double halide perovskites (VO DHPs) by conferring them with designable optoelectronic properties. Here, we report confocal mapping of Gd doped Cs₂SnCl₆ along with the macroscopic photoluminescence studies. The insertion of Gd³⁺ ions into the crystal structure facilitates an additional stable room temperature low intensity PL emission at ca. 615 nm (~2.0 eV) in addition to the major emission at ca. 445 nm (~2.7 eV) due to the creation of defect states. Both the pristine (Cs₂SnCl₆) and Gd:Cs₂SnCl₆ exhibit crystalline cubic structure with the space group of Fm3̄m. The Rietveld refinement correlates well with the experimental X-ray diffraction data, while the SEM studies confirm the anisotropic growth, forming large micron sized octahedral structures of pristine (>20 μm) and partly distorted crystals of Gd:Cs₂SnCl₆ (<5 μm). This study enhances the understanding of hitherto unknown 2nd emission at room temperature of larger crystals of Gd:Cs₂SnCl₆ having implications in quantum photonics.</p>
46.	<p>Controlling air pollution in data centers using green data centers S Dey, S Pal - 2023 IEEE/ACM International Symposium on Cluster, Cloud and Internet Computing Workshops (CCGridW 2023), 2023</p> <p>Abstract Growing air pollution has become a global threat to the environment. Controlling this global threat is very challenging and costly. Therefore, this paper proposes an air pollution control measure using green metrics (GMs). For doing this, we minimize the carbon emission from traditional data centers (DCs) by designing the 'Green Data Centers' (GDCs). GDCs are the control mechanism, which includes a set of different green protocols. GDCs are designed in such a way that they can minimize the carbon emission (i.e., CO, and CO₂) from the traditional DCs. The design of GDCs is also responsible for optimizing energy consumption, cost-effectiveness, efficient network infrastructures, load scheduling algorithms, and the number of used devices like switches, ports, and linecards. GDCs are constructed by taking care of the idle server because it consumes massive energy than the computing server. This paper also presents a taxonomy of the existing research work, which contains the research of GDCs related to DCs, like cloud computing and cooling techniques. Apart from this, we discuss various green metrics (GMs), green computing, and networking proposals of GDCs.</p>
47.	<p>Cosecure domination: Hardness results and algorithms Kusum, A Pandey - International Workshop on Combinatorial Algorithms, 2023</p> <p>Abstract For a simple graph $G=(V,E)$ without any isolated vertex, a cosecure dominating set S of G satisfies two properties, (i) S is a dominating set of G, (ii) for every vertex $v \in S$, there exists a vertex $u \in V \setminus S$ such that $uv \in E$ and $(S \setminus \{v\}) \cup \{u\}$ is a dominating set of G. The minimum cardinality of a cosecure dominating set of G is called the cosecure domination number of G and</p>

	<p>is denoted by $\gamma_{cs}(G)$. The MINIMUM COSECURE DOMINATION problem is to find a cosecure dominating set of a graph G of cardinality $\gamma_{cs}(G)$. The decision version of the problem is known to be NP-complete for bipartite, planar, and split graphs. Also, it is known that the MINIMUM COSECURE DOMINATION problem is efficiently solvable for proper interval graphs and cographs.</p> <p>In this paper, we work on various important graph classes in an effort to reduce the complexity gap of the MINIMUM COSECURE DOMINATION problem. We show that the decision version of the problem remains NP-complete for doubly chordal graphs, chordal bipartite graphs, star-convex bipartite graphs and comb-convex bipartite graphs. On the positive side, we give an efficient algorithm to compute the cosecure domination number of chain graphs, which is an important subclass of bipartite graphs. In addition, we show that the problem is linear-time solvable for bounded tree-width graphs. Further, we prove that the computational complexity of this problem varies from the classical domination problem.</p>
48.	<p>Current and emerging techniques for the detection of environmental contaminants V Vaishampayan, R Dahake, GK Athira...S Gumfekar - <i>Molecularly Imprinted Polymers for Environmental Monitoring: Fundamentals and applications: Book Chapter</i>, 2023</p> <p>Abstract</p> <p>The burden to public health of diseases and deaths linked to environmental contamination is evolving as a worldwide challenge. Industries and natural and artificial human activities are the key contributors to generating ecological contaminants in wastewater, microplastics, pathogenic contaminants, electronic waste (e-waste), etc. These contaminants contain a plethora of hazardous organic groups, synthetic chemicals, heavy metals, and so on. Their generation has raised a serious concern in recent years because of their potential threats and continuous output. Often, the level of exposure to these contaminants is unknown and the lack of monitoring makes it difficult to select further treatment methods. The cumulative exposure and long latency period of these materials create hurdles in separating the contaminants from the environment. The existing methods to determine the contaminants quantitatively are sophisticated and bulky. Hence, researchers are developing new generations of sensors for the analytical estimation of these contaminants. This chapter presents a holistic picture of environmental contaminants, their current existing detection methods, and new developing methods. Further, we discuss the integration of these sensing mechanisms with futuristic technologies for better monitoring.</p>
49.	<p>Dependence of persistent photoconductivity on the thickness of β-Ga₂O₃ thin film photodetectors on c-plane sapphire via magnetron sputtering D Kaur, R Dahiya, M Kumar - <i>Journal of Vacuum Science & Technology A</i>, 2023</p> <p>Abstract</p> <p>β-Ga₂O₃ is a next-generation, ultra-wide bandgap semiconductor with intrinsic solar-blindness having the potential to replace Si for photodetection applications especially for the UV-C range. The material itself shows excellent photoconductive gain but is quite prone to the menace of the persistent photoconductivity, or the PPC. The fabricated devices become slower because of PPC and it also leads to reliability issues for photodetection logic. Herein, we report the dependence of the PPC effect on the different thickness of β-Ga₂O₃ thin film based solar-blind photodetectors. The polycrystalline films are grown on c-plane sapphire via RF magnetron sputtering at an elevated temperature of 500 °C. Optical bandgap of the films decreases with increasing thickness while their grain size increases. The oxygen-related defects studied using x-ray photoelectron spectroscopy are responsible for the observation of the enhanced PPC effect for the thinner films. The device performance is intimately connected with the quality of the thin film, its stoichiometry and the amount of oxygen defects present in the system. Better quality films with lower amount of oxygen vacancies show an improved performance with the least amount of PPC. This work shows that oxygen vacancies play an important role in determining the ultimate device performance and need to be engineered for high performance photodetectors.</p>

50.	<p>Design and analyses of planar antenna for bluetooth based IoT applications R Raina, LK Baghel, S Kumar - International Conference on Microwave, Antenna and Communication (MAC 2023), 2023</p> <p>Abstract Bluetooth is the most preferred wireless technology for low-power, short-range Internet of Things (IoT) applications. Bluetooth-based IoT devices being smaller in size, require compact antennas. In this regard, various 2.45 GHz antennas have been proposed in the literature; however, they possess certain limitations, for instance, large size, difficult to fabricate, and costly. Hence, in order to address these concerns, a compact and modified Meandered Inverted F Antenna (MIFA) is proposed in this paper. The proposed antenna possesses a simulated bandwidth percentage of 8.09 %, 1.61 dBi gain, 91.07 % radiation efficiency, and an omnidirectional radiation pattern at 2.45 GHz. Additionally, a comparative analysis between the simple inverted F antenna and the proposed compact and modified meandered inverted F antenna has been made for the improved performance evaluation of the proposed antenna. The proposed antenna design is fabricated on an FR4 substrate with 35 mm x 35 mm x 1.6 mm dimensions and is simulated on Ansys Electronics Desktop 2021R1. Also, numerous experiments have been performed in real-time to validate the proposed design.</p>
51.	<p>Design methodology of near-field transmitter coil antenna for maximizing efficiency of the WPT system A Bharadwaj, VK Srivastava, CC Reddy ... - 17th European Conference on Antennas and Propagation (EuCAP), 2023</p> <p>Abstract This article provides a comprehensive stepwise procedure to develop a transmitter (Tx) coil antenna for a near-field WPT system. The design procedure enables to determine the parameters such as distance between Tx and Receiver (Rx) coils (h), side-length (2a), the number of turns (N t), and resonant frequency (f c) of Tx coil. These parameters are optimized based on the application scenario, maximum magnetic field strength (H), safety guidelines, and quality factor (Q). Further, the analytical H-field results are verified by the EM simulator. Moreover, by choosing an appropriate load resistance (R L) and optimal circuit parameters, the link efficiency (η) between Tx-Rx coils and system efficiency (η_{dc-dc}) are maximized using the LT-Spice circuit simulator.</p>
52.	<p>Design of a bifunctional catalyst by alloying Ni with Ru-supported H-beta for selective hydrodeoxygenation of bisphenol A and polycarbonate plastic waste A K Manal, GV Shanbhag, R Srivastava - Applied Catalysis B: Environmental, 2023</p> <p>Abstract The valorization of waste plastic to renewable chemicals is essential for human civilization. Bimetallic bi-functional catalysts can promote liquid-phase hydrodeoxygenation to produce liquid fuels and value-added chemicals. Ru-Ni/H-Beta bi-functional catalyst is demonstrated for the hydrodeoxygenation of bisphenol A, a monomer of polycarbonate (PC), and PC plastic waste under mild reaction conditions, afforded a complete conversion and > 90% selectivity of propane-2,2-diylidicyclohexane (P7), a JET fuel range C₁₅ cycloalkanes. The process was scaled to 2 g of plastic waste. The catalyst exhibited excellent activity (TOF-309 h⁻¹ at 0.3 h), reusability, and substrate diversity. The performance of Ru-Ni/H-Beta catalysts depends on the synergy between Ru and Ni, with the best performance observed at the Ni/Ru weight ratio of 0.5. The bimetallic Ru-Ni catalytic strategy and mechanistic understanding presented in this work provide promising insight into catalyst design and could be applied to other chemical transformations requiring efficient hydrodeoxygenation catalysts.</p>
53.	<p>Design of a high precision CMOS programmable gain and data rate delta sigma ADC MA Saeed, RK Srivastava, D Sehgal, DM Das - Analog Integrated Circuits and Signal</p>

	<p>Processing, 2023</p> <p>Abstract</p> <p>This paper presents a general purpose high precision Delta Sigma () ADC with a common mode rejection of 100 dB, developed for data acquisition of sensors used in a satellite launch vehicle telemetry system. To make ADC suitable for various sensor outputs such as temperature sensor, pressure sensor, strain sensor etc., the ADC offers eight digitally programmable gain values (X1, X2, X4, X8, X16, X32, X64 and X128). This ADC uses a second order delta sigma modulator (DSM) followed by a digital sinc filter. The output data rate of the ADC is also digitally programmable and can be set to any value of 312.5 Hz, 625 Hz, 1.25 kHz and 2.5 kHz. The ADC is also equipped with on chip offset and gain calibration features to reduce the offset and gain errors. The serial interface of ADC is SPI compatible. The proposed ADC is designed and fabricated in single poly, 4-metal, 0.18 μm CMOS process at Semi-Conductor Laboratory (SCL). The ADC is clocked at 5.12 MHz and consumes a total power of 4 mW and occupies 2.25 mm of silicon area. The ADC requires a supply voltage of 3.3 V and 1.8 V and can operate in a wide temperature range of 55 to 125 C. The proposed ADC achieves a maximum ENOB of 19.15 bits at a data rate of 312.5 Hz with a full scale range of 1.22 V.</p>
54.	<p>Design of porphyrin-based frameworks for efficient visible light-promoted reduction of CO₂ from dilute gas: Combined experimental and theoretical investigation R Das, R Belgamwar, SS Manna...CM Nagaraja - Journal of Colloid and Interface Science, 2023</p> <p>Abstract</p> <p>The photocatalytic carbon dioxide reduction (CO₂R) coupled with hydrogen evolution reaction (HER) constitutes a promising step for a sustainable generation of syngas (CO + H₂), an essential feedstock for the preparation of several commodity chemicals. Herein, visible light/sunlight-promoted catalytic reduction of CO₂ and protons to syngas using rationally designed porphyrin-based 2D porous organic frameworks, POF(Co/Zn) is demonstrated. Indeed, POF(Co) showed superior catalytic performance over the Zn counterpart with CO and H₂ generation rates of 1104 and 3981 $\mu\text{mol g}^{-1}\text{h}^{-1}$, respectively. The excellent catalytic performance of Co-based POF is aided by the favorable transfer of photo-excited electrons from Ru-sensitizer to the Co^{II} catalytic site, which is not feasible in the case of POF(Zn), revealed from the theoretical investigation. More importantly, the POF(Co) catalyzes the reduction of CO₂ even from dilute gas (13% CO₂), surpassing most reported framework-based photocatalytic systems. Significantly, the catalytic performance of POF(Co) was increased under natural sunlight conditions suggesting sunlight-promoted enhancement in syngas generation. The in-depth theoretical investigation further unveiled the comprehensive mechanistic pathway of the light-promoted concurrent CO and H₂ generation. This work showcases the advantages of porphyrin-based frameworks for visible light/sunlight-promoted syngas generation by utilizing greenhouse gas (CO₂) and protons under mild eco-friendly conditions.</p>
55.	<p>Design of power system stabilizer for DFIG-based wind energy integrated power systems under combined influence of PLL and virtual inertia controller B Sahu, BP Padhy - Journal of Modern Power Systems and Clean Energy, 2023</p> <p>Abstract</p> <p>Wind Energy Systems (WES) based on DFIG have enormous potential to meet the demand for clean energy in the future. Due to the low inertia and intermittency nature of power injection, WES are enabled with a virtual inertia controller (VIC) to support the system during a frequency event. The frequency deviation measured by Phase Locked Loop (PLL) installed on point of common coupling (PCC) bus is the input signal to VIC. However, VIC with improper inertial gain could deteriorate the damping of the power system, which may lead to instability. To address this issue, a mathematical formulation for calculating the synchronizing and damping</p>

	torque coefficients of the WES integrated Single Machine Infinite Bus (SMIB) system while taking PLL and VIC dynamics into consideration has been proposed in this paper. Further, the PSS design methodology has been proposed in a WESs integrated power system to enhance electromechanical oscillation damping. The small signal stability assessment is performed using the infinite bus connected to a synchronous generator (SG) of higher-order dynamics integrated with VIC-equipped WES. Finally, the performance and robustness of the proposed PSS is demonstrated through timedomain simulation in the SMIB system and nine bus test systems integrated with WES considering several case studies.
56.	<p>Determining the strain rate of controlled-strain loading consolidation test with hydraulic conductivity M Raheena, RG Robinson - Canadian Geotechnical Journal, 2023</p> <p>Abstract This note presents a rational procedure to determine the initial strain rate of controlled-strain loading (CSL) consolidation test and control the strain rate during the test within the permissible limits of pore pressure ratio. The initial strain rate is determined by measuring the hydraulic conductivity of soil specimen by conducting a rapid falling head hydraulic conductivity test using a stand pipe of 3 mm diameter. The strain rate is controlled during the test by restricting the maximum allowable pore pressure ratio at the base of the specimen close to 15%. The testing procedure is validated by performing a series of experiments on reconstituted and undisturbed soil samples. The results from the proposed method are compared with those obtained from the incremental loading consolidation test. The test results proved that the proposed method can be conveniently used to perform the CSL consolidation tests for the determination of the consolidation properties of soils.</p>
57.	<p>Development, characterization and high-temperature oxidation behaviour of hot-isostatic-treated cold-sprayed thick titanium deposits P Singh, H Singh, S Singh... - Machines, 2023</p> <p>Abstract In this work, thick deposits of pure titanium (Ti), with a thickness of around 15 mm, were additively manufactured using high-pressure cold spraying. Nitrogen was employed as the process gas. Subsequently, the deposits were subjected to hot isostatic pressing (HIP). The HIP-treated Ti deposits were analyzed for their metallurgical and mechanical characteristics with the aim of exploring the viability of using cold spraying for the additive manufacturing of Ti components. Moreover, high-temperature cyclic oxidation testing was also performed on the HIP-treated Ti deposit to understand its stability at high temperatures. SEM/EDS showed a dense structure with marginal porosity for the HIP-treated Ti deposits, without any oxide formation, which was further confirmed via XRD analysis. An average microhardness of 214 HV was measured for the HIP-treated Ti deposits, which is close to that of the commercially available bulk titanium (202 HV). The high-temperature oxidation studies revealed that the cold-sprayed HIP-treated Ti has very good oxidation resistance, which could be attributed to the formation of protective titanium dioxide in its oxide scale.</p>
58.	<p>Development of a diagnostic kit for point-of-care biosensors: Fundamentals and applications V Vaishampayan, P Kulabhushan, I Dasgupta...SP Gumfekar - Point-of-Care Biosensors for Infectious Diseases: Book Chapter, 2023</p> <p>Summary Historically, the gold standards for biomedical diagnostics and chemical and biomolecular analyses have been centralized laboratories equipped with sophisticated equipment. The benchmarked techniques and approved protocols enable the delivery of standardized results to the users. However, the scenario of healthcare facilities is rapidly changing due to social, economic, and technical reasons. There is an impetus to make healthcare diagnostics accessible</p>

	<p>to all sections of society to improve health standards and promote timely diagnosis of epidemic diseases. In this context, World Health Organization (WHO) has designated the ASSURED (Affordable, Sensitive, Specific, User-friendly, Rapid and robust, Equipment-free, and Deliverable to end users) criteria to emphasize the need of developing diagnostics platforms to improve global healthcare standards. Point-of-care (POC) testing is ideally meant to be simple, low cost, and patient-centered. The advances in microfabrication techniques and microfluidics have significantly enhanced the capabilities of POC testing devices, thus enabling them to move toward meeting the goal of ASSURED criteria. The proposed chapter covers the fundamental building blocks for biosensors, including a selection of substrates, fabrication methods, biorecognition elements, readout mechanisms with applications for the infectious diseases.</p>
59.	<p>Development of a multilayer Iliac crest numerical model for simulating honeybee stinger-inspired hollow needle insertion R Nadda, R Repaka, AK Sahani - Journal of Engineering and Science in Medical Diagnostics and Therapy, 2023</p> <p>Abstract Minimally invasive biopsy needles are frequently inserted into the desired body regions while performing the bone marrow biopsy (BMB) procedure. The key problem with needle insertion in tissues is that the insertion force damages the tissue and deviates the needle path, leading the needle to miss the desired target and reducing biopsy sample integrity. To address these shortcomings, the present work developed a unique bio-inspired barbed biopsy needle design that reduces insertion/extraction forces and needle deflection. This study established several design parameters, including barb geometry and shape (viz., the height of barb, barbed front angle, barbed back angle, and length of portion containing barbs), and examined the impact of these factors on insertion/extraction force and deflection. A Lagrangian surface-based nonlinear finite element (FE) approach has been used to numerically simulate the BMB procedure on a three-dimensional (3D) multilayered heterogeneous model of the human iliac crest. The proposed honeybee stinger-inspired needle design has been found to reduce both insertion and extraction forces because of the decreased frictional surface of the biopsy needle.</p>
60.	<p>Do You Really Mean That? Content Driven Audio-Visual Deepfake Dataset and Multimodal Method for Temporal Forgery Localization Z Cai, K Stefanov, A Dhall... - 2022 International Conference on Digital Image Computing: Techniques and Applications (DICTA 2022), 2022</p> <p>Abstract Due to its high societal impact, deepfake detection is getting active attention in the computer vision community. Most deepfake detection methods rely on identity, facial attributes, and adversarial perturbation-based spatio-temporal modifications at the whole video or random locations while keeping the meaning of the content intact. However, a sophisticated deepfake may contain only a small segment of video/audio manipulation, through which the meaning of the content can be, for example, completely inverted from a sentiment perspective. We introduce a content-driven audio-visual deepfake dataset, termed Localized Audio Visual DeepFake (LAV-DF), explicitly designed for the task of learning temporal forgery localization. Specifically, the content-driven audio-visual manipulations are performed strategically to change the sentiment polarity of the whole video. Our baseline method for benchmarking the proposed dataset is a 3DCNN model, termed as Boundary Aware Temporal Forgery Detection (BA-TFD), which is guided via contrastive, boundary matching, and frame classification loss functions. Our extensive quantitative and qualitative analysis demonstrates the proposed method's strong performance for temporal forgery localization and deepfake detection tasks.</p>
61.	<p>Driveline system effects on powertrain mounting optimization for vibration isolation under actual vehicle conditions J Singh, AK Sarna, N Kumar... - SAE International Journal of Commercial Vehicles, 2023</p>

	<p>Abstract</p> <p>Vehicle vibration is the key consideration in the early stage of vehicle development. The most dynamic system in a vehicle is the powertrain system, which is a source of various frequency vibration inputs to the vehicle. Mostly for powertrain mounting system design, only the uncoupled powertrain system is considered. However, in real situations, other subsystems are also attached to the powertrain unit. Thereby, assuming only the powertrain unit ignores the dynamic interactions among the powertrain and other systems. To address this shortcoming, a coupled powertrain and driveline mounting system problem is formulated and examined. This 16 DOF problem is constructed around a case of a front engine-based powertrain unit attached to the driveline system, which as an assembly resting on other systems such as chassis, suspensions, axles, and tires. First, the effect of a driveline on torque roll axis and other rigid body modes decoupling is examined analytically in terms of eigensolutions and frequency responses. It is observed from the analysis that when the optimized uncoupled powertrain system is introduced in real vehicle conditions, the vibration isolation level of the powertrain mountings gets degraded. Then, a new improved approach of considering coupled powertrain and driveline systems in the initial design phase itself is proposed. The mounting system parameters such as mount location, mount orientation angle, and stiffness rate are optimized and redesigned for the proposed system. The results of the redesigned system show that the decoupling of the rigid body mode parameters is improved and consequently powertrain vibration performance is also improved in static and dynamic conditions of the vehicle. Overall, the findings of this study suggest that considering the driveline along with the powertrain as a coupled system at the early phase of the mounting system design itself improves the vibration performance of the vehicle during real-life situations.</p>
62.	<p>DSM-IDM-YOLO: Depth-wise separable module and inception depth-wise module based YOLO for pedestrian detection S Panigrahi, USN Raju - International Journal on Artificial Intelligence Tools, 2023</p> <p>Abstract</p> <p>Pedestrian detection is one of the most challenging research areas in computer vision. Compared to traditional hand-crafted methods, convolutional neural networks (CNNs) have superior detection results. The single-stage detection networks, particularly the state-of-The-Art You Only Look Once (YOLO) network, have attained a satisfactory performance without compromising the computation speed in object detection. YOLO framework can be leveraged in pedestrian detection as well. In this work, we propose an improved YOLOv2, called DSM-IDM-YOLO. The proposed model uses a modified DarkNet19 integrated with three new modules, two depth-wise separable convolution modules and one inception depth-wise convolution module, leading to a comprehensive feature of an object in the image. The modules are integrated on top of features from multiple levels of the network. The proposed framework is computationally less expensive owing to its convolution design and a moderate number of layers. It aims to improve performance with minimal computational overhead. The proposed method is compared with state-of-The-Art detection methods, i.e., Faster R-CNN, YOLOv2, YOLOv3, YOLOv4-Tiny and Single Shot Multibox Detector (SSD). The performance results attest that the proposed method has effectively improved the detection. Three benchmark pedestrian datasets are used for experimental analysis: INRIA, PASCAL VOC 2012 and Caltech.</p>
63.	<p>edAttack: Hardware trojan attack on on-chip packet compression A Kumar, D Deb, S Das... - IEEE Design & Test, 2023</p> <p>Abstract</p> <p>Modern MultiProcessor System-on-Chip (MPSoC) designs use third-party intellectual property (IP) to reduce design costs and meet deadlines. In a Network-on-Chip (NoC)-based MPSoC, most NoC components that connect multiple IPs, are third-party IPs. NoC carries cache misses</p>

	<p>and cache blocks as request-reply packets. Since reply packets may contain repetitive data patterns, compressing them reduces latency and energy consumption. Nevertheless, some IPs in NoC may contain Hardware Trojans (HT). While researchers investigated the possibility of HTs in NoC routing protocols and Network Interfaces (NIs), this work investigates the prospect of a new HT in NoC routers, or NIs, that targets on-chip packet compression techniques.</p>
64.	<p>Electrochemical production of hydrogen from hydrogen sulfide using cobalt cadmium sulfide K Garg, M Kumar, S Kaur...T C Nagaiah... - ACS Applied Materials & Interfaces, 2023</p> <p>Abstract The electrocatalytic decomposition of H₂S is a promising technology for H₂ production as well as for targeting environmental pollution. But due to the lack of low-cost and efficient electrocatalysts, this technology for H₂ production is not being explored much. Moreover, the highly toxic and copious waste H₂S released from industries is rarely encountered in the scientific domain. Herein, we have designed a highly efficient electrocatalyst, i.e., CoCd(x:y)Sn, as an anode catalyst for sulfide oxidation reaction (SOR). This optimized catalyst could drive the anode reaction at an onset potential of 0.25 V vs reversible hydrogen electrode (RHE), which was 1.27 V lower than that required for the water oxidation reaction. Moreover, we have achieved 98% H₂ Faradaic efficiency with remarkable stability of 120 h. Thus, this method paves a path to high-value utilization of hazardous waste H₂S and demonstrates its great potential for hydrogen production and sulfur toward sustainable energy applications.</p>
65.	<p>Electrochemical synthesis and reactivity of three-membered strained carbo- and heterocycles R Kumar, N Banerjee, P Kumar, P Banerjee - Chemistry: A European Journal, 2023</p> <p>Abstract Three-membered carbocyclic- and heterocyclic ring structures are versatile synthetic building blocks in organic synthesis owing to their biological importance. Also, the inherent strain of these three-membered rings led to their ring-opening functionalization via C-C, C-N, and C-O bond cleavage. Traditional synthesis and ring-opening methods of these molecules require the usage of acid catalysts or transition-metals. Recently, electroorganic synthesis has emerged as a powerful tool for initiating new chemical transformations. In this review, the synthetic and mechanistic aspects of electro-mediated synthesis and ring-opening functionalization of three-membered carbo- and heterocycles are highlighted.</p>
66.	<p>EMG based clinical evaluation of an unpowered exoskeleton device RS Halder, B Basumatary, A Pandya...AK Sahani - 2023 IEEE International Symposium on Medical Measurements and Applications, (MeMeA), 2023</p> <p>Abstract This paper reports a clinical study to characterize reduction in load on the major muscles of the back by use of an unpowered, lightweight, protective and therapeutic exoskeleton device named JaipurBelt that supports the spine and waist. Seventy nine subjects underwent Institutional Ethical Committee approved clinical trial at Santokba Durlabhji Memorial Hospital (SDMH), Jaipur, India. The protocols used for this study incorporate without device without load (WOJBWOL), without device with load (WOJBWL), with device without load at a medium level of support (WJBMidWOL), with device with load at a medium level of support (WJBMidWL), with device with load at a maximum level of support (WJBMaxWL). The EMG was recorded from six major back muscles. The result showed that, average reduction of muscle activity in all six muscles for Stoop Bending Up (SBU) is about 7.62%, and for Stoop Bending Down (SBD) is about 12.19% in without load condition. In with load condition and maximum level of support (WJBMaxWL), the overall maximum reduction of muscle activity was 80.97% for Ninth Thoracic Vertebra of Erector Spine (EST9), 44.39% for Fourth Lumbar Vertebra of Erector Spine (ESL4), 24.62% for Multifidus (MF), 10.18% for Quadratus Lumborum (QL), 37.54% for Gluteus maximus (GM), 40.23% for Rectus Femoris (RF). In this clinical study, with</p>

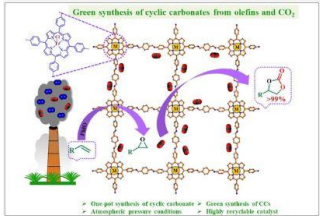
	<p>the use of this unpowered exoskeleton device, it was found that there is a substantial reduction in muscle force requirements for load lifting, frequent bending ups, bending down and stooping activities by reducing the load from back and abdominal muscles. Thus, use of this device can potentially helps in reducing the risk of lower back disorders, fatigue, musculoskeletal problems, spinal disorders like slip disc and associated pain. This study was conducted after registration with Central trial register of India (CTRI registration number CTRI/2017/01/007649dtd 16/01/2017).</p>
67.	<p>Energy aid volatility across developing countries: a disaggregated sectoral analysis P Jain, S. Bardhan - <i>International Economics and Economic Policy</i>, 2023</p> <p>Abstract Empirical evidence on general aid volatility reveals that it is a limiting factor that impedes aid effectiveness. Unlike the previous studies focusing on aggregate aid volatility, this paper seeks to analyze the energy aid volatility across sub-sectors of energy aid in 67 aid-recipient countries during 2002–2019, given that energy aid effectiveness is essential for achieving the targets of sustainable development goals (SDG)-7. Specifically, we examine the contribution of different sub-sectors of energy aid in total energy aid volatility, identify sectoral volatility trends, and explore the interlinkages between the aid shocks of various sectors of energy aid. Volatility measures are based on the squared residuals obtained from a regression of aid on trend and the trend square, calculated separately for each country and energy aid sector. Findings reveal that renewable aid is the most important contributor to total energy aid volatility, particularly in lower-middle-income countries. Policy aid volatility is highest in low-income countries. We hardly observe a decline in the volatility of energy aid and its sub-sectors, except for nuclear aid. Moreover, we notice a lack of sectoral greening of energy aid as donors do not shift disbursement targets from non-renewable to renewable energy generation sources. From a policy perspective, these findings suggest that donors and recipients need to work on reducing energy aid volatility by focusing on specific energy aid sectors that majorly cause volatility to enhance energy aid effectiveness. Findings also call for understanding the factors that inhibit the greening of energy aid in terms of shifting concession resources from non-renewable to renewable energy generation.</p>
68.	<p>Energy-absorbing characteristics of an ABS-M30i-based 3D-printed periodic surface and strut-based lattice structure AI Ansari, NA Sheikh, N Kumar - <i>Journal of The Institution of Engineers (India): Series C</i>, 2023</p> <p>Abstract High permeable sandwich structure (foam) or scaffolds are prerequisites in the field of Biomedical, Aerospace, and Automotive sector, due to its energy-absorbing characteristics and tissue formation or cell generation properties. The architecture was previously distant to manufacture but is now feasible, thanks to Additive manufacturing methodology or 3D-printing technology. Fused deposition technology is a method of 3D printing to fabricate the complex shapes and prototypes for large-scale real-world applications. The purpose of this study is to use theoretical and experimental methods to compare the structural strength of three distinct lattice designs at 0.001 S-1 strain rates. The body centered cubic (BCC), Schwarz primitive (TPMS based Design), and simple cubic-double ring lattice (SC-DRL) are investigated using a combination of mechanical compressive testing and finite element analysis (FEA). We evaluate the stress–strain graph, elastic modules, breakdown strengths, deformation methods, and predicted stress distributions of these lattice configurations under compressive pressure force, as well as to assess the structure for load capacity behavior at post-yielding phases depending on its lattice design to accurately represent the behaviors of 3D-printed polymeric crystal lattice structure composed of Acrylonitrile Butadiene Styrene (ABS-M30i) material. The Finite Element Analysis models</p>

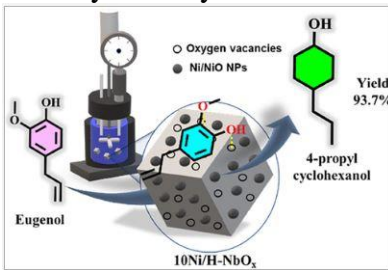
	<p>are designed to describe the compressive deformation performance of three distinct lattices. Such simulations are employed to realize as well as deliver accurate data on failure causes as well as the interaction between the different layers for the compressive deformations and lattice architectures. The influence of three distinct lattice models on the experimental mechanical performance of ABS-M30i specimens produced using FDM, each with a different porosity and structural design, are explored in this research. The finding shows that the finite element analysis derived compressive behavior closely fits the experimental results, as well as the structural behavior, that the strain and plastic dissipation energy are not distributed uniformly throughout each layer.</p>
69.	<p>Environmental impact assessment: A case study of construction of metro rail Nagpur, Maharashtra (India) BR Ambade, CB Ambade - SSRG International Journal of Recent Engineering Science, 2023</p> <p>Abstract In recent years, the metro rail system implemented in major Indian cities has contributed to major changes in the country's transportation infrastructure and intra-city connectivity. Nagpur is Maharashtra's third-largest city and the state's winter capital. From March to April 2018, the environmental impact assessment of metro rail construction on five squares in Nagpur city was conducted. Portable Air Quality Detectors were used to research the PM 1, PM 2.5, PM 10, API Index, HCHO and TVOC variants. Other impacts are analyzed in a 100 m radius, such as vibration, traffic congestion, injuries, water use, vibration and noise pollution. In order to minimize these impacts during the implementation of the project, remedial steps are recommended.</p>
70.	<p>EWSmethods: an R package to forecast tipping points at the community level using early warning signals, resilience measures, and machine learning models DA O'Brien, S Deb, S Sidheekh....PS Dutta... - Ecography, 2023</p> <p>Abstract Early warning signals (EWSs) represent a potentially universal tool for identifying whether a system is approaching a tipping point, and have been applied in fields including ecology, epidemiology, economics, and physics. This potential universality has led to the development of a suite of computational approaches aimed at improving the reliability of these methods. Classic methods based on univariate data have a long history of use, but recent theoretical advances have expanded EWSs to multivariate datasets, particularly relevant given advancements in remote sensing. More recently, novel machine learning approaches have been developed but have not been made accessible in the R (www.r-project.org) environment. Here, we present EWSmethods – an R package (www.r-project.org) that provides a unified syntax and interpretation of the most popular and cutting edge EWSs methods applicable to both univariate and multivariate time series. EWSmethods provides two primary functions for univariate and multivariate systems respectively, with two forms of calculation available for each: classical rolling window time series analysis, and the more robust expanding window. It also provides an interface to the Python machine learning model EWSNet which predicts the probability of a sudden tipping point or a smooth transition, the first of its form available to R (www.r-project.org) users. This note details the rationale for this open-source package and delivers an introduction to its functionality for assessing resilience. We have also provided vignettes and an external website to act as further tutorials and FAQs.</p>
71.	<p>Exclusive mass-energy distributions of the fast fission fragments in the 40Ca+144 Sm reaction EM Kozulin, AA Bogachev, GN Knyazheva... PP Singh... - Physics of Atomic Nuclei, 2023</p> <p>Abstract The dependence of the properties of the fission fragments formed both in the fusion-fission and fast fission processes on the angular momentum still remains very unclear from an experimental as well as theoretical point of view. To study the properties of fast fission fragments of preactinide nuclei as function of the interaction energy and introduced angular momentum, the mass-energy distributions of 184184Pb fission fragments formed in the 40Ca+14440Ca+144Sm</p>

	<p>reaction at energies above the Coulomb barrier have been measured using the double-arm time-of-flight spectrometer CORSET at the ^{40}Ca ions' energies of 212, 231, 244, and 277 MeV. The mass-energy distributions of the fast fission fragments have been extracted by subtracting the mass-energy matrices corresponding to the compound nucleus fission from those of all measured fissionlike events. The asymmetric fragments with masses 76 and 108 u were found to be the most probable in the fast fission of ^{184}Pb. With increasing ^{40}Ca energy from 231 to 277 MeV the mass distributions of fast fission fragments change weakly, whereas an increase in the TKE is about 20 MeV. The properties found for the fast fission fragments indicate the incomplete mass relaxation and not full energy dissipation.</p>
72.	<p>Experimental investigation on slow thermal pyrolysis of real-world plastic wastes in a fixed bed reactor to obtain aromatic rich fuel grade liquid oil Subhashini, T Mondal - Journal of Environmental Management, 2023</p> <p>Abstract Plastic wastes have become one of the biggest global environmental issues and thus recycling such massive quantities is targeted. Thermal pyrolysis has been the most suitable approach to convert the waste plastic into a source of energy. This study aims to compare the thermal pyrolysis of waste plastic with that of the modal plastic compounds in a fixed bed reactor. The liquid oil, obtained from the thermal pyrolysis of HDPE, LDPE, PP and PS wastes were characterized using FT-IR, GC-MS and ^1H NMR. Also, their fuel properties such as viscosity and calorific values were characterized using parallel plate rheometer and bomb calorimeter respectively. $\text{C}_{10}\text{--C}_{44}$ paraffins and $\text{C}_{10}\text{--C}_{22}$ olefins were obtained along with aromatics and alcohols in different type of plastic waste pyrolysis oil. The viscosity of the plastic oil is within kerosene and diesel range. The calorific values of the oils are at par with the Petro fuels.</p>
73.	<p>Experimental study on laser bending of mild steel with buckling mechanism R Yadav, R Yadav, R Kant - Optics & Laser Technology, 2023</p> <p>Abstract Laser bending has emerged as a promising technique for shaping metallic sheets with high precision and flexibility. However, the traditional temperature gradient mechanism (TGM) of laser bending faces limitations in achieving large bend angle especially for low-thickness and high-conductive sheets. The buckling mechanism (BM) has the potential to overcome this limitation, as it does not require a high temperature gradient. Despite this potential, the BM has not been widely explored experimentally. In this study, the BM is comprehensively investigated, and analyzed the effect of laser power, scanning speed, worksheet width and laser beam diameter on bend angle, top surface temperature, and mechanical and metallurgical properties. It is found that the bend angle first increases and then decreases with the increase in laser power and scanning speed, while it increases with worksheet width and laser beam diameter. The top surface temperature increases with the number of scans and decreases with beam diameter and worksheet width. Furthermore, the BM results in grain refinement within the scanned region, and improvements in tensile strength and hardness, albeit at a reduction in ductility. The bend angle achieved with BM is found to be 100% greater than TGM. The results of this study demonstrate the potential of the BM for high-precision manufacturing applications.</p>
74.	<p>Experiments and geochemical modelling of arsenic interaction with clay-dominated soil from Rupnagar district of Punjab, India H Nazir, VA Loganathan - Water Security, 2023</p> <p>Abstract The present study investigates the interaction of the soil in Garhbagha village, located in the Rupnagar district of Punjab, India for As(V) adsorption under the influence of pH, contact time</p>

	<p>and varying arsenic concentrations. To understand the geochemical controls of arsenic mobilization in the region, batch sorption experiments were performed using soil obtained from arsenic contaminated district of Punjab. This study presents a novel approach by employing surface complexation models (SCMs) to investigate arsenic adsorption onto natural soils in the Punjab region, which has not been explored in previous literature. Furthermore, a comparison between Fe-based models, assuming ferrihydrite binding, and general composite (GC) approach, assuming adsorption on soil component surfaces, has not been conducted before, adding to the originality of this research. The adsorption kinetic experiment indicates about 70% adsorption of As(V) in about 4 h. The results of batch isotherm experiment shows that As(V) adsorption saturation onto the soil is reached at an aqueous concentration of about 0.89 mgL^{-1}. The results of the pH edges study shows a maximum As(V) adsorption of 93.88% at a pH of 4. The Langmuir's isotherm was the best fitted because the value of linear regression coefficient ($R^2 = 0.997$) which verifies the monolayer adsorption of As(V). It was observed that the pseudo first order model best fitted for explaining the kinetic of As(V) adsorption onto the soil because it showed higher value of linear regression coefficient ($R^2 = 0.995$). Further, three different diffused layer models under varied assumptions were used to capture the batch experimental results. The surface complexation model with general-composite (GC) approach fairly predicted the experimental results when compared to Fe-oxide based models. The GC model was able to capture the observed experimental results for adsorption isotherm and pH edges for the soil within reasonable RMSE of 6.22 % and 7.97 %, respectively.</p>
75.	<p>Explainable image classification: The journey so far and the road ahead K Vidhya, CK Narananan - AI, 2023</p> <p>Abstract Explainable Artificial Intelligence (XAI) has emerged as a crucial research area to address the interpretability challenges posed by complex machine learning models. In this survey paper, we provide a comprehensive analysis of existing approaches in the field of XAI, focusing on the tradeoff between model accuracy and interpretability. Motivated by the need to address this tradeoff, we conduct an extensive review of the literature, presenting a multi-view taxonomy that offers a new perspective on XAI methodologies. We analyze various sub-categories of XAI methods, considering their strengths, weaknesses, and practical challenges. Moreover, we explore causal relationships in model explanations and discuss approaches dedicated to explaining cross-domain classifiers. The latter is particularly important in scenarios where training and test data are sampled from different distributions. Drawing insights from our analysis, we propose future research directions, including exploring explainable allied learning paradigms, developing evaluation metrics for both traditionally trained and allied learning-based classifiers, and applying neural architectural search techniques to minimize the accuracy–interpretability tradeoff. This survey paper provides a comprehensive overview of the state-of-the-art in XAI, serving as a valuable resource for researchers and practitioners interested in understanding and advancing the field.</p>
76.	<p>External electric field modulation of single-layer MoSe₂ electronic and optical properties: A first-principles investigation A Chafai, M Behloul, I Essaoudi, R Ahuja... - Micro and Nanostructures, 2023</p> <p>Abstract A wisely applied external electric field could effectively develop the optoelectronic properties of single-layer materials. The optical and electronic characteristics of monolayer molybdenum diselenide (ML-MoSe₂) are deeply studied by means of density functional computations (DFT) to pinpoint the effect of the out-of-plane applied electric field (F//Oz). In fact, variations in the applied electric field strength gradually increase the energy of the electronic band gap (E_g) from 1.44 eV at $0\text{V}/\text{\AA}$ to 1.51 eV at $\pm 0.6\text{V}/\text{\AA}$. We also probed a sharp drop in the energy gap at high intensities. However, dielectric function, reflectivity, and loss function are studied for</p>

	<p>unpolarized and polarized incident light. Interestingly, the 001-polarization of the incident light affects the dielectric function's magnitude and position; this effect is more emphasized in the presence of an electric field with positive strengths. Furthermore, we found that the applied negative/positive electric field enhances the UV–visible reflectivity. Also, blue shifts of the ML-MoSe₂ optical properties spectrum appear when subjected to the 001-polarized incident light. However, the loss function exhibits a weak response to the applied F. Additionally, we obtain that the 001-light polarization improves a plasmonic peak around 100 nm. Our results will provide a new view to understanding the controllable optical and electronic properties of MoSe₂ monolayer, which is valuable for the design of new optoelectronic and plasmonic devices under development.</p>
77.	<p>Fast deterministic gathering with detection on arbitrary graphs: The power of many robots AR Molla, K Mondal, WK Moses - 2023 IEEE International Parallel and Distributed Processing Symposium (IPDPS 2023), 2023</p> <p>Abstract Over the years, much research involving mobile computational entities has been performed. From modeling actual microscopic (and smaller) robots, to modeling software processes on a network, many important problems have been studied in this context. Gathering is one such fundamental problem in this area. The problem of gathering k robots, initially arbitrarily placed on the nodes of an n-node graph, asks that these robots coordinate and communicate in a local manner, as opposed to global, to move around the graph, find each other, and settle down on a single node as fast as possible. A more difficult problem to solve is gathering with detection, where once the robots gather, they must subsequently realize that gathering has occurred and then terminate. In this paper, we propose a deterministic approach to solve gathering with detection for any arbitrary connected graph that is faster than existing deterministic solutions for even just gathering (without the requirement of detection) for arbitrary graphs. In contrast to earlier work on gathering, it leverages the fact that there are more robots present in the system to achieve gathering with detection faster than those previous papers that focused on just gathering. The state of the art solution for deterministic gathering [Ta-Shma and Zwick, TALG, 2014] takes (Equation Presented) rounds, where is the smallest label among robots and hides a polylog factor. We design a deterministic algorithm for gathering with detection with the following trade-offs depending on how many robots are present: (i) when $k \geq$ (Equation Presented), the algorithm takes $O(n^3)$ rounds, (ii) when $k \geq$ (Equation Presented), the algorithm takes $O(n^4 \log n)$ rounds, and (iii) otherwise, the algorithm takes (Equation Presented) rounds. The algorithm is not required to know k, but only n.</p>
78.	<p>Fatigue life estimation of TMT reinforcing steel bar considering pitting corrosion and high temperature impacted surface topography S Chauhan, S Muthulingam - International Journal of Fatigue, 2023</p> <p>Abstract Surface topography of steel changes considerably when subjected to pitting corrosion and high temperature leading to a reduction in its fatigue life. Based on experiments, including microstructural studies and employing multiple linear regression methods, prediction models for surface topographic feature parameters such as arithmetic mean height, total height, ten-point height, profile mean spacing as a function of pitting severity, corrosion level severity, and temperature are developed. Using identical parameters, prediction models for surface topographic feature variable in stress concentration factor and defect size parameter are also developed. Further, a framework for estimating high-cycle fatigue life is proposed, incorporating the developed models. The proposed framework is validated by comparing the fatigue life estimated by incorporating the developed models with experimental data from the literature.</p>
79.	<p>Fault ride through with conformance to grid voltage limits in photovoltaic grid connected inverters</p>

	<p>AH Lone, AI Gedam, KR Sekhar - 2023 IEEE IAS Global Conference on Emerging Technologies (GlobConET), 2023</p> <p>Abstract</p> <p>Short-duration voltage sags and swells are common in utility grids. This can activate the over-voltage/under-voltage protection relays in grid-connected solar inverters, thus disconnecting them from the main grid. This rapid separation might trigger a catastrophic voltage breakdown in utility networks with a substantial proportion of energy originating from solar power plants. Furthermore, the ensuing power imbalance might cause frequency or angular instability in the main grid. This paper presents a control technique capable of accomplishing both high voltage ride through (HVRT) and low voltage ride through (LVRT) in grid-connected solar inverters. When voltage sags occur, the provided control technique boosts the terminal voltage to meet the utility-regulated voltage restrictions. In the event of a voltage surge, the control technique decreases the terminal voltage to meet the utility's voltage limitations. The conformance to utility set voltage band can be achieved only in case of photovoltaic power plants with large power rating. The control given also decreases the voltage imbalance factor to the grid norms. This reduces the double frequency power flow oscillations in the inverter. The inverter's remaining power capacity is used to support the grid for real power. The inverter is used to its full apparent power capacity. These multiple fault ride through objectives are met while adhering to the inverter's maximum current capacity restriction. The control technique is evaluated for various voltage sags and swells in the Matlab/Simulink environment. This paper presents the findings.</p>
80.	<p>Fe(III)-anchored porphyrin-based nanoporous covalent organic frameworks for green synthesis of cyclic carbonates from olefins and CO₂ under atmospheric pressure conditions G Singh, K Prakash, CM Nagaraja - Inorganic Chemistry, 2023</p> <p>Abstract</p> <p>The utilization of carbon dioxide (CO₂) as a C1 source coupled with olefins, readily accessible feedstocks, offers dual advantages of mitigating atmospheric carbon dioxide and green synthesis of valuable chemicals. In this regard, herein we demonstrate the application of Fe(III)-anchored porphyrin-based covalent organic framework (P-COF) as a promising recyclable catalyst for one-step generation of cyclic carbonates (CCs), value-added commodity chemicals from olefins and CO₂, under mild atmospheric pressure conditions. Moreover, this one-pot synthesis was applied to transform various olefins (aliphatic and aromatic) into the corresponding CCs in good yield and selectivity. In addition, the Fe(III)@P-COF showed good recyclability and durability for multiple reuse cycles without losing its catalytic activity. Notably, this one-step synthesis strategy presents an eco-friendly, atom-economic alternative to the conventional two-step process requiring epoxides. This work represents a rare demonstration of porphyrin COF-catalyzed one-pot CC synthesis by utilizing readily available olefins at atmospheric pressure of carbon dioxide.</p> 
81.	<p>Finding analog/RF performance of inserted high-K FinFET for Sub-5 nm technology node A Goel, A Rawat, B Rawat - 2022 IEEE International Conference on Emerging Electronic (ICEE 2022), 2022</p> <p>Abstract</p>

	<p>In this paper, the analog/RF performance of an emerging inserted-oxide FinFET (i-FinFET) is being explored and benchmarked with their counterparts nanosheet field-effect transistor (NS-FET) and FinFET for sub-5 nm technology node using a fully calibrated three-dimensional (3-D) technology computer-aided design (TCAD) simulation. The three-channel stacked i-FinFET exhibits the cut-off frequency (f_T)/ maximum oscillation frequency (f_{max}) of around 275/203 GHz at fixed I_{ON} of 0.25 mA/μm, which is nearly 1.54 x higher than that for NS-FET and FinFET. To gain insight into the practical i-FinFET, we investigate the f_T/f_{max} optimization by varying the technology node, spacer material, and channel stacking number. Since 3 nm technology node FinFET have successfully scaled to production for analog/RF design, the extension to i-FinFET for beyond 3 nm technology node could help in realizing high frequency/low power RF and SoC circuits.</p>
82.	<p>Fine-tuning of Ni/NiO over H-NbO_x for enhanced eugenol hydrogenation through enhanced oxygen vacancies and synergistic participation of active sites G S More, BP Singh, R Bal...R Srivastava - <i>Inorganic Chemistry</i>, 2023</p> <p>Abstract The hydrogenation of lignin-derived phenolics to produce valuable chemicals is a promising but challenging task. This study successfully demonstrates the use of sustainable transition metal-based catalysts to hydrogenate lignin-derived phenolics. A defect-induced oxygen vacancy containing H-NbO_x prepared from commercial Nb₂O₅ was employed as a catalyst. H-NbO_x exhibited higher oxygen vacancies (158.21 μmol/g) than commercial Nb₂O₅ (39.01 μmol/g), evaluated from O₂-TPD. Upon supporting 10 wt % Ni, a Ni/NiO interface was formed over H-NbO_x, which was intrinsically active for the hydrogenation of phenolics. 10Ni/H-NbO_x exhibited a two-fold increase in activity than 10Ni/Nb₂O₅, achieving >99% eugenol conversion and affording ~94% 4-propyl cyclohexanol selectivity, wherein ~63% eugenol conversion and ~73% 4-propyl cyclohexanol selectivity were obtained over 10Ni/Nb₂O₅. The Ni/NiO formation was confirmed by X-ray photoelectron spectroscopy, HR-TEM, and H₂-TPR analysis, while the oxygen vacancies were verified by Raman spectroscopy and O₂-TPD analysis. The resulting interface enhanced the synergy between Ni and H-NbO_x and facilitated hydrogen dissociation, confirmed by H₂-TPD. Remarkably, 10Ni/H-NbO_x maintained its catalytic activity for five tested cycles and demonstrated exceptional activity with various phenolics. Our findings highlight the potential of a sustainable transition metal catalyst for the hydrogenation of lignin-derived phenolic compounds, which could pave the path to producing valuable chemicals in an environmentally friendly manner.</p> 
83.	<p>First examples of room-temperature discotic nematic liquid crystals exhibiting ambipolar charge carrier mobilities M Gupta, Krishna KM Abhinand, S Sony... - <i>Chemical Communications</i>, 2023</p> <p>Abstract Four new room-temperature nematic liquid-crystalline (LC) dimers consisting of a wedge-shaped 3,4,5-tridecyloxy gallic ester molecule linked to either cyanobiphenyl, cholesteryl, pentaalkynylbenzene or triphenylene based moieties are reported. Dimers with pentaalkynylbenzene and triphenylene moieties in their room-temperature discotic nematic (N_D) mesophase show ambipolar charge carrier mobilities of the order of 10⁻⁵ cm² V⁻¹ s⁻¹ and</p>

	$10^{-3} \text{ cm}^2 \text{ V}^{-1} \text{ s}^{-1}$, respectively, as measured using a time-of-flight (ToF) technique.
84.	<p>First-principles calculations to investigate the dielectric and optical anisotropy in two-dimensional monolayer calcium and magnesium difluorides in the vacuum ultraviolet V Kumar, RK Mishra, H Jeon...R Ahuja - Journal of Physics and Chemistry of Solids, 2023</p> <p>Abstract Anisotropic dielectric and optical properties of two-dimensional (2D) calcium and magnesium difluorides were investigated in the vacuum ultraviolet (VUV) region of the electromagnetic spectrum (EM) using the first principles density functional theory (DFT). The anisotropy between the in-plane and out-of-plane directions shows that these materials are uniaxial, exhibiting optical and dielectric anisotropy. The optical functions of these anisotropic materials- optical absorption, photoconductivity, refractive index, reflection and extinction coefficients, and electron energy loss (EEL) spectra-are calculated in the framework of DFT. The low refractive index values and relatively small extinction coefficient make these materials alternative low-index 2D materials for the long wavelengths in the VUV region of the EM spectrum. The reflection and transmission spectra indicate the antireflective property of these materials. The calculated EEL function shows less energy loss of fast-traveling electrons in the material's medium. The maxima in the EEL spectrum are the main feature of plasma oscillations. The dissipation in the incident light radiation energy propagating through the dielectric medium is estimated with the dielectric loss tangent ($\tan\delta$). The magnesium difluoride is identified as a less dielectric loss medium than calcium difluoride in the VUV region. The present results suggest that these 2D materials are promising in low refractive index, high reflective, and antireflective coating materials in optoelectronic device applications. Also, electronic studies revealed that these are excellent materials for gate insulators in field-effect transistors based on 2D electronic materials.</p>
85.	<p>First-principles insights into the optical and electronic characteristics of barium intercalated AB-stacked bilayer grapheme A Chafai, L Bouziani, S Bouhou...R Ahuja... - The European Physical Journal Plus, 2023</p> <p>Abstract The present study describes the electronic and optical characteristics of barium atoms (an alkaline earth metal) intercalated within AB-stacked bilayer graphene (AB-2LG). Using state-of-the-art first-principles computations and taking into account the dispersion forces between the diverse nanosheets, we determined that the intercalation of barium atoms (Ba) into AB-2LG increases the interlayer distance from 3.357 to 5.584 Å, and no C–Ba bond formation has been observed. In addition, our findings reveal that the presence of Ba atoms inside the AB-2LG induces a change in the Space group number from 164 (pure AB-2LG) to 156 (Ba-intercalated AB-2LG). Concurrently, we observed that the AB-2LG band structure exhibits a Dirac cone at the K-point, which is a characteristic signature of a semi-metallic character. By contrast, the electronic behavior of the barium-intercalated AB-2LG is found to be metallic. Also, we noticed that the confinement of Ba atoms into the AB-2LG shifts the Dirac point under the Fermi level. Additionally, upon examining the optical properties under the 001 and 100-polarization of the incident light, we found that all optical parameters of both under-investigated bidimensional materials exhibit an anisotropic character. Interestingly, under the 001-polarization, we observed that the intercalation of AB-2LG with Ba atoms reduces the optical absorption to zero in the visible region, and blueshifts are the absorption peak observed in the infrared region. Furthermore, in the case of 001-polarization, the presence of Ba atoms enhances the optical absorption in the 7–9 eV spectral range. However, the obtained data exhibit a remarkable decrease in the refractive index after the Ba intercalation process, for both considered polarization directions.</p>
86.	Flow instability in Buoyancy-Assisted and opposed flows through a vertical pipeline in the laminar regime of mixed convection- a numerical study

	<p>S Gorai, D Samanta, S K Das - 8th Thermal and Fluids Engineering Conference (TFEC), 2023</p> <p>Abstract</p> <p>A detailed numerical investigation on laminar mixed convection has been carried out to understand the flow instability in buoyancy-aiding and buoyancy-opposing flows through a vertical pipe subjected to uniform heat flux. Two-dimensional axisymmetric steady simulations are performed with the available commercial software for aiding as well as opposing flows of water through a vertical pipe of length to diameter ratio of 500. The structured grids used for the simulation such that; it is uniform in axial and non-uniform in radial direction. The effects of Reynolds number ($100 \leq Re \leq 2300$) and Grashof number ($10^3 \leq Gr \leq 1.19 \times 10^7$) on heat transfer and fluid flow are analysed by employing SIMPLE algorithm for solving pressure-velocity coupling and second order UPWIND scheme for solving momentum and various energy equations. The Boussinesq approximation has been considered for the analysis. The Richardson number (Ri) varies from 0.1 to 1.5 for the present range of Re and Gr. Results show that the heat transfer increases in case of buoyancy-assisting flow as compared to buoyancy-opposing flow for same Ri. It is inferred from the velocity profile and skin friction coefficient (C_f) plots that the pressure drop is more in case of opposing flow as that of aiding flow. An increase in heat flux advances the transition from laminar to turbulent in opposing flows whereas it delays in aiding flows. The point of inflection in aiding flows and the flow separation from the wall in opposing flows have been observed with further increase of Ri which ensures the presence of flow instability.</p>
87.	<p>Flow-switching and mixing phenomena in electroosmotic flows of viscoelastic fluids MB Khan, F Hamid, N Ali...C Sasmal... - Physics of Fluids, 2023</p> <p>Abstract</p> <p>The present study uses numerical simulations and experiments to investigate the electroosmotic flows of viscoelastic fluids through a microchannel containing a cylindrical obstacle. As the electric field strength gradually increases, the flow dynamics within this microfluidic setup becomes chaotic and fluctuating. Notably, numerical simulations reveal a flow-switching phenomenon in viscoelastic fluids when the applied electric field strength exceeds a critical value, which is absent in simple Newtonian fluids under identical conditions. Corresponding experiments confirm these observations. Additionally, this study demonstrates the successful mixing of two viscoelastic fluids using the flow-switching phenomenon within the present microfluidic setup. To gain insight into the dynamics of coherent flow structures arising from the flow-switching phenomenon and their impact on the mixing process, data-driven dynamic mode decomposition (DMD) analysis is employed. Importantly, the DMD analysis uncovers the presence of upstream elastic instability, which is not discernible through traditional velocity or concentration field plots. Overall, this study aims to advance our understanding of the electrokinetic flow behavior of viscoelastic fluids in complex systems like porous media. Furthermore, it proposes a relatively simple and fabricable microfluidic technique for efficiently mixing viscoelastic fluids.</p>
88.	<p>Forward and inverse optimization of a solar or waste heat operated modified Goswami cycle A Singh, R Das - 5th International Conference on Energy, Power and Environment: Towards Flexible Green Energy Technologies (ICEPE), 2023</p> <p>Abstract</p> <p>A modified Goswami cycle (MGC) is presented when it is operated in multigenerational mode through solar/waste heat input. For this, the conventional Goswami cycle (CGC) is transformed by adding supplementary refrigeration and heating assembly to its existing configuration. The arrangement of the refrigeration assembly is similar to that of the conventional absorption refrigeration cycle with an exception that the refrigerant vapor is generated from the hot liquid condensate of the CGC through flashing process. The heating facilities utilize the waste heat</p>

	<p>outputs of the refrigeration assembly for both preheating the basic solution and producing hot water. For the optimization of MGC, first different standalone energy (turbine power, sensible cooling output, latent cooling output and heating output) and exergy based objectives are formulated, which are solved by dragonfly algorithm. It is seen that there is no single standalone objective which generates maximum possible exergy efficiency of 27.39% and also have overall exergy destruction close to 88.97 kW (minimum possible value). So, these standalone objectives are clubbed to form two equally weighted forward and inverse objective functions, which are also minimized by dragonfly algorithm. The results show that the value of exergy efficiency for the forward (28.05%) and inverse (28.43%) based objectives are found to be higher than any of their standalone objective. Also, the overall exergy destruction for these forward (89.73 kW) and inverse (92.09 kW) based objectives are quite less than for the standalone case when exergy efficiency is 27.39 % (113.62 kW).</p>
89.	<p>Fractional poisson processes of order k and beyond N Gupta, A Kumar - Journal of Theoretical Probability, 2023</p> <p>Abstract In this article, we introduce fractional Poisson fields of order k in n-dimensional Euclidean space of positive real valued vectors. We also work on time-fractional Poisson process of order k, space-fractional Poisson processes of order k and a tempered version of time-space fractional Poisson processes of order k. We discuss generalized fractional Poisson processes of order k in terms of Bernstein functions. These processes are defined in terms of fractional compound Poisson processes. The time-fractional Poisson process of order k naturally generalizes the Poisson process and the Poisson process of order k to a heavy-tailed waiting-times counting process. The space-fractional Poisson process of order k allows on average an infinite number of arrivals in any interval. We derive the marginal probabilities governing difference–differential equations of the introduced processes. We also provide the Watanabe martingale characterization for some time-changed Poisson processes.</p>
90.	<p>From symbolic to agential: The evolution of natural representation in Indian eco-sensitive films RK Pankaj, D Rey – Quarterly Review of Film and Video, 2023</p> <p>Abstract The Indian eco-sensitive cinema from the 1990s to the post-millennial time shows a certain thematic mutation from Nature’s anthropocentric preservationism to agential assertion. In other words, this paper describes that the early Indian eco-sensitive cinema (canonized by the National Film Award for Environment Conservation/Preservation, starting from the early 1990s) was less about Nature itself, and more about the human characters’ vested interest in the preservation of the former, leading to a narrow, homocentric attempt to explain away the natural agency. However, in the post-millennial phase, through a series of multilingual films, we observe a more complex hybrid of anthropic decadence, super-natural myths and sylvan invasion along with a theme of fear and reverence: Nature is now alive, invading the lives of the urbane and the indigene alike, actively influencing/destabilising the anthropocentric vision of it by establishing a “metamorphic dynamism of nature with commingled wonder and horror”(Moreland 2018, 35). We also argue that this mutation is concurrent with the evolution of ecocritical philosophy. Both Glotfelty and Buell have argued that the 1990s inception of ecocriticism was marked by the treatment of Nature as a mystical ‘other’, in desperate need of preservation by the very entities that endangered it in the first place: humans. This, as predicted by the duo, would eventually change into a unique and empowered Natural representation, evoking a mix of reverence and disquiet from the anthropos: “fusion of domestic sphere, biological environment, and the sacred”(Buell 2011, 99). Divided into two parts, the paper first draws a parallel between the anthropic.</p>
91.	<p>Gallium oxide nanoparticle-loaded, quaternized Chitosan-oxidized sodium alginate hydrogels for treatment of bacteria-infected wounds</p>

	<p>D Negi, Y Singh - ACS Applied Nano Materials, 2023</p> <p>Abstract</p> <p>Delayed wound healing usually involves bacterial infection and hemorrhage. Antibiotic resistance and biofilm formation caused by the overuse and misuse of antibiotics further worsen the problem. Nanoparticle hydrogel systems aimed at controlling hemorrhage and bacterial infection, without the chances of developing resistance, have recently generated significant research interest as efficient wound dressings. In this work, we have developed a multifunctional, β-Ga₂O₃ nanoparticle-loaded quaternized chitosan-oxidized sodium alginate hydrogels for antibacterial, antibiofilm, and hemostatic applications. The hydrogels demonstrated enhanced reactive oxygen species scavenging activity of >85%, broad-spectrum antibacterial ability of around 90% against both Staphylococcus aureus and Escherichia coli, antibiofilm activity, and hemostatic potential by taking advantage of intrinsic hemostatic, antioxidative, and antibacterial properties of quaternized chitosan along with the antibacterial and antibiofilm properties of gallium nanoparticles. The scratch assay performed on L929 cells showed the complete closure of scratch in 24 h, emphasizing its potential as a drug-free, multifunctional material in wound dressings. As per our knowledge, this is for the first time that the effect of β-Ga₂O₃ nanoparticle-loaded quaternized chitosan-oxidized sodium alginate hydrogels has been investigated as a treatment strategy for bacteria-infected wounds.</p>
92.	<p>Glucose oxidation assisted hydrogen and gluconic/gluconic acid production using NiVP/Pi bifunctional electrocatalyst</p> <p>N Thakur, D Mandal, A Chaturvedi ...TC Nagaiah... - Journal of Materials Chemistry A, 2023</p> <p>Abstract</p> <p>Hydrogen is an efficient green energy source due to its high energy density and environmental friendliness. Water electrolysis, which involves hydrogen generation at the cathode and O₂ production at the anode, is a promising approach for H₂ production. But, its sluggish oxygen evolution reaction (OER) limits the overall large-scale application of hydrogen. Thus, replacing the OER with anodic glucose oxidation, which occurs at a lower potential, makes it energy efficient and further produces higher value-added products such as gluconic acid, glucaric acid, and gluconolactone. Herein, we report nickel vanadium phosphide/phosphate-Vulcan carbon (NiVP/Pi-VC) as an effective bifunctional electrocatalyst for the hydrogen evolution reaction coupled with glucose oxidation, which exhibits a low cell voltage of 1.3 V to reach a current density of 10 mA cm⁻², which is 280 mV lower compared to water splitting. The catalyst offers a new prospect for the development of other valuable products along with hydrogen generation.</p>
93.	<p>Graphene metamaterials</p> <p>GP Singh, N Sardana - Recent Advances in Graphene and Graphene-Based Technologies: Book Chapter, 2023</p> <p>Abstract</p> <p>In this chapter, the applications of graphene-based metamaterials are broadly divided into imaging (absorber, lenses, and modulators), communication (antennas, transparency, and encryption), and sensing.</p>
94.	<p>Growth of harmonic mappings and baernstein type inequalities</p> <p>S Das, A Sairam Kaliraj – Potential Analysis, 2023</p> <p>Abstract</p> <p>Seminal works of Hardy and Littlewood on the growth of analytic functions contain the comparison of the integral means $M_p(r, f)$, $M_p(r, f')$, $M_q(r, f)$. For a complex-valued harmonic function f in the unit disk, using the notation $\nabla f = (fz ^2 + fz^- ^2)^{1/2}$ we explore the relation between $M_p(r, f)$ and $M_p(r, \nabla f)$. We show that if ∇f grows sufficiently slowly, then f is continuous on the closed unit disk and the boundary function satisfies a Lipschitz condition. We</p>

	<p>also prove that for $1 \leq p < q \leq \infty$, it is possible to give an estimate on the growth of $M_q(r, f)$ whenever the growth of $M_p(r, f)$ is known. We notably obtain Baernstein type inequalities for the major geometric subclasses of univalent harmonic mappings such as convex, starlike, close-to-convex, and convex in one direction functions. Some of these results are sharp. A growth estimate and a coefficient bound for the whole class of univalent harmonic mappings are given as well.</p>
95.	<p>Haunted by the past: Understanding history and the aftermath of war in Michael Ondaatje's Anil's Ghost A Nandha, S Reji - Arcadia, 2023</p> <p>Abstract This article explores the spectral presence of the past in the form of skulls and emotional trauma in a story about a country ravaged by a protracted war. It analyzes Anil's Ghost (2000), a novel by Michael Ondaatje, a Sri Lankan Canadian writer renowned for constructing revisionist and fictional historiographic narratives. The novel speaks about a phase of the ethno-nationalist civil war in contemporary Sri Lanka, and the article expounds on the deconstruction and understanding of war and history as represented in this piece of fiction. In deprecating a unilateral and cohesive representation of history, the novel presents multiple voices and subverts the notion of a single truth, thereby challenging the unity and logic of representing history in fiction. It also highlights the lingering effects of past violence and buried memories haunting the present for the purpose of closure in the form of splintered personal memories resurfacing at random moments.</p>
96.	<p>HierChain: A hierarchical blockchain-based data management system for smart healthcare V Agarwal, S Pal – IEEE Internet of Things Journal, 2023</p> <p>Abstract Healthcare is a crucial element of human lives that produces a substantial amount of medical data every year. A major difficulty faced by e-Health systems is the secure storage and sharing of this data without compromising its integrity and privacy. Being a trustless, traceable, and immutable technology, blockchain has the potential to address these issues. In this paper, we propose HierChain, a hierarchical blockchain-based data storage and sharing system for healthcare. This framework provides a trustless environment that is decentralized and tamper-resistant for efficient management of data. We first introduce an optimization problem aimed at identifying the optimal data storage solution for maximum efficiency. Next, we classify the health data based on its specific features, sensitivity, and storage requirements. This classified data is then stored on three different blockchains (Ethereum, Hyperledger Sawtooth, and MultiChain) according to their optimal attributes. We utilize fog nodes for providing computational services to the resource-constrained Internet of Things (IoT) nodes, enabling us to perform data preprocessing and eliminate redundant information from the collected data. Moreover, we use differential privacy on the fog layer to ensure that sensitive medical data remains protected throughout the analysis process. Finally, we present a comprehensive attack evaluation and performance analysis by implementing our framework on a real-world medical dataset. The simulation results indicate that HierChain outperforms existing algorithms in terms of scalability and security of health data without degrading the performance of the IoT network.</p>
97.	<p>Honeybee stinger-based biopsy needle and influence of the barbs on needle forces during insertion/extraction into the iliac crest: A multilayer finite element approach R Nadda, R Repaka, A K Sahani - Computers in Biology and Medicine, 2023</p> <p>Abstract Bone marrow biopsy (BMB) needles are frequently used in medical procedures, including extracting biological tissue to identify specific lesions or abnormalities discovered during a medical examination or a radiological scan. The forces applied by the needle during the cutting</p>

	<p>operation significantly impact the sample quality. Excessive needle insertion force and possible deflection might cause tissue damage, compromising the integrity of the biopsy specimen. The present study aims at proposing a revolutionary bioinspired needle design that will be utilized during the BMB procedure. A non-linear finite element method (FEM) has been used to analyze the insertion/extraction mechanisms of the honeybee-inspired biopsy needle with barbs into/from the human skin-bone domain (i.e., iliac crest model). It can be seen from the results of the FEM analysis that stresses are concentrated around the bioinspired biopsy needle tip and barbs during the needle insertion process. Also, these needles reduce the insertion force and reduce the tip deflection. The insertion force in the current study has been reduced by 8.6% for bone tissue and 22.66% for skin tissue layers. Similarly, the extraction force has been reduced by an average of 57.54%. Additionally, it has been observed that the needle-tip deflection got reduced from 10.44 mm for a plain bevel needle to 6.3 mm for a barbed biopsy bevel needle. According to the research findings, the proposed bioinspired barbed biopsy needle design could be utilized to create and produce novel biopsy needles for successful and minimally invasive piercing operations.</p>
98.	<p>Hormonal and non-hormonal oral contraceptives given long-term to pubertal rats differently affect bone mass, quality and metabolism K Porwal, S Sharma, S Kumar.. – <i>Frontiers in Endocrinology</i>, 2023</p> <p>Abstract</p> <p>Introduction: We investigated the effects of hormonal and non-hormonal oral contraceptives (OCs) on bone mass, mineralization, composition, mechanical properties, and metabolites in pubertal female SD rats.</p> <p>Methods: OCs were given for 3-, and 7 months at human equivalent doses. The combined hormonal contraceptive (CHC) was ethinyl estradiol and progestin, whereas the non-hormonal contraceptive (NHC) was ormeloxifene. MicroCT was used to assess bone microarchitecture and BMD. Bone formation and mineralization were assessed by static and dynamic histomorphometry. The 3-point bending test, nanoindentation, FTIR, and cyclic reference point indentation (cRPI) measured the changes in bone strength and material composition. Bone and serum metabolomes were studied to identify potential biomarkers of drug efficacy and safety and gain insight into the underlying mechanisms of action of the OCs.</p> <p>Results: NHC increased bone mass in the femur metaphysis after 3 months, but the gain was lost after 7 months. After 7 months, both OCs decreased bone mass and deteriorated trabecular microarchitecture in the femur metaphysis and lumbar spine. Also, both OCs decreased the mineral: matrix ratio and increased the unmineralized matrix after 7 months. After 3 months, the OCs increased carbonate: phosphate and carbonate: amide I ratios, indicating a disordered hydroxyapatite crystal structure susceptible to resorption, but these changes mostly reversed after 7 months, indicating that the early changes contributed to demineralization at the later time. In the femur 3-point bending test, CHC reduced energy storage, resilience, and ultimate stress, indicating increased susceptibility to micro-damage and fracture, while NHC only decreased energy storage. In the cyclic loading test, both OCs decreased creep indentation distance, but CHC increased the average unloading slope, implying decreased microdamage risk and improved deformation resistance by the OCs. Thus, reduced bone mineralization by the OCs appears to affect bone mechanical properties under static loading, but not its cyclic loading ability. When compared to an age-matched control, after 7 months, CHC affected 24 metabolic pathways in bone and 9 in serum, whereas NHC altered 17 in bone and none in serum. 6 metabolites were common between the serum and bone of CHC rats, suggesting their potential as biomarkers of bone health in women taking CHC.</p> <p>Conclusion: Both OCs have adverse effects on various skeletal parameters, with CHC having a greater negative impact on bone strength.</p>

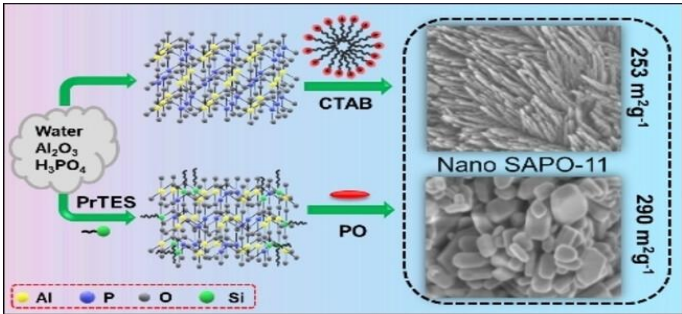
99.	<p>Humbert generalized fractional differenced ARMA processes N Bhootna, MS Dhull, A Kumar... - Communications in Nonlinear Science and Numerical Simulation, 2023</p> <p>Abstract In this article, we use the generating functions of the Humbert polynomials to define two types of Humbert generalized fractional differenced ARMA processes. We present stationarity and invertibility conditions for the introduced models. The singularities for the spectral densities of the introduced models are investigated. In particular, Pincherle ARMA, Horadam ARMA and Horadam–Pethe ARMA processes are studied. It is shown that the Pincherle ARMA process has long memory property for $u=0$. Additionally, we employ the Whittle quasi-likelihood technique to estimate the parameters of the introduced processes. Through this estimation method, we attain results regarding the consistency and normality of the parameter estimators. We also conduct a comprehensive simulation study to validate the performance of the estimation technique for Pincherle ARMA process. Moreover, we apply the Pincherle ARMA process to real-world data, specifically to Spain's 10 years treasury bond yield data, to demonstrate its practical utility in capturing and forecasting market dynamics.</p>
100.	<p>Hybrid relaying based cross layer MAC protocol using variable beacon for cooperative vehicles S Bhattacharyya, P Kumar, S Darshi...B Kumbhani... - IEEE Transactions on Vehicular Technology, 2023</p> <p>Abstract The onset of network coded cooperation (NCC) and its applications in vehicle-to-everything (V2X) scenarios have allowed vehicular networks to relish both reliability and throughput which are the key factors in an on-road scenario. However, a typical NCC based network uses a time division multiple access (TDMA) based data transmission aided by a relay employing a fixed relaying scheme. This puts a concern on the system's quality-of-service (QoS). We thus propose a dual threshold-based hybrid (DTH) relaying scheme where the relay vehicle dynamically decides the relaying scheme or asks for a re-transmission to improve the QoS. The decision to select a relaying scheme is based on the instantaneous signal-to-noise ratio (SNR). Consequently, an acknowledgement frame structure is proposed to convey the crucial information to the destinations which are required during data extraction. A variable beacon interval is also proposed where the relay vehicle dynamically changes the beacon transmission time based on the number of re-transmissions which helps new users to join the system. Metrics like outage probability, achievable rate and throughput have been considered as the QoS metrics to compare the performance of the proposed model with respect to other existing works. Extensive simulations in MATLAB show that the proposed scheme experiences a better outage performance than amplify-and-forward (AF) whereas a worse performance when compared with decode-and-forward (DF). However, the better performance in the case of DF comes with a trade-off in terms of throughput when compared to the proposed scheme.</p>
101.	<p>Hybridisation effect of carboxyl graphene and silica nanofillers on environmentally aged composite acrylonitrile butadiene rubber AK Jha, N Kumar, K Suresh - Journal of Rubber Research, 2023</p> <p>Abstract Filler hybridisation in elastomers has become a subject of both scientific and industrial interest. Consequently, the use of nanofillers has attracted researchers looking to enhance the performance of elastomers. Therefore, carboxyl graphene (CG) and silicon dioxide (SiO_2) nanofillers have been hybridised for the combined effect study of composite NBR (acrylonitrile butadiene rubber) elastomers in various accelerated environmental ageing conditions (high temperature, low temperature, and QUV). The inorganic filler (SiO_2) had enhanced dispersion</p>

	<p>upon hybridising with CG on the surface of a composite NBR elastomer. To evaluate the mechanical and dynamic mechanical properties, unfilled and filled (CG/SiO₂) composite NBR elastomer samples were prepared by mixing and rolling methods. Furthermore, the prepared samples were kept in various ageing chambers. The results of mechanical testing exhibited that tensile strength improvement was greater for filled elastomers than unfilled elastomers after ageing. Moreover, the filled elastomers were also able to retain the reduction in elongation at break after ageing. However, after ageing, the hardness of composite NBR elastomers increased marginally with the addition of CG/SiO₂. Moreover, the loss factor (tan δ) of a composite NBR elastomer (CG/SiO₂: 15/7.5), compared to that of the unfilled NBR elastomer before and after ageing, decreased but was still much higher than that of the aged unfilled NBR elastomer. The reason behind that was that CG/SiO₂ dispersion in the composite NBR elastomer matrix acted as a barrier against ageing. CG/SiO₂ hybridising is an effective way to develop high-performance composite NBR elastomers with good potential in industrial applications.</p>
102.	<p>Hybridisation effect of steel–polypropylene fibres in high-volume fly ash concrete O Mishra, S P Singh, S Mishra - Magazine of Concrete Research, 2023</p> <p>Abstract The paper presents the results of an investigation conducted to investigate the effects of hybrid fibres (polypropylene (PP) and steel (S) fibres on the workability, compressive strength, flexural strength and flexural toughness of high-volume fly ash concrete (HVFAC). Different combinations of PP and S fibres (PP fibre 0–100% and S fibre 100–0%) were incorporated to a total fibre volume fraction of 1.0%. Three different code methods were used for a comparative evaluation of various properties of the HVFAC (toughness, residual strength, cracking strength, etc.). It was found that the mixes with a higher percentage of PP fibre resulted in lower workability as compared to the mixes made with a higher percentage of S fibres. The HVFAC mix made with 25% PP fibre and 75% S fibre showed the best results of all concrete mixes and this combination is thus considered to be the most appropriate for fibre hybridisation in HVFAC.</p>
103.	<p>Hydrogen fueled low-temperature combustion engines MR Saxena, RK Maurya - Hydrogen for Future Thermal Engines: Book Chapter, 2023</p> <p>Abstract Energy security concerns, rapid depletion of crude oil reserves, and stringent emission norms demand cleaner and efficient combustion technology for engines. Advanced low-temperature combustion (LTC) regimes such as HCCI, RCCI, etc., have demonstrated improved thermal efficiency and simultaneous reduction of NO_x and soot emissions. These combustion regimes are fuel flexible. Characteristics of hydrogen fuel (such as wider flammability range, higher laminar and turbulent burning velocities, and better flame stability) and its improved performance motivates its application in LTC engine. Hydrogen can be effectively used as a fuel in CI engines with advanced LTC strategies. This chapter presents the characteristics of hydrogen-fueled conventional dual-fuel, HCCI, and RCCI engines. First, the fuel injection strategy for conventional dual fuel, HCCI, and RCCI combustion modes is discussed. Secondly, a detailed analysis of performance (including specific fuel consumption, thermal efficiency), combustion (including ignition delay, heat release rate, combustion phasing and duration, ringing intensity), and emission (including NO_x, soot, CO, and HC) characteristics are presented. Lastly, the challenges associated with hydrogen in HCCI and dual-fuel engines and future prospects of hydrogen with LTC engines are also discussed. © 2023, The Author(s), under exclusive license to Springer Nature Switzerland AG.</p>
104.	<p>Hydrogen Storage in a Ti-Functionalized metal carbyne framework: Insights from a first-principles study P Beniwal, TJ Dhilip Kumar - ACS Applied Energy Materials, 2023</p> <p>Abstract</p>

	<p>Hydrogen (H₂) has the ability to be a future green-energy source for the automotive industry due to its versatility, clean nature, and efficiency as an energy carrier. The biggest obstacle to achieving hydrogen as a potential energy source is the nonavailability of effective hydrogen storage materials. In this proposed work, the hydrogen storage capacity and reversibility of a Ti-functionalized metal carbyne framework (MCF) having carbyne as an organic linker and Mg₄O as an inorganic moiety are explored. All structural relaxation and simulation calculations are performed by employing the dispersion-corrected density functional theory computation. In this Ti-functionalized MCF, each Ti can adsorb up to five H₂ molecules via the Kubas mechanism, with adsorption energy lying between 0.33 and 0.44 eV, which falls within the range outlined by the U.S. Department of Energy (DOE). For a detailed study of the thermal stability of framework, hydrogen reversibility, and mechanism of hydrogen sorption, Born-Oppenheimer molecular dynamics (BOMD) simulations are carried out at various temperatures. From the findings of BOMD simulations, the Ti-functionalized MCF can reversibly adsorb the H₂ molecules with a high gravimetric density of about 9.4 wt %. This proposed Ti-functionalized MCF stands out as a potential hydrogen storage medium meeting the standards established by the DOE.</p>
105.	<p>Hydrogeochemical constraints on uranium contamination of groundwater for drinking water supplies and associated health risks M Verma, VA Loganathan - Groundwater for Sustainable Development, 2023</p> <p>Abstract The groundwater quality of Punjab, India is of huge concern owing to the presence of various toxic contaminants that includes uranium and other trace elements. The focus of this study is to identify the hydrogeochemical processes responsible for uranium mobilization in groundwater and evaluation of groundwater quality in uranium contaminated zones for drinking, irrigation use along with associated health risks. The study was conducted using the water quality data obtained from 302 sampling locations covering the entire state of Punjab reported by Central Ground Water Board between 2019 and 2020. It was observed that around 50% of the samples were exceeding the drinking water acceptable limits for total alkalinity, magnesium, pH, and Total Dissolved Solids. Around 25% of the samples were above drinking water acceptable limit for uranium in groundwater. A comprehensive multiplicative water quality index (M_{ED}-WQI) well represented the consolidated perspective of all individual water quality parameters wherein 40 sampling locations in districts viz. Bathinda, Fazilka, Ferozepur, Jalandhar, Kapurthala, Ludhiana, Muktsar and Sangrur fall under heavily-polluted water quality class due to high levels of uranium, alkalinity, and hardness. The Piper plots and Gibbs diagram depicted that the majority of groundwater samples were characterized as Na⁺-HCO₃⁻, Ca²⁺-Mg²⁺-HCO₃⁻ systems driven by rock-water interactions. Speciation analysis indicates that the dominant uranium species in groundwater of U-affected regions was primarily associated with calcium and alkalinity and exist in the form of CaUO₂(CO₃)₃²⁻, Ca₂UO₂(CO₃)₃(aq), UO₂(CO₃)₃⁴⁻, and UO₂(OH)₃⁻. Various irrigation indices depict that the groundwater in majority of the state, barring few districts in Malwa region, was suitable for irrigation. Further, a non-carcinogenic health risk assessment model showed association of high health risk with heavily-polluted water quality class. The results of this study would aid regulatory authorities in designing remedial strategies and frame policy actions toward groundwater quality improvement in the uranium-affected regions of Punjab.</p>
106.	<p>Identification of diphenylurea derivatives as novel endocytosis inhibitors that demonstrate broad-spectrum activity against SARS-CoV-2 and influenza A virus both in vitro and in vivo IM Taily, P Singh, C Singh ...P Banerjee... - PLoS Pathogens, 2023</p> <p>Abstract Rapid evolution of severe acute respiratory syndrome coronavirus 2 (SARS-CoV-2) and influenza A virus (IAV) poses enormous challenge in the development of broad-spectrum</p>

	<p>antivirals that are effective against the existing and emerging viral strains. Virus entry through endocytosis represents an attractive target for drug development, as inhibition of this early infection step should block downstream infection processes, and potentially inhibit viruses sharing the same entry route. In this study, we report the identification of 1,3-diphenylurea (DPU) derivatives (DPUDs) as a new class of endocytosis inhibitors, which broadly restricted entry and replication of several SARS-CoV-2 and IAV strains. Importantly, the DPUDs did not induce any significant cytotoxicity at concentrations effective against the viral infections. Examining the uptake of cargoes specific to different endocytic pathways, we found that DPUDs majorly affected clathrin-mediated endocytosis, which both SARS-CoV-2 and IAV utilize for cellular entry. In the DPUD-treated cells, although virus binding on the cell surface was unaffected, internalization of both the viruses was drastically reduced. Since compounds similar to the DPUDs were previously reported to transport anions including chloride (Cl⁻) across lipid membrane and since intracellular Cl⁻ concentration plays a critical role in regulating vesicular trafficking, we hypothesized that the observed defect in endocytosis by the DPUDs could be due to altered Cl⁻ gradient across the cell membrane. Using in vitro assays we demonstrated that the DPUDs transported Cl⁻ into the cell and led to intracellular Cl⁻ accumulation, which possibly affected the endocytic machinery by perturbing intracellular Cl⁻ homeostasis. Finally, we tested the DPUDs in mice challenged with IAV and mouse-adapted SARS-CoV-2(MA10). Treatment of the infected mice with the DPUDs led to remarkable body weight recovery, improved survival and significantly reduced lung viral load, highlighting their potential for development as broad-spectrum antivirals.</p>
107.	<p>Identification of the significant parameters in spatial prediction of landslide hazard A Tyagi, RK Tiwari, N James - <i>Bulletin of Engineering Geology and the Environment</i>, 2023</p> <p>Abstract</p> <p>Landslides are the most commonly occurring natural hazard in the hilly regions of the world. Tehri Garhwal in the Uttarakhand State of India is one such region where several landslide events have been reported. Several researchers have performed landslide susceptibility mapping (LSM) studies for the Tehri region. However, these studies lack consistency in selecting landslide-causing parameters for the susceptibility analysis and mapping. The variability in selecting parameters for the same region by various researchers has made it difficult to compare the models' prediction accuracies. Hence, this study presents a scientific method to identify the most significant landslide-causing parameters for an enhanced LSM analysis. The selected combination of parameters was further validated on the two landslide-prone test sites with similar terrain conditions. To achieve these objectives, first, the landslide inventory map of 332 historical landslide events was prepared for the Tehri region. Second, the statistical relevance of 21 landslide-causing parameters for predicting landslide susceptibility was investigated using multicollinearity analysis considering Pearson correlation and the artificial neural network (ANN) model's sensitivity analysis. Out of 21 parameters considered for the Tehri region, 11 were found to be significant for LSM and achieved the prediction accuracy of 0.93 area under curve (AUC) value. Third, the relevance of these 11 parameters in predicting the landslide susceptibility was checked for the two test sites of the Himalayan region. For this purpose, these parameters and their hierarchy were imported into the analytical hierarchy process (AHP) framework for predicting the LSM of the Tehri region and two landslide-prone sites, namely the Chamba and Bhuntar sites of Himachal Pradesh. The AHP-based LSM for Chamba, Bhuntar, and Tehri regions achieved a prediction accuracy of 0.86, 0.82, and 0.89 AUC values. Thus, this study recommends using the derived 11 landslide parameters and their hierarchy for carrying out LSM in the Himalayan region.</p>
108.	<p>Impact analysis of distributed DoS attack by multiple HTs in TCMP architectures J Philomina, RK James, S Das... - 2023 International Conference on Control, Communication and Computing (ICCC), 2023</p>

	<p>Abstract</p> <p>Tiled Chip Multicore Processors (TCMP) with packet switching Network-on-Chip (NoC) have become a common method for on-chip connectivity. The performance of the entire system may suffer if a malicious Hardware Trojan (HT) is present in the NoC routers as it might negatively disrupt communication between tiles. Detecting Trojans in complicated multi-processor System on Chips (SoCs) using traditional pre and post silicon validation approaches is a huge difficulty. In this paper the presence of multiple HTs in the routing unit is modelled and its impact analysis is done for both synthetic traffic and real benchmarks using gem5 simulator. It can be observed that the presence of multiple trojans decrease the overall performance of the system.</p>
109.	<p>Increased habitat connectivity induces diversity via noise-induced symmetry breaking A Narang, T Banerjee, PS Dutta - <i>Chaos: An Interdisciplinary Journal of Nonlinear Science</i>, 2023</p> <p>Abstract</p> <p>Stochasticity or noise is omnipresent in ecosystems that mediates community dynamics. The beneficial role of stochasticity in enhancing species coexistence and, hence, in promoting biodiversity is well recognized. However, incorporating stochastic birth and death processes in excitable slow-fast ecological systems to study its response to biodiversity is largely unexplored. Considering an ecological network of excitable consumer-resource systems, we study the interplay of network structure and noise on species' collective dynamics. We find that noise drives the system out of the excitable regime, and high habitat patch connectance in the ordered as well as random networks promotes species' diversity by inducing new steady states via noise-induced symmetry breaking.</p>
110.	<p>Infection prevalence at a tertiary hospital in Hail, Saudi Arabia: A single-center study to identify strategies to improve antibiotic usage M Alanazi, HM Alqahtani, MK Alshammari...JA Malik... - <i>Infection and Drug Resistance</i>, 2023</p> <p>Abstract</p> <p>Objective: Identifying the burden of disease and the condition of the Saudi population is in high demand from both a surveillance and analytical standpoint. The objective of this study was to determine the most prevalent infections among hospitalized patients (both community-acquired and hospital-acquired), the antibiotics prescribing pattern, and their relationship with patient characteristics like age and gender.</p> <p>Methods: A retrospective study was conducted comprising 2646 patients with infectious diseases or complications admitted to a tertiary hospital in the Hail region of Saudi Arabia. A standardized form was used to collect information from patient's medical records. Demographic data such as age, gender, prescribed antibiotics, and culture-sensitivity tests were included in the study.</p> <p>Results: Males represented about two-thirds (66.5%, n = 1760) of the patients. Most patients (45.9%) who suffered from infectious diseases were between the ages of 20 and 39. The most prevalent infectious ailment was respiratory tract infection (17.65%, n = 467). Furthermore, the most common multiple infectious diseases were gallbladder calculi with cholecystitis (40.3%, n = 69). Similarly, COVID-19 had the greatest impact on people over 60. Beta-lactam antibiotics were the most commonly prescribed (37.6%), followed by fluoroquinolones (26.26%) and macrolides (13.45%). But performing culture sensitivity tests were rather uncommon (3.8%, n = 101). For multiple infections, beta-lactam antibiotics (such as amoxicillin and cefuroxime) were the most commonly prescribed antibiotics (2.26%, n = 60), followed by macrolides (such as azithromycin and Clindamycin) and fluoroquinolones (eg, ciprofloxacin and levofloxacin).</p> <p>Conclusion: Respiratory tract infections are the most prevalent infectious disease among hospital patients, who are primarily in their 20s. The frequency of performing culture tests is low. Therefore, it is important to promote culture sensitivity testing in order to support the prudent use</p>

	of antibiotics. Guidelines for anti-microbial stewardship programs are also highly recommended.
111.	<p>Influence of additives and growth inhibitors in improving the physicochemical properties of silicoaluminophosphate molecular sieve, SAPO-11 AK. Manal, JH. Advani, N Kanna...R Srivastava - Chemistry: An Asian Journal, 2023</p> <p>Abstract Silicoaluminophosphates (SAPOs) are microporous crystalline materials extensively utilized as adsorbents and catalysts. The present work utilized two strategies to synthesize nanocrystalline SAPO-11. The first strategy involves a surfactant as a mesoporegen to reduce the crystallite size and increase the surface area for the materials synthesized at 200 °C in 2 days. In the second strategy, the synthesis temperature and time were significantly reduced to 160 °C and 3 h using propylene oxide as a pH accelerator. The reduction in the particle size and the improvement in the surface area were achieved using propyltriethoxysilane, which inhibited the growth of SAPO-11 particles. The materials were thoroughly characterized using XRD, N₂-sorption, FTIR, pyridine-adsorbed FTIR, electron microscopy, XPS, and NMR. The surfactant-assisted synthesis formed a nanorod morphology with a large external and BET surface area. The low-temperature synthesis involving silane as a growth inhibitor and propylene oxide as a pH modulator demonstrated a rectangular nanoplatelet morphology with a large surface area. The synthesis was scaled up to 10 g with no change in the experimental parameters. A synthesis strategy facilitating nuclei formation and retarding the growth of particle size will attract academia and industrial researchers to utilize these strategies for the manufacturing of zeolites of different frameworks on a large scale.</p> 
112.	<p>Integrated experimental and theoretical studies on structural and magnetic properties of thin films of double perovskite ruthenates: Ba₂DyRuO₆ & Sr₂DyRuO₆ S Dani, R Kumar, H Sharma... - Physical Chemistry Chemical Physics, 2023</p> <p>Anstract Thin films of double perovskite ruthenates, viz., Ba₂DyRuO₆ (BDRO) and Sr₂DyRuO₆ (SDRO), have been successfully grown on a SrTiO₃ substrate using the pulsed laser deposition technique. The BDRO samples crystallizes in cubic structure, while SDRO exhibits monoclinic structure as revealed in their X-Ray diffraction examination. Temperature-dependent magnetization measurements suggest the presence of ferromagnetism in BDRO, while paramagnetism is present for the SDRO thin film. Surprisingly, both films show canted antiferromagnetism at ~T = 5 K as revealed in their isothermal magnetization curves. The inverse susceptibility has been fitted to the Curie–Weiss law for the SDRO sample, where the Curie temperature (T_C ~ –336.6 K) has been obtained, thus suggesting the prevalence of antiferromagnetic interactions. The existence of the canted magnetism at a lower temperature may be attributed to the Dzyaloshinskii–Moriya (D–M) interactions in the monoclinic SDRO sample due to structural distortion. However, the emergence of canted antiferromagnetism at lower temperatures (5 K) in the BDRO sample with cubic symmetry having no D–M interactions may be attributed to the various modifications at the surface of the thin films. Overall, a comparison made between the magnetic properties of both the thin films i.e., BDRO & SDRO, reveals the suppression of bulk</p>

	<p>magnetic ordering when compared to their bulk counterparts. The possible reason for the absence of any magnetic ordering in these thin films may be due to any modifications in superexchange interactions, any exchange bias, stress–strain, or uncompensated spins present in these types of thin films. UV-visible measurements for both the samples reveal a direct influence of the A-site element (Sr/Ba) on their band gaps, <i>i.e.</i>, 3.66 eV and 2.59 eV for BDRO and SDRO samples, respectively, hence suggesting their insulating nature. We have also carried out first principles calculations with DFT using the CASTEP software to gain more insights into the experimental data. These thin films with insulating-antiferromagnetic properties may be crucial for “spintronics devices”.</p>
113.	<p>Interfacial-mixing and band engineering induced by annealing of CdS and a-Ga₂O₃ n-n-type thin-film heterojunction and its impact on carrier dynamics for high-performance solar-blind photodetection D Kaur, R Wadhwa, Nisika...M Kumar - ACS Applied Electronic Materials, 2023</p> <p>Abstract Heterojunctions of dissimilar materials are increasingly being used in optoelectronics for their superior properties. However, the heart of the heterojunction—its interface—and its impact on the device performance are seldom studied in detail. Herein, we report on the band alignment modification of heterojunction formed between amorphous Ga₂O₃ and CdS, two intrinsically n-type materials, with high optical absorbance but different band gaps. The resultant heterostructure-based devices remain solar-blind and outperform the singular bare photodetectors. To further improve upon device performance, the heterostructure is subjected to a moderate annealing of 300 °C. The annealed heterojunction device shows a reduction in dark current by more than 1 order of magnitude along with an enhanced photocurrent. The response time of the devices reduces from 1.35 s/2.87 s (rise/fall time) to about 0.38 s/0.75 s upon annealing. To study this change in the device performance between the pristine and the annealed interface, the two heterojunctions are compared using X-ray photoelectron spectroscopy depth profiling, and results show that the pristine heterostructure has a sharp interface whereas upon annealing, it leads to a sort of diffuse interface. This produces a reduced valence band offset, resulting in a change in the band alignment from type II to type I. The carrier dynamics across the two interfaces therefore changes and is further validated using Kelvin probe force microscopy. This study reveals how the change at the interface by mere annealing can lead to a huge alteration in the band alignment and thus, the carrier dynamics, thereby completely altering the ultimate device performance.</p>
114.	<p>Investigation of CeO₂ nanoparticles on the performance enhancement of insulating oils O Rahman, A Ali, A Hussain... - Heliyon, 2023</p> <p>Abstract Integrating nanotechnology in dielectric fluid significantly inhibits losses and boosts overall dielectric fluid performance. There has been research done on the effects of introducing various nanoparticles, such as titania, alumina, silica nanodiamonds, etc. In this paper, a novel nanoparticle, Ceria (CeO₂), has been used, and its properties were examined using the FTIR (Fourier Transform Infrared) spectrum, the XRD (X-ray Diffraction) spectrum, the SEM (Scanning Electron Microscopy), and the TEM (Transmission Electron Microscopy). This paper illustrates an efficient dielectric fluid prepared by the successful dispersion of Cerium Oxide (CeO₂) nanoparticles in various concentrations into four commercial oils, namely mineral oil, rapeseed oil, synthetic ester oil, and soybean oil, to enhance and improve their dielectric characteristics. The performance investigation emphasises breakdown strength enhancement and other dielectric properties of the colloidal solution comprising different nanoparticle (NP) concentrations. Various commercial oils are used as a base in nano-oil to diversify their</p>

	<p>applicability as dielectric fluids by measuring the correlation in dielectric parameters and statistically assessing their applicability with normal and Weibull distributions. The obtained experimental data sets were analyzed using the Statistics and Machine Learning Toolbox in MATLAB. The aging measurement has been done only on mineral oil, and results were matched using a predictive model of statistics and the Machine Learning Toolbox in MATLAB. Well-dispersed CeO₂ NPs in the insulating oils lead to a significant increase in AC breakdown strength. The effect of ageing on the dielectric properties of nano oils yields better results than conventionally aged oil. It has been observed that the breakdown voltage is enhanced by up to 30% for mineral oil at an optimal concentration of 0.01 g/L, 9% for synthetic ester oil at 0.03 g/L, 18% for rapeseed oil at 0.02 g/L, and 19% for soybean oil at 0.03 g/L nanoparticle concentration. Following the dispersion of CeO₂ nanoparticles, the dielectric constant of all insulating oils has also significantly improved.</p> <p>The overall experimental results are promising and show the potential of the CeO₂ NPs-based nano oil as an efficient and highly performing dielectric oil for different power applications.</p>
115.	<p>IoT-QWatch: A novel framework to support the development of quality aware autonomic IoT applications K Fizza, PP Jayaraman, A Banerjee ...N Auluck... - IEEE Internet of Things Journal, 2023</p> <p>Abstract The unprecedented growth of Internet of Things (IoT) is leading to its increased usage in various domains, such as manufacturing, health, and smart cities. A majority of IoT applications are autonomic, i.e., they operate under minimal/no human intervention, and make decisions/actuators based on machine-to-machine communication and data analytics. A key challenge in the development of such applications is the ability to measure their quality while they are working in a diverse and heterogeneous IoT ecosystem. In this paper, we propose an agent based Internet of Things-Quality Watch (IoT-QWatch) framework that provides the ability to measure IoT quality metrics at each stage of the autonomic IoT application life cycle running in the IoT ecosystem. We envision that IoT-QWatch will enable the development of a new generation of quality-aware autonomic IoT applications that are able to be resilient to the heterogeneous and uncertain nature of IoT ecosystems. We present architectural details and implementation of IoT-QWatch, and corresponding models used to measure IoT quality metrics at different stages. We conduct extensive experiments using a real-world IoT test bed from the domain of manufacturing to validate the efficacy of IoT-QWatch. Experimental outcomes provide promising results in realising IoT-QWatch in real-world deployment, while the framework itself offers significant extensibility to include new models for measuring IoT quality metrics.</p>
116.	<p>Janus functionalized Boron-Nitride nanosystems as a potential application for absorber layer in solar cells B Roondhe, V Roondhe, A Shukla...R Ahuja... - Advanced Electronic Materials, 2023</p> <p>Abstract Janus nanosystems enable one to achieve complementary properties in a single entity. In the current study, the fundamental properties like structural, electronic, and dynamical of Janus hexagonal boron nitride (h-BN) by selectively hydrogenating and fluorinating a h-BN surface are systematically examined, using density functional theory. Functionalization of h-BN introduces partial sp³ (buckled) character in the predicted materials as compared to planar sp² h-BNs. Fully fluorinated and hydrogenated h-BN have a direct bandgap of 3.42 and 3.37 eV, respectively. All the investigated configurations are predicted to be dynamically stable. Furthermore, optical properties including dielectric function, absorption spectra, refractive index, and reflectivity are evaluated to realize the optical and photocatalytic behavior of considered systems. The dielectric</p>


	<p>function $\epsilon_2(\omega)$ shows fundamental absorption edge arising at 3.2, 3.9, 2.8, and 3.4 eV for hydrogen on boron and nitrogen, hydrogen on boron and fluorine on nitrogen, fluorine on boron and hydrogen on nitrogen (FBNH) and fluorine on boron and nitrogen which is comparable to the bandgap of respective monolayers. Solar cell parameters of all considered BN structures are calculated using the Shockley–Queisser (SQ) limit. The highest short-circuit current density (J_{sc}) for FBNH is found to be 2.1 mA cm^{-2} providing the efficiency of 8.27% making FBNH a potential candidate for absorber layer in solar cells.</p>
117.	<p>Lateral capacity of concrete bridge piers with steel rebar reinforcement and glass fibre reinforced polymer P Maheshwari, PH Malini, P Kamatchi... - Proceedings of 17th Symposium on Earthquake Engineering, 2023</p> <p>Abstract Corrosion remains a challenge for maintenance of important infrastructure like bridges and researchers are involved in looking for alternative materials for replacement of steel reinforcement. Studies are reported in literature on fabrication and characterisation of engineering properties of Glass Fibre Reinforced Polymer (GFRP) rebars. Non-degradable property of GFRP rebars against alkaline and corrosive environment is the major desirable characteristics for infrastructure located at severe corrosive sites like offshore. Studies are reported in literature on the use of GFRP rebars for bridge decks. In the present study, three-span continuous steel girder composite bridge consisting of two bents with two piers each with a concrete deck slab has been considered. Two types of reinforcements are considered for bridge piers viz., steel rebar reinforcement and GFRP rebar reinforcement. Stress–strain and other engineering properties of GFRP rebars are adopted from literature. Lateral capacity of bridge bents is evaluated through pushover analyses. Base shear capacity of bridge piers with GFRP reinforcement is observed to be similar to the base shear capacity of bridge pier with steel reinforcement however, ductility is observed to be very less for bridge pier with GFRP reinforcement. Hence it will be desirable to use GFRP rebars and steel rebars in combination in order to achieve desirable inelastic behaviour of bridge piers for highly corrosive sites located at high seismic prone zones.</p>
118.	<p>Layer by layer self-assembled MoS2-ZnO heterostructure for near room temperature NO2Gas sensor R Gond, P Shukla, M Bhagoria ...B Rawat... - 2022 IEEE International Conference on Emerging Electronic (ICEE 2022), 2022</p> <p>Abstract Due to their excellent chemical and electronic properties, two-dimensional MoS2 has emerged as a viable candidate for developing room temperature NO2sensors. However, the MoS2-based gas sensor suffers from low sensitivity and incomplete recovery. Therefore, in this work, we fabricate and characterize layer-by-layer self-assembled MoS2-ZnO heterostructure for near-room temperature NO2gas sensor. The results reveal that MoS2 -ZnO heterostructure exhibits high response and complete recovery for NO2gas with the excellent cross-sensitivity against CO, CO2, NH3 and SO2 gases. Moreover, the long-term durability of the sensor is evident from the stable response curves even after 15 days. Further, the MoS2 -ZnO heterostructure sensor exhibits the room temperature response and recovery times of around 2.1 min. and 27.9 min., respectively, for 50 ppm NO2gas with the lowest detection limit of about 1 ppm.</p>
119.	<p>Leishmania LPG interacts with LRR5/LRR6 of macrophage TLR4 for parasite invasion and impairs the macrophage functions S Mazumder, A Sinha, S Ghosh...D Pal... - Pathogens and Disease, 2023</p> <p>Abstract Visceral Leishmaniasis (VL) is a severe form of leishmaniasis, primarily affecting the poor in</p>

	<p>developing countries. Although several studies highlighted the importance of toll-like receptors (TLRs) in the pathophysiology of leishmaniasis, however, the role of specific TLRs and their binding partners involved in <i>Leishmania donovani</i> uptake are still elusive. To investigate the mechanism of <i>L. donovani</i> entry inside the macrophages, we have found that the parasites lipophosphoglycan (LPG) interacted with the macrophage TLR4 leading to parasite uptake without any significant alteration of macrophage cell viability. Increased parasite numbers within macrophages markedly inhibited LPS-induced pro-inflammatory cytokines gene expression. Silencing of macrophage-TLR4, or inhibition of parasite-LPG, significantly stemmed parasite infection in macrophages. Interestingly, we observed a significant enhancement of macrophage migration, and generation of reactive oxygen species (ROS) in the parasite-infected TLR4-silenced macrophages, whereas, parasite infection in TLR4-overexpressed macrophages, exhibited notable reduction of macrophage migration and ROS generation. Moreover, mutations at the leucine-rich repeats (LRRs), particularly LRR5 and LRR6, significantly prevented TLR4 interaction with LPG, thus inhibiting cellular parasite entry. All these results suggest that parasite LPG recognition by the LRR5 and LRR6 of macrophage-TLR4 facilitated parasite entry, and impaired macrophage functions. Therefore, targeting LRR5/LRR6 interactions with LPG could provide a novel option to prevent VL.</p>
120.	<p>Leveraging task variability in meta-learning A Aimen, B Ladrecha, S Sidheekh...CK Narayanan - SN Computer Science, 2023</p> <p>Abstract Meta-learning (ML) utilizes extracted meta-knowledge from data to enable models to perform well on unseen data that they have not encountered before. Typically, this meta-knowledge is acquired from randomly sampled task batches, and a critical assumption in the meta-learning is that all tasks in a batch equally contribute to the meta-knowledge. However, this assumption may not always hold true. In this study, we explore the impact of weighting tasks in a batch based on their contribution to meta-knowledge. We achieve this by introducing a learnable “task attention module” that can be integrated into any episodic training pipeline. We demonstrate that our approach improves the quality of the meta-knowledge obtained on standard meta-learning benchmarks such as miniImagenet, FC100, and tieredImagenet, as well as on noisy and cross-domain few-shot benchmarks. Additionally, we conduct a comprehensive analysis of the proposed task attention module to gain insights into its operation.</p>
121.	<p>Life cycle assessment to reduce environmental and carbon footprints of ultrasonic-assisted turning N Khanna, J Airao, P Maheshwari...CK Nirala... - Sustainable Materials and Technologies, 2023</p> <p>Abstract This work emphasizes life cycle assessment (LCA) for conventional and ultrasonic assisted turning (UAT) of Inconel 718 under six different combinations of cooling/lubricant strategies (LCO₂, MQL, and EMQL). The results indicate that when LCO₂ is flown on the rake whereas EMQL on the flank face, the tool wear, surface roughness, and energy consumption are significantly reduced compared to other strategies. The surface roughness is lowered approximately by 3–43% in the UAT compared to CT. The LCA results show that the combination of EMQL-MQL has more impact on the environment as it had a separate setup for charging the mist particles by a high voltage, followed by LCO₂-EMQL and LCO₂-MQL technique. The major impact is on the Ecosystem by 76.2%, 74.2%, and 75.3% in LCO₂-EMQL, EMQL-MQL, and LCO₂-MQL. It is concluded that LCO₂-EMQL is the best strategy for creating a balance between both technical and environmental parameters.</p>
122.	<p>Linear scaling relationships for Furan hydrodeoxygenation over transition metal and bimetallic surfaces DR Kanchan, A Banerjee – ChemSusChem, 2023</p>

	<p>Abstract</p> <p>Brønsted-Evans-Polanyi (BEP) and transition-state-scaling (TSS) relationships have become valuable tools for the rational design of catalysts for complex reactions like hydrodeoxygenation (HDO) of bio-oil (containing heterocyclic and homocyclic molecules). In this work, BEP and TSS relationships are developed for all the elementary steps of furan activation (C and O hydrogenation and CH_x -OH_y scission, for both ring and open-ring intermediates) to oxygenates, ring-saturated compounds and deoxygenated products on the most stable facets of Ni, Co, Rh, Ru, Pt, Pd, Fe and Ir surfaces using Density Functional Theory (DFT) calculations. Furan ring opening barriers were found to be facile and strongly dependent on carbon and oxygen binding strength on the investigated surfaces. Our calculations suggest linear chain oxygenates form on Ir, Pt, Pd and Rh surfaces due to their low hydrogenation and high CH_x -OH_y scission barriers, while deoxygenated linear products are favoured on Fe and Ni surfaces due to their low CH_x -OH_y scission and moderate hydrogenation barriers. Bimetallic alloy catalysts were also screened for their potential HDO activity and PtFe catalysts were found to significantly lower the ring opening and deoxygenation barriers relative to the corresponding pure metals. The developed BEPs for monometallic surfaces can be extended to estimate the barriers on bimetallic surfaces for ring opening and ring hydrogenation reactions but fails to predict the barriers for open-ring activation reactions due to the change in transition state binding sites on the bimetallic surface. The obtained BEP and TSS relationships can be used to develop microkinetic models for facilitating accelerated catalyst discovery for HDO.</p>
123.	<p>LYLAA: A lightweight YOLO based legend and axis analysis method for CHART-Infographics HS Kawoosa, MS Kanroo, P Goyal - DocEng '23: Proceedings of the ACM Symposium on Document Engineering, 2023</p> <p>Abstract</p> <p>Chart Data Extraction (CDE) is a complex task in document analysis that involves extracting data from charts to facilitate accessibility for various applications, such as document mining, medical diagnosis, and accessibility for the visually impaired. CDE is challenging due to the intricate structure and specific semantics of charts, which include elements such as title, axis, legend, and plot elements. The existing solutions for CDE have not yet satisfactorily addressed these issues. In this paper, we focus on two critical subtasks in CDE, Legend Analysis and Axis Analysis, and present a lightweight YOLO-based method for detection and domain-specific heuristic algorithms (Axis Matching and Legend Matching), for matching. We evaluate the efficacy of our proposed method, LYLAA, on a real-world dataset, the ICPR2022 UB PMC dataset, and observe promising results compared to the competing teams in the ICPR2022 CHART-Infographics competition. Our findings showcase the potential of our proposed method in the CDE process.</p>
124.	<p>Machinability and surface integrity analysis of magnesium AZ31B alloy during laser assisted turning N Deswal, R Kant - Journal of Manufacturing Processes, 2023</p> <p>Abstract</p> <p>Magnesium AZ31B alloys are promising materials for biomedical, aviation, and automotive industries. Severe plastic deformation processes such as machining processes have shown capabilities to improve the performance of magnesium AZ31B alloys. However, the usage of water and oil-based coolants during the machining of magnesium AZ31B alloys generates hydrogen and hazardous gases, which can explode and create a hazardous environment for nature and human beings. Therefore, machining without using any coolants has been preferred to machine magnesium AZ31B alloys. Moreover, laser assisted turning (LAT) has emerged as a hybrid machining process to machine various materials without using any coolants and in an eco-friendly manner. Hence, an attempt has been made to analyze the machining performance of</p>

	<p>magnesium AZ31B alloy during the LAT process. In this study, the machinability and surface integrity of magnesium AZ31B alloy was compared for LAT and conventional turning (CT) processes. With the usage of laser, a substantial decrement in machining forces, surface roughness, and tool wear was achieved during LAT than CT. Though, the machining temperature was obtained to be higher for LAT in comparison to CT. Long, continuous, and ductile chips were formed in LAT. Lesser scratches, cracks, and pits were observed on the machined surface during LAT than in CT. Coarse grain microstructure was observed for both CT and LAT. However, lower microhardness was obtained in LAT than in CT. Compressive residual stresses were achieved for LAT than tensile residual stresses in CT. Corrosion resistance was enhanced by up to 50 % for the LAT process than in the CT process.</p>
125.	<p>Mechanical, electronic and thermodynamic properties of crystalline molecular hydrogen at high pressure XY Yang, R Ahuja, W Luo - Physics Letters A, 2023</p> <p>Abstract Solid molecular hydrogen exhibits a rich variety of unique properties, including insulator-to-metal transition. However, the specific structure of phase III remains unclear. Experimental evidence suggests high-pressure hydrogen shows a hexagonal close-packed lattice. Therefore, as a potential candidate for phase III, the structure, energetic, mechanical, electronic, and thermodynamic properties of P6₁22 structure are systemically studied. It is found phase III with P6₁22 space group is both mechanically and thermodynamically stable within the pressure range of 120~300 GPa. Besides, we observed significant enhancements in the bulk modulus, shear modulus, and Young's modulus. The band structures exhibit a transition from topological insulator to topological semiconductor and eventually to a Wely semimetal as the pressure increases. The electron density accumulates between pseudo “H₂” molecules in the insulating phase but it partly channels into the interlayer space in the semimetallic phase. Phase III with P6₁22 structure is barely explored previously in solid hydrogen, therefore, we believe our present investigation contributes valuable insights towards understanding the behavior of metallic hydrogen.</p>
126.	<p>Microstructure, microhardness and tribological properties of electrodeposited Ni–Co based particle reinforced composite coatings Jhalak, D Beniwal, R Garg - Coating Materials: Computational Aspects, Applications and Challenges: Book Chapter, 2023</p> <p>Abstract Electrodeposited Ni–Co coatings are employed in various industrial applications due to their corrosion and wear resistant properties. The performance of these coatings can be further enhanced by the incorporation of ceramic particles in Ni–Co matrix. The optimal selection and precise control of various parameters, such as bath composition, current density and pH, during the electrodeposition process is critical for obtaining coatings with desired quality and properties. This review consolidates the insights, gained from existing literature, into the effect of all these parameters on the microstructure, microhardness and tribological properties of nickel–cobalt based coatings reinforced with carbide, nitride and oxide particles. The optimal values of various parameters, as reported in various studies, are also presented in this review, along with an assessment of the recent advances in the development of particle-reinforced Ni–Co coatings.</p>
127.	<p>Modeling and analysis of CMOS-based folded memristive crossbar array for 3D neuromorphic integrated circuits SK Thomas, SK Vohra, R Sharma...DM Das... - 2023 IEEE 73rd Electronic Components and Technology Conference (ECTC), 2023</p> <p>Abstract The scalability of the crossbar array is critical for performing complex computation tasks, as</p>

	<p>large-scale synaptic arrays are required to complete the operations. To address the drawbacks of a 2D neuromorphic IC, such as long routing paths and large die area, 3D IC technology is considered, where the stacking of the crossbar array enhances the system's scalability. Therefore, a novel crossbar architecture for 3D neuromorphic IC is proposed where the crossbar array is folded to decrease the area by approximately 50%, thereby enhancing the architecture's synaptic density by 50%. In the proposed architecture, CMOS-based memristors are employed, which can be interconnected to the word or bit lines by simple metal lines without using TSVs or MIVs, reducing the crossbar's area and its associated parasitics. Due to the folding of the crossbar layer, the length of the word lines gets reduced by half; therefore, there will be a significant reduction in the parasitics associated with the crossbar, which will help improve the system's performance. A Q3D model of the proposed 3D architecture of the crossbar is designed to extract the parasitics associated with it and to verify and validate the proposed novel concept. An RC circuit model of the proposed architecture is built using the parasitics extracted from the Q3D model to analyze its effect on the system. The circuit is designed in 65nm CMOS technology.</p>
128.	<p>Modified knowledge-based neural networks using control variates for the fast uncertainty quantification of on-chip MWCNT interconnects K Dimple, S Guglani, A Dasgupta...R Sharma... - IEEE Transactions on Electromagnetic Compatibility, 2023</p> <p>Abstract: In this article, a modified knowledge-based artificial neural network (KBANN) metamodel is developed for the efficient uncertainty quantification of on-chip multiwalled carbon nanotube (MWCNT) interconnects. The proposed KBANN metamodel utilizes the notion of control variates to enable much faster training than what is possible with standard KBANNs. Importantly, techniques to calculate the optimal value of the control variates in an a priori manner without augmenting the training dataset have been developed in this article. Furthermore, techniques to exploit the control variates depending on whether one or multiple low-fidelity models of the MWCNT interconnects are available have also been developed in this article. The benefits of the proposed KBANN metamodel using control variates over standard KBANN metamodels have been validated using multiple MWCNT interconnect examples spanning multiple technology nodes.</p>
129.	<p>New potential energy surface and rotational deexcitation cross-sections of CNNC by para-H₂ (<i>j_p</i>=0) Ritika, TJ Dhillip Kumar - Physical Chemistry Chemical Physics, 2023</p> <p>Abstract The objective of this study is to enhance our understanding of the existence of molecules in interstellar space by determining the collisional rate coefficients with the most prevalent species. The study examines the impact of para-H₂ collisions, specifically when it is in its ground vibrational state with a nuclear spin of para-H₂, i.e., <i>j_p</i>=0, on causing the rotational deexcitation of the diisocyanogen (CNC) molecule. This scattering data comes as a result of spherically averaging a four-dimensional potential energy surface (4DPES) over the H₂ orientations. Using the CCSD(T)-F12a approach and aug-cc-pVTZ basis sets, the ab initio 4DPES for the CNC-H₂ van der Waals system is calculated. The CNC-para-H₂ 4DPES attains a global minimum of 221.38 cm⁻¹ at the CNC and H₂ center of mass distance (<i>R</i>) of 3.1 Å. The method of close coupling calculations is employed for the purpose of calculating cross-sectional data of CNC with para-H₂ (<i>j_p</i>=0), for total energies up to 1000 cm⁻¹. Rate coefficients are computed over a temperature range of 1 K to 100 K. Propensity suggests that even Δj transitions are strongly preferred. The rate coefficients for CNC-H₂ are determined to be 0.90-2.95 times of CNC-He, which implies it is not reliable to estimate the H₂ rate coefficients by multiplying the rate coefficients for CNC-He collision with a scaling factor of 1.38.</p>
130.	<p>NiCr2O4 nanozyme based portable sensor kit for on-site quantification of nerve agent mimic for environment monitoring</p>

	<p>M Kumar, N Kaur, N Singh - Sensors and Actuators B: Chemical, 2023</p> <p>Abstract</p> <p>Nerve agents are among the most dangerous chemical known to the human being. On account of an incident by utilizing nerve agents, the fabrication of a cost-effective and ready-to-use device for the convenient identification of nerve agents is needed. Herein, we developed a easy-to-use, portable sensor kit based on NiCr2O4 artificial nanozyme mimic to quantify diethyl-chlorophosphate (DCP). The synthesized NiCr2O4 artificial nanozyme showed good oxidase and peroxidase-like catalytic activity for the conversion of colorless tetramethylbenzidine (TMB) to bluish-green oxTMB. It is recognized that the presence of DCP can assist the oxidation of TMB due to the easy binding of DCP with the amine group of TMB and enhance the catalytic process. Therefore, this mechanism is utilized to fabricate a colorimetric sensor kit for naked-eye quantification of DCP, which gives yellowish color after interaction with oxTMB. Furthermore, the practicability of a portable sensor kit was performed for the quantification of DCP in soil and water samples, and results showed a detection limit of 15.4 nM (3σ method). Thus, the proposed portable sensor kit's naked eye detection paves the way for an affordable and practical platform for the easy-to-use, reliable, and quick colorimetric quantification of DCP for environment monitoring.</p> 
131.	<p>Nonlinear transient response of sandwich beams with functionally graded porous core under moving load W Songsuwan, N Wattanasakulpong, S Kumar - Engineering Analysis with Boundary Elements, 2023</p> <p>Abstract</p> <p>Nonlinear transient response of sandwich beams possessing functionally graded porous core under the action of moving load was examined in this study. With this regard, Reddy's third-order shear deformation theory and the geometrical nonlinearity of von Kármán assumption were utilized to construct the governing equation system. The set of governing equations was solved by the Gram-Schmidt-Ritz method in conjunction with iterative procedures based on the time-integration of Newmark for the convergence in time and geometrical domains. According to the methodology, we received accurately stable results of nonlinear free and forced vibration of the sandwich beams. Several important parameters such as slenderness ratio, layer thickness's ratio, porous coefficient, types of porous distribution, etc. that have a significant impact on nonlinear deflection of the beams were taken into account. Based on numerical experiments, it can be disclosed that the sandwich beams carrying porous distribution in form of functionally graded materials are much better than the beams with uniform porous distribution in terms of strength and stiffness. The porous coefficient also plays an important role in changing the ability of loading resistance.</p>
132.	<p>NTIRE 2023 image shadow removal challenge report F-A Vasluianu, T Seizinger.. SS Phutke, A Kulkarni, MDR Khan, S Murala, SK Vipparthi.. - Proceedings of the IEEE/CVF Conference on Computer Vision and Pattern Recognition, 2023</p> <p>Abstract</p> <p>This work reviews the results of the NTIRE 2023 Challenge on Image Shadow Removal. The</p>

	described set of solutions were proposed for a novel data set, which captures a wide range of object-light interactions. It consists of 1200 roughly pixel aligned pairs of real shadow free and shadow affected images, captured in a controlled environment. The data was captured in a white-box set up, using professional equipment for lights and data acquisition sensors. The challenge had a number of 144 participants registered, out of which 19 teams were compared in the final ranking. To posed solutions extend the work on shadow removal, improving over the performance level describing state-of-the art methods.
133.	<p>Numerical modelling of transport and fate of chromium (VI) in sub-surface porous media S Ganguly, S Ganguly - Lecture Notes in Civil Engineering, 2023</p> <p>Abstract Chromium (VI) is used in major industries like stainless steel production, electroplating, leather tanning and textile dye synthesis. If Cr (VI) is disposed without any proper treatment, it might leach into the soil and pollute the groundwater. Chromium (VI) is a known carcinogen and is thus extremely harmful if consumed. The present study numerically models the transport and fate of chromium (VI) leached from a stainless steel plant located in the Rupnagar District, Punjab, for a period of 20 years using COMSOL Multiphysics simulation software. A contaminant transport model is developed including the processes of advection, dispersion and sorption. A uniform recharge through precipitation is considered from the topmost layer of the soil profile in the study. The numerical model is validated using standard analytical solutions of the advection–dispersion equation.</p>
134.	<p>Numerical study of the effect of Péclet number on miscible viscous fingering with effective interfacial tension YF Deki, Y Nagatsu, M Mishra... - Journal of Fluid Mechanics, 2023</p> <p>Abstract Viscous fingering or Saffman–Taylor instability shows fingering interfacial patterns when a more mobile fluid displaces a less mobile one in porous media. The effective interfacial tension(EIT) is like capillary force, acting at the miscible interface on timescales shorter than interface relaxation. It has been numerically reported so far that the fingers are wider with EIT compared with those without EIT. A recent experiment observed finger widening with increasing flow rate in a miscible system with EIT, which is not observed in classical immiscible and miscible systems. In this study, we have numerically investigated the effect of Pe(which corresponds to the injection flow rates in the experiment) on miscible viscous fingering with/without EIT. We have shown that the fingers are monotonically thinner with an increase in Pe in the system without EIT, while finger widening with increasing Pe is observed in the system with EIT. Furthermore, we have also examined a one-dimensional underlying concentration profile and EIT profile by using a one-dimensional diffusion–convection model because EIT is proportional to the squared concentration gradient. We have then shown that the concentration gradient is steeper and, thus, the EIT is larger as Pe I larger. Therefore, this is the first numerical study that can theoretically verify finger widening with increasing flow rate, which occurs only in a miscible system with EIT to the extent of our targeting EIT values, and explain the mechanism by one-dimensional analysis.</p>
135.	<p>Optimal synthesis of reconfigurable manipulators for robotic assistance in vertical farming N Chitre, A Dogra, E Singla - Robotica, 2023</p> <p>Abstract Due to the ever-increasing demand for food commodities and issues arising in their transport from rural to urban areas, commercial agricultural practices with the help of vertical farming are being taken up near urban regions. For the realization of agricultural practices on high-rise vertical farms, where human intervention is quite laborious, robotic assistance would be an effective solution to perform agricultural processes like seeding, transplanting, harvesting, health</p>

	<p>monitoring, nutrient-water supply, etc. The requirements and complexities of these tasks to be performed are different such as end-effector requirement, payload capacity required, amount of clutter while performing the task, etc. In such cases, an individual robotic configuration would not serve all the purposes and each task may require a different configuration. Purchasing a large number of configurations, as per requirement, is not economical and will also increase the cost of maintenance. Thus, the design of a reconfigurable robot manipulator is proposed in this work which can cater to modular layouts. A thorough study of the processes involved in the farming of leafy vegetables is done and the tasks to be performed by the manipulator are identified. Constrained optimization is performed based on reachability, while minimizing DoF, for the tasks of transplanting, plant health monitoring, and harvesting to find the optimal configurations which can perform the given tasks. The study resulted in 5-DoF, 4-DoF, and 6-DoF configurations for transplanting, plant health monitoring, and harvesting, respectively, thus emphasizing the need of a reconfigurable solution. The configurations are realized using modular library and verified to satisfy reachability to provide a complete solution.</p>
136.	<p>Optimization of cooling condition and energy parameters during laser bending of Duplex-2205 R Yadav, R Kant – <i>Materials and Manufacturing Processes</i>, 2023</p> <p>Abstract In this study, the impact of process parameters on bend angle was explored under varying cooling conditions. Optimization of process parameters and cooling conditions was performed to maximize bend angle with minimum energy input. A regression fit function was generated and experimentally validated, and the mechanical and metallurgical properties at the optimum condition were analyzed. The study revealed that forced cooling at the lower surface significantly improved the bend angle, achieving a 35.2% increase compared to natural cooling. Process parameters were found to have varying effects at different cooling conditions. Optimization using Pareto front optimality and genetic algorithm resulted in a 7.5% increase in bend angle and a 22.14% improvement in bend angle per line energy rate. The tensile strength and hardness of the bend specimen at the optimum condition were increased at the expense of ductility, attributed to phase distribution rearrangement in the laser irradiation region.</p>
137.	<p>Organocatalytic (3+3)-cycloaddition of <i>ortho</i>-substituted phenyl nitrones with aryl cyclopropane carbaldehydes: a facile access to enantioenriched 1,2-oxazinanest A Hazra, A Ghosh, N Yadav, P Banerjee - <i>Chemical Communications</i>, 2023</p> <p>Abstract The first asymmetric (3+3)-cycloaddition of <i>ortho</i>-substituted phenyl nitrones with aryl cyclopropane carbaldehydes has been demonstrated by secondary amine catalysts. While the other <i>ortho</i>-substituents gave 1,2-oxazinanest, <i>ortho</i>-hydroxy ones provided a novel class of tetrahydrochromeno-1,2-oxazine cores <i>via</i> rare 1,3-aryl migration, followed by cyclization. An unusual type of asymmetric approach was also recognized.</p>
138.	<p>Organocatalytic activation of donor-acceptor cyclopropanes: A tandem (3 + 3)-cycloaddition/aryl migration toward the synthesis of enantioenriched tetrahydropyridazines A Hazra, R Dey, A Kushwaha, TJ Dhilip Kumar, P Banerjee - <i>Organic Letters</i>, 2023</p> <p>Abstract An organocatalytic enantioselective (3 + 3)-cycloaddition reaction of racemic cyclopropane carbaldehydes and aryl hydrazones has been demonstrated for the first time. A wide range of enantioenriched tetrahydropyridazines with an exocyclic double bond were obtained with moderate to good yields and good to excellent enantiomeric excesses. Mechanistic investigations hinted toward a matched/mismatched kinetic resolution, and control experiments and DFT calculations unveiled that 1, 3-aryl migration was concerted and intramolecular and proceeds via a four-membered transition state.</p>

139.	<p>Orthogonal signal based single phase FLL with minimum computational overhead for adverse grid conditions M Satyanarayana, AV Ravi Teja - IEEE Journal of Emerging and Selected Topics in Industrial Electronics, 2023</p> <p>Abstract In this paper, a frequency locked loop (FLL) is proposed for distorted single phase grid systems. The proposed algorithm estimates the grid phase and frequency angle with minimal errors by using the orthogonal signal of Harmonic Flag-Modified second-order generalized integrator (HF-MoSOGI) and digital estimator stage. The proposed method achieves these estimates independently without using trigonometric and division operations. The implementation of the proposed FLL is straightforward and has minimum computational overhead. The proposed algorithm, along with the detailed procedure for hardware implementation, is explained in this paper. The simulation and hardware results are presented at various grid adversities to verify the proposed algorithm's improved dynamic response and effectiveness under steady grid disturbances(harmonics and dc offset). The Proposed FLL is also used to implement the single-phase grid-tied inverter using hysteresis current control, and the results in simulation and hardware are reported.</p>
140.	<p>Oxidized pullulan exhibits potent antibacterial activity against S. aureus by disrupting its membrane integrity S Roy, M Halder, P Ramprasad, Y Singh...D Pal... - International Journal of Biological Macromolecules, 2023</p> <p>Abstract The capability of bacteria to withstand the misuse of antibiotics leads to the generation of multi-drug resistant strains, posing a new challenge to curb wound infections. The biological macromolecules, due to their biocompatibility, biodegradability, and antimicrobial properties, have been explored for a variety of antimicrobial and therapeutic purposes. This work reports that a single-step oxidation of pullulan polymer leads to the formation of oxidized pullulan (o-pullulan), which shows striking antibacterial and antibiofilm activities against the Gram-positive bacteria, <i>Staphylococcus aureus</i>, implicated in wound-related infections. Oxidation of pullulan generates 28 % aldehyde groups (3.462 mmol/g) which exerted 97 % bactericidal activity against <i>S. aureus</i> by targeting cell wall-associated membrane protein SpA (Staphylococcal protein A). The molecular docking, gene silencing, and fluorescence quenching studies revealed a direct binding of o-pullulan with the B and C domains of SpA, which alters the membrane potential and inhibits Ca^{2+}-Mg^{2+}-ATPase pumps. O-pullulan also exhibited scavenging activity against intracellular reactive oxygen species (ROS), and non-immunotoxic activity and was found to be non-toxic to mammalian cells. Thus, o-pullulan shows great promise as an antimicrobial polymer against <i>S. aureus</i> for chronic wound management.</p>
141.	<p>Performance evaluation of Indian electricity distribution companies: An integrated DEA-IRP-TOPSIShttps://www.sciencedirect.com/science/article/abs/pii/S0140988323002943 approach VS Patyal, R Kumar, K Lamba... - Energy Economics, 2023</p> <p>Abstract Energy is a fundamental building block of human growth and plays a significant role in developing emerging economies such as India. The Indian electricity sector has a strong generation and transmission system but a weak distribution system. This is considered the weakest link in the electricity sector's value chain, and regulators are primarily concerned with the performance of electricity distribution companies (DISCOMs). Despite numerous reforms introduced to attain financial sustainability, most DISCOMs consistently incur losses and are financially unsustainable. Therefore, evaluating the performance of DISCOMs is essential by</p>

	<p>measuring their efficiency to ensure competition among them and to make reforms successful. This study aimed to identify and compare the performance efficiencies of 48 electricity DISCOMs from 24 states across India between 2015/16 and 2018/19. This study used the integrated DEA-IRP-TOPSIS technique to segment efficient and inefficient DISCOMs. The study recommends that states provide operational and financial autonomy to power Discoms. The study will be helpful for DISCOMs professionals to understand their performance and design suitable strategies based on efficiency assessments and their position concerning their peers. By comparing Indian DISCOMs with their contemporaries, this study contributes new evidence at the policy level and to the literature on the efficiency analysis of Indian DISCOMs.</p>
142.	<p>Performance measurement and discharge data based analysis of ultrasonic assisted μEDM for Ti6Al4V Sohaib Raza, Jay Airao, CK Nirala - Journal of Micro and Nano-Manufacturing, 2023</p> <p>Abstract Unconventional machining of difficult-to-cut conductive materials with high accuracy, low heat-affected zone formation, and the ability to cut intricate geometries entitles micro-electrical discharge machining (μEDM) as the most versatile technology in micromachining. Ultrasonic vibration assistance further enhances the material-removing ability of the μEDM process while imparting several other benefits. The present work proposes a comparative study between the unassisted and ultrasonic vibration assisted μEDM to the tool electrode for machining microslots on Ti6Al4V material using an in-house developed tool holder. The characteristics of the discharge waveforms were captured using a data acquisition system at high sampling rates. The pulse discrimination system is used to perform an in-depth study of the discharge pulses. μEDM milling experiments were performed to machine microslots at varying input voltages, capacitances, and feed rates. The ultrasonic vibrations proved beneficial in addressing the primary issue associated with the μEDM process, i.e., the material removal rate (MRR) with a maximum of 35% increment. Applying ultrasonic vibrations reduced the recast layer and tool wear rate (TWR) and increased the surface finish.</p>
143.	<p>Performance of two-dimensional MoS₂ Field-Effect transistor in the presence of oxide-channel imperfection A Rawat, A Goel, B Rawat - 2022 IEEE International Conference on Emerging Electronic(ICEE 2022), 2022</p> <p>Abstract In this work, we propose a more accurate description of the interface trap in the MoS₂ field-effect transistor using a quantum-mechanical modeling framework. Introducing an interface trap based on tight-binding parameter substitution at an atomic site is found to be a more effective way to include its effect on the device electrostatics and the carrier transport. Further, lower energy interface traps from conduction band are found to significantly impact the device performance, with severe degradation in subthreshold slope and ON-current. Our proposed model reveals that charge trapping in the interface trap causes substantial degradation in the drive current for high gate biases, whereas source-to-drain tunneling through trap limits the performance for low gate biases.</p>
144.	<p>Photocatalytic and thermoelectric performance of a symmetrical two-dimensional Janus aluminum chalcogenides Z Haman, M Kibbou, N Khossossi ...R Ahuja... - Journal of Physics: Energy, 2023</p> <p>Abstract Through a density functional theory-driven survey, a comprehensive investigation of two-dimensional(2D)Janus aluminum-based monochalcogenides(Al₂XY with X/Y = S, Se, and Te) has been performed within this study. To begin with, it is established that the examined phase, in which the Al-atoms are located at the two inner planes while the (S, Se, and Te)-atoms occupy</p>

	<p>the two outer planes in the unit cell, are energetically, mechanically, dynamically, and thermally stable. To address the electronic and optical properties, the hybrid function HSE06 has been employed. It is at first revealed that all three mono layers display a semiconducting nature with an indirect band gap ranging from 1.82 to 2.79 eV with a refractive index greater than 1.5, which implies that they would be transparent materials. Furthermore, the monolayers feature strong absorption spectra of around 10^5 cm^{-1} within the visible and ultraviolet regions, suggesting their potential use in optoelectronic devices. Concerning the photocatalytic performance, the conduction band-edge positions straddle the hydrogen evolution reaction redox level. Also, it is observed that the computed Gibbs free energy is around 1.15 eV, which is lower and comparable to some recently reported 2D-based Janus monolayers. Additionally, the thermoelectric properties are further investigated and found to offer a large thermal power as well as a high figure of merit (ZT) around 1.03. The aforementioned results strongly suggest that the 2D Janus Al-based monochalcogenide exhibits suitable characteristics as a potential material for high-performance optoelectronic and thermoelectric applications.</p>
145.	<p>Photonic structure induced enhancement in the triplet state dynamics of organic phosphors at room S S Behera, A Ghorai, S Garain ...RV Nair... - Advanced Optical Materials, 2003</p> <p>Abstract Triplet state modification in organic phosphorescence molecules for a desired color and quantum yield is typically pursued by chemical modification. A facile methodology is introduced to tune the triplet state dynamics of a phosphorescent molecule by changing the host-matrix parameters. An organic phosphor, Br₂PmDI (2-Bromo pyromellitic diimide), dispersed at dilute levels (1.5 wt.%) in a semicrystalline high-κ relaxer ferroelectric host matrix emit room-temperature phosphorescence accompanied by a delayed fluorescence component. The host relaxer ferroelectric polymer film can be engineered to form a photonic matrix with a regular micropore structure of refractive index contrast ≈ 0.6 that can increase the density of optical states and introduce photonic coupling. The phosphorescence quantum yield of Br₂PmDI in this photonic matrix increases by ≈ 2.3 fold, and the lifetime reduces by a factor of three. The coupled quantum states are investigated by time-resolved spectroscopy at different temperatures and pump intensities.</p>
146.	<p>Physician's knowledge and attitudes on antibiotic prescribing and resistance: A cross-sectional study from hail region of Saudi Arabia K Almansour, JA Malik, I Rashid... - Healthcare, 2023</p> <p>Abstract Background: Antibiotic (AB) resistance is caused partly by overuse, varies by region, and is influenced by prescriber perspectives. This study sought to determine physicians' knowledge and attitudes toward AB prescribing, particularly in the Hail region of Saudi Arabia. Methods: An interdisciplinary team created and validated an electronic questionnaire via the test-retest method that measured reliability and consistency. The 19 questions covered the following subjects: demographic information (7), experience with AB resistance in daily work (3), AB prescribing behavior (2), communication with patients regarding AB resistance (3), and prescribing practices (4). The revised questionnaire was prepared and distributed to physicians in the Hail region via multiple electronic communication channels. Inferences were drawn based on descriptive statistics and multivariate regression analysis. Results: The questionnaire responses of 202 participants were eligible for analysis. A total of 70 (34.80%) participants were general practitioners, 78 (38.12%) were engaged in daily work that was only mildly related to AB resistance, and 25 (12.37%) performed work that was substantially related to AB resistance. A total of 88 (43.56%) physicians believed that prescribing behavior contributed to the emergence of AB resistance, whereas 68 (33.66%) did not. Regarding exposure, 51 (25.24%) physicians</p>

	<p>reported encountering instances of AB resistance monthly, whereas 104 (51.48%) reported seeing cases of AB resistance very rarely. In terms of prescribing practices, 99 (49.0%) physicians prescribed ABs to patients daily and 73 (36.13%) weekly. Regarding AB-resistance-related communication with patients, 73 (36.13%) physicians frequently discussed AB resistance with patients suffering from infections, whereas 13 (6.4%) never discussed it with patients. Conclusion: General practitioners in the Hail region exhibited comprehensive awareness of the elements that contribute to AB resistance but only rarely communicated about the issue with their patients, presuming the latter to be oblivious to the science behind AB resistance. Our findings suggest that the features underlying practitioners' AB prescribing behavior could be a powerful strategy for lowering AB resistance.</p>
147.	<p>Pinning of graphene for conformal wrinkling over a soft corrugated substrate through prestretch-release process M Pandey, BK Parida, M Ranjan, R Ahuja, R Kumar - <i>Applied Surface Science Advances</i>, 2023</p> <p>Abstract The adhesion of a 2D material to a substrate is facilitated by the van der Waals (vdW) interactions, which is significantly influenced by the roughness and wettability of the substrate. It is challenging to achieve good as well as conformal adhesion of mechanically exfoliated 2D materials to a hydrophobic soft substrate like polydimethylsiloxane (PDMS). In addition, the mechanical folding instabilities are inevitably observed in 2D elastic nanosheets over a smooth PDMS substrate under higher compressions in a prestretch-release process. However, the manipulation of the soft substrate's surface roughness may provide an essential degree of freedom for tailoring the conformation level and topography of the 2D elastic nanosheets. Herein, we propose a technique to improve the interfacial adhesion of the graphene membrane to a periodically trenched PDMS substrate by suppressing the mechanical folding instabilities in a prestretch-release process. The conformal wrinkling of the graphene membrane, as confirmed through atomic force microscopy (AFM) imaging, is found to result from its pinning into the trenches via snap-through transition. We also show the impact of the substrate's topography on the buckling behavior of the graphene membrane under the stress loading-unloading cycle by surface-engineering of the PDMS substrate using ion beam irradiation. This study offers fundamental as well as practical insights into the adhesion mechanics of the 2D elastic nanosheets over the corrugated soft substrates under the prestretch-release process. The wrinkled topography of the membrane could be harnessed for flexible, conformal, and tunable electronic devices.</p>
148.	<p>Playing it the nation's way: tradition, cosmopolitanism, and the native-masculine of Hindi sports films P Radhakrishnan, D Ray - <i>Contemporary South Asia</i>, 2023</p> <p>Abstract The generic popularity of Hindi sports films has been overwhelming in recent years. The article examines this genre of Hindi films through the thematic construction of the sports'man' and its evolutionary manifestation from a masculine figure symbolising India's national unitarian ethos to a megalithic, tradition-backed, orthodox patriarchy post-2010s. It elaborates this seemingly linear transformation through decade based phases, starting from the social-emancipatory athletic phenomenon of the pre-globalisation era to the neoliberal Hindi sports films of the early millennial phase. The study then explores the slow dissolution of the 'composite masculinity' that considered the ethnic variegation of Indian nationalism, and the emergence of sporting cinema on patriarchal and athletic superheroes. The article further discusses how it was nurtured within deeply insular, and ethno-religious gaming traditions of antiquity like the <i>akhara</i> wrestling, in fictional/biographical sports films like <i>Sultan</i> (Zafar 2016) and <i>Dangal</i> (Tiwari 2016). While commenting on this transformation of the 'national athlete' into the 'heritage's surrogate', the article attempts to provide a detailed methodology of</p>

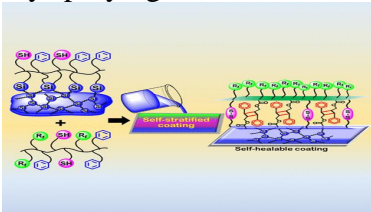
	understanding the expanding canon of Hindi sports films so far and how it aligns itself with the re-ethnicisation of India's polity in the last two decades.
149.	<p>PO⁺-He collision: Ab initio potential energy surface and inelastic rotational rate coefficients P Chahal, TJ Dhillip Kumar - Monthly Notices of the Royal Astronomical Society, 2023</p> <p>Abstract Computations involving quantum dynamics are performed to attain cross-sections corresponding to rotational de-excitation and excitation rates of the PO⁺ species including four rotational lines recently detected in the interstellar molecular clouds. New ab initio potential energy surface (PES) for PO⁺-He collision is constructed by using CCSD(T) method and basis set extrapolated to complete basis set limit (CBS) considering a rigid rotor approximation. The PES is then trained to create neural network (NN) model to construct an augmented surface with angular coordinates at 1° intervals. The PES has a global minimum located at and R = 3.1 Å. An analytical fitting is performed on the NN surface to obtain the first 41 radial coefficients needed to solve the equations of the coupled-channel method. The essentially precise close coupling approach is used to compute the rotational (de-)excitation cross-sections till 1400 cm⁻¹ with rotational states converged up to 26. Further, these cross-sections are thermally averaged to get the rate coefficients for various rotational transitions till 200 K. The propensity rule favours the odd transitions ($\Delta j = 1$) for the current study. The rate for the transition 5 → 4 is found to be higher than transition 1 → 0 by a factor of 3.1 at T = 20 K that decreases to 2.1 at T = 100 K.</p>
150.	<p>Polypyrrole nanocomposites as promising gas/vapour sensing materials: past, present and future prospects A Husain, MU Shariq - Sensors and Actuators: A. Physical, 2023</p> <p>Abstract Development of highly efficient gas/vapour sensor is an urgent necessity because of rapidly increasing emission of various hazardous and highly flammable gases/vapours. The chemical detection and quantification are extremely important to control and monitor the pollutant or toxins and flammable gases/vapours to ensure the safety of eco-system. Nano sensors have fascinated massive interest owing to their excellent performance along with being compact, easy to fabricate and cost effective. Over the years, polypyrrole (PPy) is one of the conducting polymers (CPs), proved to be excellent materials for gas/vapour sensing application at room temperature operations. But pristine PPy has some drawbacks such as poor selectivity & reversibility and poor long-term stability. However, these sensing properties can be significantly improved by making nanocomposites of PPy by adding semiconductor metal oxide and/or carbon nanomaterials which amplify adsorption, catalytic reaction and charge transport behaviour. Hence, PPy nanocomposites have been employed as the gas/vapour sensing materials for detection and monitoring of various gases such as ammonia (NH₃), liquefied petroleum gas (LPG), hydrogen disulphide (H₂S), carbon oxides (CO & CO₂), nitrogen oxides (NO & NO₂), hydrogen (H₂) and different volatile organic compounds (VOCs) such as acetone, ethanol, methanol, formaldehyde, toluene etc. Current review is focused on the gas/vapour sensing properties of PPy nanocomposites along with future prospects for the development of new PPy nanocomposites for the fabrication of highly efficient sensors.</p>
151.	<p>Portable, wireless and easy to use device for negative pressure wound therapy Ashima, VK Dubey, B Basumatary, A Sahani - 2023 IEEE International Symposium on Medical Measurements and Applications (MeMeA), 2023</p> <p>Abstract Wound healing is a natural biological process in the human body, achieved through four interdependent, precisely and highly programmed phases. Every wound is unique and is affected by various factors hence optimization of wound healing mechanism based on the complexity of wound is of utmost importance. NPWT has emerged to be a prominent systematic wound</p>

	<p>treatment practice for chronic wounds such as arterial ulcers, diabetic foot ulcers, non healing surgical wounds, pressure ulcers, traumatic wounds, vasculitic ulcers (leg), venous stasis ulcers, etc. Typically, an optimum pressure range of 88 to 125 mmHg exhibits positive and promising effects in this kind of therapy. Despite assisting the wound healing mechanism in many ways, this method poses certain problems too. The key to this process lies in optimization of the value of negative pressure, duration of negative pressure application, and the number of times the treatment has to be performed based on the type of wound. Here in this study our aim is the modification of negative-pressure wound therapy such that we make this device portable, wireless and easy to operate on different negative pressure settings. Other than these optimizations we have incorporated the process of instillation wherein wound flushing is done with help of saline, antiseptic, anti-infective drugs or growth factor solutions.</p>
152.	<p>Correction to: Prediction of the future landslide susceptibility scenario based on LULC and climate projections (Landslides, (2023), 10.1007/s10346-023-02088-6) A Tyagi, RK Tiwari, N James - Landslides, 2023</p> <p>Abstract The authors regret that the Fig. 7 that appears in the article is incorrect. The correct Fig. 7 is shown below. (Figure presented.) Sensitivity analysis of the eighteen landslide causative factors (TRI is topographic ruggedness index, RR is relative relief, SPI is stream power index, PHA is peak horizontal acceleration, TWI is topographic wetness index, and STI is sediment transport index) The original article has been corrected.</p>
153.	<p>Power saving approach of a smart watch for monitoring the heart rate of a runner A Vyas, S Pal - IEEE Transactions on Consumer Electronics (Early Access), 2023</p> <p>Abstract Heart Rate (HR) monitoring in a smart watch is a battery consuming process. Therefore, some smart watches prevent continuous HR sampling during low-level physical activities for improving the power usage of batteries. However, high acceleration events like running require continuous HR sampling for recording the varying HR readings, which consumes a lot of battery power. Therefore, the challenge is to reduce the sampling during running while recording an individual's HR variation (HRV). Our approach prevents continuous HR sampling for long-running events without missing important HR information. In this context, we analyze the existing real-life HRs and acceleration datasets recorded on humans during long runs. We design an adaptive HR sampling algorithm, A-HeaRing, from the extracted HR variation details. A-HeaRing reduces the battery power consumption of a smart watch by more than 50% while recording a running event. Additionally, we design a data regeneration system for missing HR readings. The regeneration system provides a minimum of 90% accuracy in the HR zone estimation.</p>
154.	<p>Quasi-one-andquasi-two-dimensional Bose-Fermi mixtures from weak coupling to unitarity P Kaur, S Gutam, SK Adhikari - The European Physical Journal Plus, 2023</p> <p>Abstract We study ultracold superfluid Bose-Fermi mixtures in three dimensions, with stronger confinement along one or two directions, using a non-perturbative beyond-mean-field model for bulk chemical potential valid along the weak-coupling to unitarity crossover. Although bosons are considered to be in a superfluid state, we consider two possibilities for the fermions – spin-polarized degenerate state and superfluid state. Simplified reduced analytic lower-dimensional models are derived along the weak-coupling to unitarity crossover in quasi-one-dimensional (quasi-1D) and quasi-two-dimensional (quasi-2D) settings. The only parameters in these models are the constants of the beyond-mean-field Bose-Bose and Fermi-Fermi Lee-Huang-Yang interactions and the respective universal Bertsch parameter at unitarity. In addition to the numerical results for a fully-trapped system, we also present results for quasi-2D Bose-Fermi</p>

	<p>mixtures where one of the components is untrapped but localized due to the interaction mediated by the other component. We demonstrate the validity of the reduced quasi-1D and quasi-2D models via a comparison of the numerical solutions for the ground states obtained from the reduced models and the full three-dimensional (3D) model.</p>
155.	<p>Recent advances in plasmonic enhanced nanocatalyst for oxidation of alcohol N Nath, S Chakroborty, K Pal ...N P Mishra... - Topics in Catalysis, 2023</p> <p>Abstract Plasmonic nanomaterials (PNMs) and catalytically active surfaces, when combined, provide novel opportunities for a wide range of potential applications of catalysis. When stimulated by the right kind of light, surface plasmons can be put to use to either directly cause or indirectly facilitate a wide variety of chemical reactions. PNMs are currently the center of extensive research that is being conducted for the purpose of determining whether or not they could be utilized to improve the efficiency of catalytic reactions. This is due to the fact that PNMs have the alluring ability to interact with light in a powerful fashion. These structures exhibit the singular property of localised surface plasmon resonance, which transforms light of a particular wavelength ranges into hot charge carriers, together with high local electromagnetic fields, or heat, which may all contribute in different ways to increasing the reaction efficiency. Plasmon-mediated catalysts, which go beyond the highly influential application of supported gold nanomaterials (NMs) to photo-oxidation reactions, can be utilised to create a greater variety of visible-light induced catalysts by combining various metals and supports with available Au, Ag, and Cu NMs and PNMs photocatalysts. Plasmon-mediated catalysts go beyond the highly influential application of supported gold nanomaterials (NMs) to photo-oxidation reactions. This would make it possible to develop a greater diversity of photocatalysts, which are catalysts that can be powered by visible light. This review will focus on the PNMs-based catalyst for alcohol oxidation, which will be addressed within the framework of this research.</p>
156.	<p>Recognition of bovine hemoglobin protein on molecularly imprinted polymer surfaces using nonlinear vibrational spectroscopy S Chaudhary, H Kaur, H Kaur...KC Jena - Applied Physics Letters, 2023</p> <p>Abstract Advancement in molecularly imprinted biomimetics has aided in developing robust artificial recognition-based materials, which can be customized for bio/chemo-sensing of distinct molecules. The present study reports a simple one-step synthesis and analysis of protein-imprinted polymer thin films as a recognition element directly onto a solid support. Dopamine has been explored as a versatile functional monomer for a molecularly imprinted polymer (MIP) matrix to fabricate polydopamine (PDA) thin films with bovine hemoglobin as a template protein molecule. A detailed molecular-level insight into the recognition of the template molecule at each step has been investigated using vibrational sum frequency generation (VSFG) spectroscopy. A suitable PDA-coated thin film is selected based on the extent of polymerized intermediates formed after non-imprinted polymer fabrication at different time durations. An optimally prepared film of MIP is specified by observing the spectral signature of the methyl groups from protein molecules at the air-polymer interface. The template removal from MIP films after the washing procedure and subsequent re-binding of the protein molecules were evaluated by VSFG spectroscopy. The insightful molecular-level findings from SFG spectroscopy demonstrate the fabrication of an imprinted matrix as a label-free chemical sensor.</p>
157.	<p>Release of geogenic fluoride from contaminated soils of Rajasthan, India: Experiments and geochemical modeling B Thakur, VA Loganathan, A Sharma... - Water Security, 2023</p> <p>Abstract Management of groundwater contaminants, that are primarily of geogenic origin, such as</p>

	<p>fluoride, is a major public health concern. Worldwide, around 200 million people are dependent on drinking water resources that contain elevated levels of fluoride that exceeds WHO's drinking water threshold limit of 1.5 mg/L. According to the Ministry of Drinking Water and Sanitation of India, about 11.7 million people, mostly in the Rajasthan state, are exposed to high fluoride risk. It is important to understand the soil–water interaction mechanisms to properly assess the fluoride contamination that are primarily due to geogenic origins prevalent in the region. In this study, batch desorption experiments were performed with soils obtained from varied depths at two sites in Rajasthan that has high fluoride levels in groundwater. The fluoride release kinetics followed a pseudo first-order kinetic model. The results of the batch experiments indicate higher release of fluoride from lower soil layers when compared to the upper layers. Further, the release of fluoride was dependent on pH wherein higher release was noticed under basic pH. Since the natural pH of the soils from this region is ca. pH 8 it is expected to play a vital role in the continued release of fluoride to the groundwater system. Furthermore, a simplified geochemical model, incorporating a general composite approach, has been used to simulate the experimental results that include dissolved Al and Al-F surface complexes. The model was able to capture the observed experimental results for various soils within a reasonable RMSE of 11.74%. The results of this study not only further the current understanding of the fate and transport mechanisms of fluoride in the contaminated subsurface but also would aid in designing remedial strategies to ensure future water security in this region.</p>
158.	<p>Risk perception and adoption of digital innovation in mobile stock trading S Gupta, DK Dey – Journal of Consumer Behaviour, 2023</p> <p>Abstract An increase in retail investors, trading platforms, and smartphones is facilitating digital transformation in stock trading. Investments in mobile-centered digitalization by trading firms are rapidly becoming a source of competitive advantage. Distinctive psychological aspects involving risks, make stock trading a unique individual decision-making behavior. The objective of the present research is to examine the determinants of retail investors' behavioral intentions (BI) for mobile stock trading (MoST). Across two studies using a mixed method approach we empirically test a framework comprising cognitive risk-mitigation factors, perceived risk (PR), perceived financial cost (PFC), and technology acceptance model (TAM) constructs. The results indicate information quality, privacy, and security protection to mitigate the risk perception involved in trading on mobile platforms. Further, we report the mediation of PR in the relationship between the cognitive risk-mitigating factors and BIs to adopt MoST. Moreover, we find PFC to moderate PR and the TAM constructs' relationship with BIs to adopt MoST. Our research has important theoretical contributions and managerial implications to understand digital adoption behavior by retail investors for MoST platforms.</p>
159.	<p>Rumination moderates the association between neuroticism, anxiety and depressive symptoms in Indian women P Singh, N Mishra - Indian Journal of Psychological Medicine, 2023</p> <p>Abstract Background: The higher prevalence of depressive symptoms among women demands an in-depth exploration of every possible mechanism through which depressive symptoms may prevail. Identifying any malleable mechanism may open a new pathway through which such symptoms could be targeted. We explored the association between neuroticism, rumination, anxiety, and depressive symptoms and tested a moderated mediation model with anxiety as a mediator in the relationship between neuroticism and depressive symptoms, and rumination as a moderator of the effect of neuroticism on anxiety.</p>
160.	<p>Safety and efficacy of intracavitary microwave ablation in hepatic gland tumours: Numerical and in vitro studies V Satish, R Repaka - Proceedings of the Institution of Mechanical Engineers, Part H: Journal of</p>

	<p>Engineering in Medicine, 2023</p> <p>Abstract The microwave ablation (MWA) of large hepatic gland tumour using multiple trocars operated at 2.45/6 GHz frequencies has been analysed. The ablation region (in vitro) obtained using parallel and non-parallel insertion of multiple trocars into the tissue has been analysed and compared with the numerical studies. The present study has considered a typical triangular-shaped hepatic gland model for experimental and numerical analysis. COMSOL Multiphysics software with inbuilt bioheat transfer, electromagnetic waves, heat transfer in solids and fluids and laminar flow physics has been used to obtain the numerical results. Experimental analysis has been conducted on egg white using a market-available microwave ablation device. It has been found from the present study that MWA operated at 2.45/6 GHz with the non-parallel position of multiple trocars into the tissue leads to a considerable increase in the ablation region as compared to the parallel insertion of trocars. Hence, non-parallel insertion of trocars is suitable to treat irregular-shaped large cancerous tumours (>3 cm). The non-parallel simultaneous insertion of trocars can overcome the healthy tissue ablation issue as well as the problem associated with indentation. Further, reasonable accuracy (with the difference being nearly ± 0.1 cm in ablation diameter) has been achieved in comparing the ablation region and temperature variation between experimental and numerical studies. The present study may create a new path in the ablation of large size tumours (>3 cm) with multiple trocars of all shapes by sparing the healthy tissue.</p>
161.	<p>SBI-DHGR: Skeleton-based intelligent dynamic hand gestures recognition S Narayan, AP Mazumdar, SK Vipparthi - Expert Systems with Applications, 2023</p> <p>Abstract Hand gesture recognition (HGR) plays a significant role in interpreting the meaning of sign language, human–computer interaction, and robot control. This paper proposes a real-time skeleton-based intelligent dynamic hand gesture recognition (SBI-DHGR) approach, which comprises three modules: Palm Centroid (PC), Data augmentation with the Tenet Effect, and Deep learning architecture. The palm Centroid (PC) module is introduced to identify the proposed palm center joint. Data augmentation with a tenet effect module is designed to improve the CNN model's generalizability. Further, a novel deep learning model is proposed for temporal 3D-HGR by exploiting the capabilities of a multi-channel convolutional neural network (CNN) and long short-term memory (LSTM) recurrent network. The multi-channel CNN is introduced to learn the cardinal positions of hand joints by capturing the low, average, and high-level features. LSTM is embedded to learn the temporal characteristics of hand joints. The effectiveness of the SBI-DHGR framework is evaluated over five challenging datasets: SHREC-14, SHREC-28, DHG-14, DHG-28, and FPHA, by adopting person-dependent and person-independent validation setups.</p>
162.	<p>Self-assembled amino acid microstructures as biocompatible physically unclonable functions (BPUFs) for authentication of therapeutically relevant hydrogels. V Akavaram, K Kumar, S Siram ...SK Meena... - Macromolecular Bioscience, 2023</p> <p>Abstract Counterfeited biomedical products result in significant economic losses and pose a public health hazard for over a million people yearly. Hydrogels, a class of biomedical products, are being investigated as alternatives to conventional biomedical products and are equally susceptible to counterfeiting. Here, a biocompatible, physically unclonable function (BPUF) to verify the authenticity of therapeutically relevant hydrogels are developed. The principle of BPUF relies on the self-assembly of tyrosine into fibril-like structures which are incorporated into therapeutically relevant hydrogels resulting in their random dispersion. This unclonable arrangement leads to distinctive optical micrographs captured using an optical microscope. These optical micrographs are transformed into a unique security code through cryptographic techniques which are then used to authenticate the hydrogel. The temporal stability of the BPUFs are demonstrated and additionally, exploit the dissolution propensity of the structures upon</p>

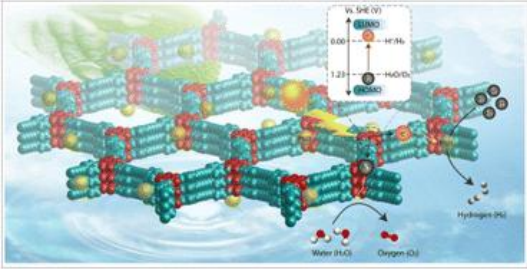
	<p>exposure to an adulterant to identify the tampering of the hydrogel. Finally, a platform to demonstrate the translational potential of this technology in validating and detecting tampering of therapeutically relevant hydrogels is developed. The potential of BPUFs to combat hydrogel counterfeiting is exemplified by its simplicity in production, ease of use, biocompatibility, and cost-effectiveness.</p>
163.	<p>Self-powered NH₃ synthesis by trifunctional Co₂B-based high power density Zn-air batteries D Gupta, A Kafle, PP Mohanty...R Ahuja... - Journal of Materials Chemistry A, 2023</p> <p>Abstract The electrochemical production of NH₃ by Zn-air batteries is a viable and economical approach to realize sustainable and competent energy conversion. We report the environment friendly, cost-effective, and energy efficient sonochemical synthesis of amorphous Co₂B nanosheets for trifunctional electrocatalysis. The catalyst exhibits a high NH₃ yield rate (2.98 mg h⁻¹ mg_{cat.}⁻¹), F.E (20.45%), and TOF of 0.74 h⁻¹ at -0.3 V vs. RHE, thereby unveiling an outstanding performance for the artificial ammonia synthesis. The reliable and true NH₃ production is premediated by following rigorous protocol that involves the purification of gas supplies, elimination of N-contaminants, and quantification of NH₃ by different methods, UV-Vis spectroscopy and ¹⁵N₂ isotope labelling experiments. More interestingly, DFT calculations on the Co₂B catalyst surface shed light on the efficient NRR owing to the presence of Co active sites and possible HER suppression. The optimized Co₂B catalyst shows outstanding oxygen bifunctional activity. When employed as an air-cathode for Zn-air batteries, it exhibited remarkable electrocatalytic activity delivering an open circuit potential of 1.45 V with a high power density of 500 mW cm⁻² and an energy density of 1078 W h kg⁻¹, which can perform NH₃ generation with an overall NH₃ production yield rate of 1.048 mg h⁻¹ mg_{cat.}⁻¹</p>
164.	<p>Self-stratified coating with multiresponsive self-healing polymer D Sharma, D Mandal - ACS Applied Polymer Materials, 2023</p> <p>Abstract Self-stratifying coating produces multicoat films by single-coat application, which offers superior performance by enhancing both the adhesion and surface properties simultaneously, suitable for many special coatings and industrial applications. Here, we have developed a well-defined multifunctional self-stratifying coating material with self-healing abilities from blending two copolymers based on fluororous/thiol/siloxane. Combinations of silyl copolymer (PMEA-co-PCMA-co-PTEPA) and fluororous copolymer (PMEA-co-PCMA-co-PHFA) offer spontaneous stratification into three layers with a gradient behavior. This transparent (>90% transmittance) coating provides a highly hydrophobic surface with good hardness (28 MPa). The polymer coating self-repairs under UV light with >80% efficiency. In addition, the healing is also conceivable by heating at 70 °C or by spraying amine due to the thiol-Michael reaction.</p> 
165.	<p>Sensors-based discharge data acquisition and response measurement in ultrasonic assisted micro-EDM drilling S Raza, R Nadda, CK Nirala - Measurement: Sensors, 2023</p> <p>Abstract Micro-electrical discharge machining (μEDM) suffers from the problem of low material removal rate (MRR) and poor surface finish, especially when there are recurring abnormal sparks. Such</p>

	<p>sparks are mainly due to the accumulation of unflushed debris in the discharge zone resulting in a frequent arcing phenomenon. Vibration assistance to μEDM has proven contributions to the MRR and surface finish enhancement, but the intrinsic information on discharge pulse modification due to the vibration is unclear. The present work proposes a pulse categorization strategy to understand the nature of discharge pulses during the conventional and ultrasonic vibration assisted μEDM. The discharge pulses were acquired at a sufficiently high sampling rate using NI LABVIEW-based data acquisition through an in-house developed pulse discrimination system (PDS). The developed PDS is simultaneously used to estimate the real-time discharge energies of individual pulses and their histograms with the machining progress. The acquired information from the developed PDS is used to justify the variations in discharge energy, discharge frequency, surface roughness and accuracy with increasing machining depth. Vibration assistance to the μEDM process was found beneficial, with an 18% increase in the discharge energy, and a 7.14% reduction in the percentage error in depth. The surface roughness at high-energy settings reduces from 3.2 μm to 0.45 μm because of ultrasonic vibration assistance.</p>
166.	<p>Separation of nanoplastics from synthetic and industrial wastewater using electrolysis-assisted flotation approach: A green approach for real-time contaminant mitigation VS Pawak, C Shekhar, VA Loganathan, M Sabapathy - Chemical Engineering Research and Design, 2023</p> <p>Abstract</p> <p>Nanoplastics pose a significant global environmental concern, as they can accumulate emerging pollutants and enter the food chain, endangering human health and ecosystems. Wastewater treatment plants (WWTPs) have been identified as the primary source of micro and nanoplastic contamination, necessitating the development of effective removal methods. This study investigates the efficacy of electrolysis-assisted flotation (EF) process for removing nanoplastics from synthetic wastewater, using polystyrene-type nanoparticles synthesized from expanded polystyrene waste (EPS) as representative nanoplastic contaminants. Electrolysis experiments were conducted using parallel aluminium electrodes under low-voltage conditions. The study systematically explores the influence of various process parameters, including electrode spacing, salt concentration, nanoplastics concentration, and applied voltage, on the removal efficiency of nanoplastics. The removal efficiency was evaluated using a turbidity meter and dynamic light scattering technique. The derived count rate (DCR) obtained from dynamic light scattering supplements the nephelometric turbidity units (NTU) and provides a reliable estimate of the nanoplastics sample concentration. Under optimized conditions, with a specified electrolyte concentration and pH of 7.2 ± 0.3, the EF process achieved an impressive removal efficiency of nearly 95% (94% per DCR). A notable advantage of the proposed method is forming a foamy layer on top of the reactor when nanoplastics and coagulants are mixed, facilitating easy removal by simple scraping. This study provides valuable insights into developing an eco-friendly and sustainable approach for the large-scale removal of nanoplastics. The results contribute to advancing wastewater treatment strategies and addressing the pressing issue of nanoplastic pollution.</p>
167.	<p>Service time maximization for data collection in multi-UAV-aided networks J Dandapat, N Gupta, S Agarwal ...B Kumbhani - IEEE Transactions on Intelligent Vehicles, 2023</p> <p>Abstract:</p> <p>Unmanned aerial vehicles (UAVs) have been enormously gaining attention to offload traffic or collect data in wireless networks due to their key attributes, such as mobility, flexibility, and cost-effective deployment. However, the limited onboard energy inhibits the UAV from serving for a longer duration. Therefore, this paper studies a UAV-aided network where multiple UAVs are launched to collect data from the mobile nodes. In particular, we aim to maximize the service time of the UAVs by jointly optimizing the three-dimensional (3D) trajectory of the UAVs and</p>

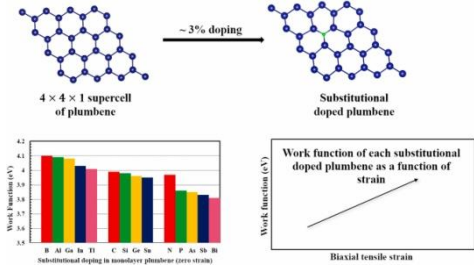
	<p>resources allocated to each node by the UAVs such that each mobile node receives a minimum specified data rate. To facilitate a solution, we construct an equivalent problem that considers the UAV's energy consumption. In particular, we minimize the maximum energy consumed by the UAVs in each time slot. To solve the problem, an iterative approach is presented that decouples the problem into two sub-problems. The optimal location of the UAVs is computed in the first sub-problem, while resource allocation is carried out in the second sub-problem. These two sub-problems are solved in an iterative manner using the alternating optimization approach. We show that the proposed approach improves the service time of the network by 20% on average compared to the existing approaches.</p>
168.	<p>Single-step generation of double emulsions in aqueous two-phase systems S Shekhar, V Mehandia, M Sabapathy - Physics of Fluids, 2023</p> <p>Abstract This communication presents a simple yet straightforward method for preparing water-in-water-in-water particle-stabilized double emulsions, also known as Pickering double emulsions. The approach involves using oppositely charged nanoparticles (OCNPs) in two distinct fluid phases, promoting self-assembly and the formation of aggregates with varying sizes and compositions. By enhancing the interfacial area through the adsorption of aggregates at the interface, this method increases the Gibbs detachment energy of particles between the two aqueous phases, forming stable double emulsions. Furthermore, we investigated the impact of the molecular weight of polyethylene oxide and dextran in the respective fluid phases and the mass ratio (M) of the OCNPs on double emulsion formation. The results demonstrate that the molecular weight of the polymers used in the aqueous phase is a critical parameter influencing the structural formation of the emulsion and the generation of double emulsions. Consequently, double emulsions are formed when equal molecular weight polymer mixtures are employed at an appropriate M, with the dispersed phase placed in the highly viscous continuous phase. The proposed method offers a one-step synthesis process, enabling easy preparation, and exhibits excellent stability for at least 30 days. This study represents the first reported approach for the one-step synthesis of multiple emulsions in an aqueous two-phase system utilizing a Pickering emulsion template.</p>
169.	<p>SNRCN2: Steganalysis noise residuals based CNN for source social network identification of digital images K Rana, G Singh, P Goyal - Pattern Recognition Letters, 2023</p> <p>Abstract Identifying the processing history of digital images related to source acquisition device, image manipulations, and Source Social Media Network (SSMN) identification is important for a forensic analyst to verify image source, trustworthiness, and integrity. Nowadays, social media networks have become a major medium of image sharing and identifying the SSMN of digital images has allured attention in the image forensic scientific community. With the precedence of deep Convolutional Neural Networks (CNNs) in the domain of image forensics, we propose a novel Steganalysis Noise Residuals based CNN (SNRCN2) for digital images SSMN identification. Inspired by the fact that image content can heavily obscures the artifacts of post-processing operations, the proposed CNN utilizes the features from steganalysis-based noise residuals to highlight the artifacts introduced by social media networks. Therefore, the given input image is high-pass filtered using well-known 30 Spatial Rich Model (SRM) filters to obtain noise residuals. Afterward, these noise residuals are passed to an efficient CNN for the extraction of high-level features related to social media networks. Lastly, a fully-connected layer is used for classification purposes. The experimental results show that the proposed model outperforms the existing techniques by providing an image-level accuracy of 99.53% and 100% on the VISION and Forchheim datasets, respectively. To further evaluate the robustness of the proposed model, we create a combined dataset that includes the images of common classes from both datasets.</p>

	The results of the combined dataset further confirm the efficacy of the proposed model.
170.	<p>Spatial stress correlations in strong colloidal gel systems DS Dagur, C Mondal, S Roy – Physical Review B, 2023</p> <p>Abstract Colloidal gel systems exhibit increasingly slow relaxation and ultra-long-ranged spatial correlations of the dynamics similar to other jammed materials. These cooperative dynamics point to the presence of long-ranged stress correlation in these systems, which remain largely uninvestigated in the literature. In this work, we systematically investigate the nature of stress correlations in soft colloidal gel materials in the limit of moderate to high packing fractions and strong attraction. In this regime, centrosymmetric potential description for particle interaction fails as strong attraction can lead to frictional contacts, as shown explicitly in previous experiments. Accordingly, we model the system similarly to the cohesive granular media with Langevin dynamics to incorporate the effects of rolling and sliding resistant contacts and thermal fluctuations. We show that the spatial stress correlations are long ranged with very slow spatial decay close to the gel point. Similarly to previous studies on the frictional granular matter, the full stress autocorrelation matrix is dictated by the pressure and torque autocorrelations due to mechanical balance and material isotropy constraints. Surprisingly, it is observed that the gel materials do not behave as a normal elastic solid <i>close to the gel point</i> as assumed loosely in the literature because the real-space pressure fluctuations decay slower than normal. Furthermore, we link the abnormal pressure fluctuations to the non-hyperuniform behavior of the system (granular matter and gel) with respect to the local packing fraction fluctuations, thus relating the deviations from the normal elastic behavior across various jammed systems under a common framework.</p>
171.	<p>Spatially random disorder in unitary fermion system in $(4 - \epsilon)$-dimensions and effective action at finite temperature RK Gupta, Meenu – Journal of High Energy Physics, 2023</p> <p>Abstract Non-relativistic conformal field theory is significant to understand various aspects of an ultra-cold system. In this paper, we study a non-relativistic system of two-component fermions interacting with a complex boson with Yukawa-like interactions near $d = 4$-spatial dimensions in the presence of a quenched disorder. The homogeneous theory flows to an interacting fixed point describing a unitary fermion system. In the presence of the disorder, we find that the system has an interesting phase structure in the space of the coupling constants and exhibits an interacting disorder fixed point in ϵ-expansion. The correlation function obeys Lifshitz scaling behaviour at the disorder fixed point with the anisotropic exponent being $z = 2 + \gamma_E$. We also study the disorder system at finite temperature and compute the leading contribution to the 1PI effective action.</p>
172.	<p>Stability of ecosystems under oscillatory driving with frequency modulation S Bhandary, T Banerjee, PS Dutta - Physical Review E, 2023</p> <p>Abstract Consumer-resource cycles are widespread in ecosystems, and seasonal forcing is known to influence them profoundly. Typically, seasonal forcing perturbs an ecosystem with time-varying frequency; however, previous studies have explored the dynamics of such systems under oscillatory forcing with constant frequency. Studies of the effect of time-varying frequency on ecosystem stability are lacking. Here we investigate isolated and network models of a cyclic consumer-resource ecosystem with oscillatory driving subjected to frequency modulation. We show that frequency modulation can induce stability in the system in the form of stable synchronized solutions, depending on intrinsic model parameters and extrinsic modulation</p>

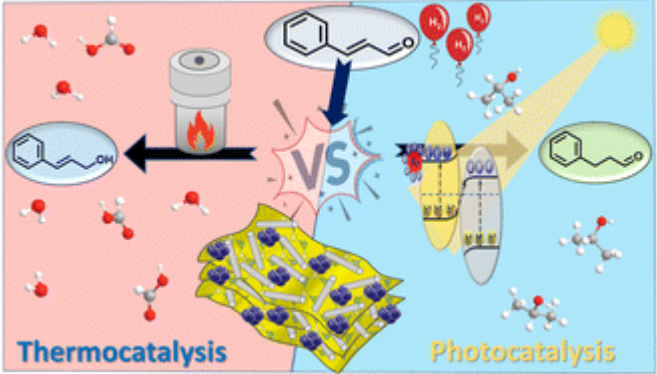
	<p>strength. The stability of synchronous solutions is determined by calculating the maximal Lyapunov exponent, which determines that the fraction of stable synchronous solution increases with an increase in the modulation strength. We also uncover intermittent synchronization when synchronous dynamics are intermingled with episodes of asynchronous dynamics. Using the phase-reduction method for the network model, we reduce the system into a phase equation that clearly distinguishes synchronous, intermittently synchronous, and asynchronous solutions. While investigating the role of network topology, we find that variation in rewiring probability has a negligible effect on the stability of synchronous solutions. This study deepens our understanding of ecosystems under seasonal perturbations.</p>
173.	<p>Strain engineering of the electrocatalytic activity of nitrogen-rich BeN₄ Dirac monolayer for hydrogen evolution reaction X Yang, R Ahuja, W Luo - Nano Energy, 2023</p> <p>Abstract</p> <p>The strong bond energy and short bond length of N≡N triple bond make it a challenging target for synthesizing nitrogen-rich compounds. However, recent research has successfully fabricated atomic-thick BeN₄ layers under high pressure (Bykov et al., 2021). Beryllonitrene, a new 2D material, consists of a Be atom and polymeric nitrogen chains and has anisotropic Dirac cones located near the Fermi level. This distinguishes it from graphene, which has isotropic Dirac cones, bulk PtTe₂ and 2D borophene, which have Dirac cones located far from the Fermi energy. The anisotropic Dirac cones in beryllonitrene result in ultrahigh carrier mobility and the potential for direction-dependent quantum devices. In this study, we systematically investigated the hydrogen evolution reaction (HER) catalytic activity of nitrogen-rich, non-precious BeN₄ monolayer using first-principles DFT calculations. Our results demonstrate that BeN₄ monolayer is thermally stable, and Be vacancy is the most energetically favorable site for hydrogen adsorption. We also found the Gibbs free energy (ΔG_H) of H* coverage can be tuned to an optimal value of $\Delta G_H \leq 0.2$ eV through strain engineering, significantly enhancing the HER electrocatalytic activity of BeN₄ monolayer. Furthermore, we examined both the homolytic Tafel reaction and heterolytic Heyrovsky reaction for HER mechanism using reaction kinetics and AIMD simulations. These findings can contribute to the development of high-performance, non-precious, and nitrogen-rich 2D catalysts for HER in future research.</p>
174.	<p>Strategic design of covalent organic frameworks (COFs) for photocatalytic hydrogen generation K Prakash, B Mishra, DD Díaz, CM Nagaraja - Journal of Materials Chemistry A, 2023</p> <p>Abstract</p> <p>Covalent organic frameworks (COFs) are an emerging class of crystalline materials that are attracting increasing attention due to their high porosity, crystallinity, and tunable properties. Consequently, the strategic design of COF-based photocatalysts for various applications, including energy and environmental remediation, has attracted considerable interest. In particular, the sustainable production of clean fuel – hydrogen (H₂) – by water splitting is a promising means to meet the global energy demand and to address the atmospheric CO₂ concentration caused by the excessive use of fossil fuels. In this regard, COFs offer potential advantages due to their modular nature, which facilitates their rational design from suitable organic building blocks to achieve optimal properties of visible light harvesting properties and easy charge transport. As a result, extensive research has been devoted to the design of photoresponsive COFs for efficient water splitting to generate hydrogen. Here, we provide a comprehensive review of recent developments in the strategic design of COF-based photocatalysts for solar fuel production <i>via</i> water splitting. The various organic linkers used in the construction of photocatalytic COFs and their structure–property correlations are discussed in detail. The role of bandgap engineering in tuning the hydrogen evolution efficiency of COFs is also discussed. Furthermore, the current challenges and future perspectives of COF-based solid catalysts for green and sustainable clean fuel production are presented. Indeed, this review</p>

	<p>demonstrates the importance of COF-based photocatalysts for the visible-light-driven hydrogen evolution reaction (HER) and can be beneficial for the future design of photocatalytic systems.</p> 
175.	<p>Structural insights into mechanical anisotropy in ambrisentan polymorphs J Haneef, D Markad, R Cahdah ...N Kumar... - CrystEngComm, 2023</p> <p>Abstract</p> <p>Mechanical properties of drug molecules largely affect pharmaceutical processing into a finished product. Structural insights together with computational prediction tools help develop a crystal engineering approach to modulate crystal mechanical parameters. This study focuses on mechanical anisotropy in ambrisentan polymorphs (form I and II). Nanoindentation experiments revealed higher hardness (H) and elastic modulus I of form I as compared to form II, while form II showed lower H/E (0.03) as compared to form I (0.08). These properties were rationalized based on the potential slip plane in form II, which exhibited relatively larger d-spacing and lack of hydrogen bonding interaction across plane. On the contrary, form I revealed the presence of an interlocked 3D clustering network that may retard the gliding of the slip planes under the indentation stress. These features were found to be consistent with the predicted mechanical parameters. Besides, the energy framework calculation displays relatively higher interlayer energy in form I, which is attributed to the cohesive crystal lattice. However, in form II, a smaller number of intertwined cylinders resulted in a smaller energetic barrier for sliding molecular layer under applied load during the nanoindentation experiment. In addition, AFM studies have indicated higher surface roughness in form II pointing towards softer and less brittle crystal than form I responsible for ease of elasticity under external stress. Hence, in-depth knowledge of structural features together with mechanical properties helps to establish structure-mechanical property relationships. Overall, form II (metastable form) exhibited higher plasticity and good tabletability than form I, which is attributed to the differential crystal packing, slip systems, strength of intermolecular interactions, surface contacts, and surface roughness. The present study showcases the implications of the crystal structure anisotropy on the mechanical performances that would aid in the selection of the right solid form in formulation development.</p>
176.	<p>Sulfonyl diazaborine ‘Click’ chemistry enables rapid and efficient bioorthogonal labeling A Chowdhury, S Chatterjee, A Kushwaha, S Nanda, TJ Dhillip, A Bandyopadhyay - Chemistry: A European Journal, 2023</p> <p>Abstract</p> <p>Finding an ideal bioorthogonal reaction that responds to a wide range of biological queries and applications is of great interest in biomedical applications. Rapid diazaborine (DAB) formation in water by the reactions of ortho-carbonyl phenylboronic acid with α-nucleophiles is an attractive conjugation module. Nevertheless, these conjugation reactions demand to satisfy stringent criteria for bioorthogonal applications. Here we show that widely used sulfonyl hydrazide (SHz) offers a stable DAB conjugate by combining with ortho-carbonyl phenylboronic acid at physiological pH, competent for an optimal biorthogonal reaction. Remarkably, the reaction conversion is quantitative and rapid ($k_2 > 10^3 \text{ M}^{-1} \text{ s}^{-1}$) at low micromolar concentrations, and it preserves comparable efficacy in a complex biological milieu. DFT calculations support that SHz facilitates DAB formation via the most stable hydrazone intermediate and the lowest energy transition state compared to other biocompatible α-</p>

	<p>nucleophiles. This conjugation is extremely efficient on living cell surfaces, enabling compelling pretargeted imaging and peptide delivery. We anticipate this work will permit addressing a wide range of cell biology queries and drug discovery platforms exploiting commercially available sulfonyl hydrazide fluorophores and derivatives.</p>
177.	<p>Surface integrity analysis of aluminum 3003 alloy during ultrasonic-vibration-laser assisted turning N Deswal, R Kant - Proceedings of the Institution of Mechanical Engineers, Part B: Journal of Engineering Manufacture, 2023</p> <p>Abstract Surface integrity of the machined surface is an important aspect considering their surface alterations, metallurgical effects, and mechanical characteristics during the machining process. Industries have been seeking a capable machining technology that can improve the machining process capabilities especially in an eco-friendly manner. Hybrid machining processes have shown significant improvement in machining performance when compared with the conventional turning (CT) process without using any cutting fluids. Moreover, a recently developed hybrid machining technology, that is, ultrasonic-vibration-laser assisted turning (UVLAT) has shown better machinability than the CT process. Therefore, an attempt has been made to improve the surface integrity of aluminum 3003 alloy in terms of machining forces, surface roughness, surface damage, microstructure, microhardness, residual stresses, and corrosion behavior during the UVLAT process. A comparative surface integrity analysis has been performed among the CT, ultrasonic vibration assisted turning (UVAT), laser assisted turning (LAT), and UVLAT processes. Significant improvement in the surface integrity has been observed for the aluminum 3003 alloy during the UVLAT process in comparison to the CT, UVAT, and LAT processes. The periodic separation of the cutting tool and thermal softening of the workpiece material, simultaneously during the UVLAT process is the possible reason for the improvement in surface integrity. Results demonstrated that the UVLAT process has an excellent potential to enhance the surface integrity of aluminum alloys and is better than the CT, UVAT, and LAT processes.</p>
178.	<p>Synthesis and electrochemical corrosion behaviour of high entropy alloys N Neeraj, D Singh, L Thakur...R Kumar... - Transactions of the Indian Institute of Metals, 2023</p> <p>Abstract High entropy alloys (HEAs) are alloys based on a minimum of five principal elements, which can also have some minor elements for improving the properties according to the applications. The present study deals with the minor elements (Al and Mn) containing CoCrFeNiTi-based HEAs and discusses the effect of Ti on the corrosion behaviour of the HEAs. The HEAs were synthesized in an inert atmosphere using a vacuum arc melting furnace. The as-synthesized HEA samples were characterized for microstructure, phases, hardness, and density. The hardness and density were influenced by changing the amount of Ti in HEAs. The electrochemical corrosion behaviour was analysed using a potentiostat in 3.5% NaCl and 0.1M H₂SO₄ solutions. The corrosion results suggest that the high Ti-containing HEAs show better corrosion resistance in the NaCl and H₂SO₄ solutions due to the formation of TiO₂ on the sample surface.</p>
179.	<p>Systematic study of gamma decay hindrance factors YP Singh, V Kumar, A Shukla...K Jha... - Physics of Particles and Nuclei Letters, 2023</p> <p>Abstract In the present work, Weisskopf hindrance factor for electric and magnetic multipole transitions has been analyzed in the mass range A. An empirical correlation between the variation in as a function of multipolarity has been determined. The pattern of as a function of multipolarity and as a function of the degree of forbiddenness are found indirectly similar to the pattern of the conversion coefficient with multipolarity. The odd-even nucleon staggering effect on is discussed.</p>

180.	<p>Tailoring electronic properties and work function of monolayer plumbene by substitutional doping and biaxial strain P Jamwal, S Kumar, M Muruganathan, R Kumar - Surfaces and Interfaces, 2023</p> <p>Abstract Recent advancements in two-dimensional materials have revealed remarkable electronic and physical properties for their applications in nanoelectronics and optoelectronics. In this research article, we have investigated the electronic properties of plumbene, a recently discovered two-dimensional material using first-principle calculations. We investigated the effect of substitutional doping with atoms from groups 13–15 of the periodic table and biaxial strain on the electronic properties and work function of plumbene. Our calculations show that doped plumbene exhibit a systematic change in the work function value on substitutional doping from groups 13–15, further modulated by strain. By substitutional doping and biaxial strain, the work function of plumbene is found to vary over a wide range of 3.80eV – 4.14eV. Tunability of the electronic properties indicate the potential for the experimental implementation of plumbene-based optoelectronic devices.</p> 
181.	<p>The evidence for repurposing anti-epileptic drugs to target cancer M Aroosa, JA Malik, S Ahmed... - Molecular Biology Reports, 2023</p> <p>Abstract Abstract: Antiepileptic drugs are versatile drugs with the potential to be used in functional drug formulations with drug repurposing approaches. In the present review, we investigated the anticancer properties of antiepileptic drugs and interlinked cancer and epileptic pathways. Our focus was primarily on those drugs that have entered clinical trials with positive results and those that provided good results in preclinical studies. Many contributing factors make cancer therapy fail, like drug resistance, tumor heterogeneity, and cost; exploring all alternatives for efficient treatment is important. It is crucial to find new drug targets to find out new antitumor molecules from the already clinically validated and approved drugs utilizing drug repurposing methods. The advancements in genomics, proteomics, and other computational approaches speed up drug repurposing. This review summarizes the potential of antiepileptic drugs in different cancers and tumor progression in the brain. Valproic acid, oxcarbazepine, lacosamide, lamotrigine, and levetiracetam are the drugs that showed potential beneficial outcomes against different cancers. Antiepileptic drugs might be a good option for adjuvant cancer therapy, but there is a need to investigate further their efficacy in cancer therapy clinical trials.</p>
182.	<p>The Role of interface trap states in MoS₂-FET performance: A full quantum mechanical simulation study A Rawat, B Rawat - IEEE Transactions on Electron Devices, 2023</p> <p>Abstract As the fabrication of short-channel MoS₂-FET has made significant progress, there is a growing need to understand the factors affecting the transfer characteristics for overcoming the variability issue. Even though several experimental works on the MoS₂-oxide interfaces have reported the presence of high-density interface trap charge, insight into the device-level performance</p>

	<p>degradation is still unexplored. To address this gap, we introduce the description of the interface trap states in the self-consistent solutions of 2-D Poisson's equation and dissipative nonequilibrium Green's function (NEGF) by modifying the on-site potential energy in the atomic description of the channel. Our results indicate that interface trap states with energy toward the mid-gap energy level from the conduction band significantly increase the OFF-state current due to phonon-assisted source–drain tunneling current with trap states, while the charge trapping in the interface states reduces the ON-state current. It is found that the interface trap states close to the mid-gap severely affect the key device performance metrics, such as OFF-state current (), subthreshold slope (SS), and threshold voltage (), for the sub-18 nm gate length. Additionally, the inelastic tunneling through trap states marginally enhances the temperature dependency in SS and of MoS2-FET. The simulation results suggest that minimizing the interface trap states with energy close to mid-gap energy level and trap position around the middle of the channel can considerably reduce the leakage current and improve the short-channel MoS2-FET performance.</p>
183.	<p>Thermal modeling of fluid flow and heat transfer in direct contact membrane distillation KS Chauhan, H Tyagi - Energy Conversion and Management, 2023</p> <p>Abstract</p> <p>In this paper, a mathematical model was developed, and numerical simulations were conducted to analyze the direct contact membrane distillation process (DCMD) utilizing solar energy. The objective is to identify the optimal operating point, flow parameters, dimensions, and membrane properties of membrane module in terms of permeate water flux and GOR. The novel aspect of this paper is to analyze the flow patterns in the feed and permeate regions on performance of DCMD to maximize water production by optimizing the balance between permeate water flux and GOR. Additionally, the study will identify the most suitable location for installing the MD system based on factors such as solar energy availability and average annual temperature. The results show that the polyethylene (PE) membrane provides the highest permeate water flux, while the polytetrafluoroethylene (PTFE) membrane provides the highest GOR. A significant increase in permeate water flux and GOR is observed when the flow changes from laminar to turbulent. The study also examines the effect of membrane module dimensions, where increasing the length decreases flux but increases GOR, while increasing the width increases flux but decreases GOR. The study also reveals that countries with high annual average temperatures produce higher permeate water flux and GOR. The paper also delves into the effect of membrane properties on water flux and GOR. It is observed that a membrane with high porosity, low thickness, and having a pore size greater than 0.14 μm is desirable.</p>
184.	<p>Thermal performance index based characterization and experimental validation for heat dissipation by unconventional arrayed micro pin-fins H Kishore, CK Nirala, A Agrawal - Thermal Science and Engineering Progress, 2023</p> <p>Abstract</p> <p>Cross-section profiles of micro pin-fins (MPFs) have significantly affected the overall heat transfer performance in natural and forced convection through passive and active cooling techniques. Unconventional, such as piranha, droplet, and aerofoil, cross-sectional profiles of MPFs have proven to enhance heat dissipation in MEMS and macro devices. The present study evaluated the thermal performance of in-house fabricated unconventional cross-sections arrayed MPFs in staggered and inline arrangements. Reverse-μEDM and laser beam micromachining (LBμM) are integrated to fabricate near-net-shape MPFs heat sinks cross-sections in desired aspect ratios. A single-phase fluid flow testing facility is designed and developed to compare and validate the thermal performance of fabricated MPFs with numerical modelling. Thermal parameters, including maximum thermal resistance, Nusselt number, and pressure drop, have been evaluated at constant heat load in the laminar flow regime. Upon comparison, arrayed piranha MPFs in staggered and inline arrangements showed better thermal performances with increasing Reynolds numbers due to their geometrical cross-section. The results obtained from</p>

	<p>the iterative experimentation are analyzed and compared in terms of the thermal performance index (TPI), where the pumping power is of great concern in high-performance MEMS devices.</p>
185.	<p>Thermocatalytic and photocatalytic chemoselective reduction of cinnamaldehyde to cinnamyl alcohol and hydrocinnamaldehyde over Ru@ZnO/CN A Chauhan, R Ghalta, R Bal, R Srivastava - Journal of Materials Chemistry A, 2023</p> <p>Abstract The selective hydrogenation of α-β unsaturated carbonyl compounds requires a catalyst with a suitable combination of the support and active sites to activate a specific functional group. In this work, ZnO and g-C₃N₄(CN) nanocomposite (ZnO/CN) supported Ru catalysts were synthesized for thermal and photochemical selective hydrogenation of cinnamaldehyde (CAL). Under thermal conditions, formic acid (FA) was employed as a hydrogenating agent in water, and 85% cinnamyl alcohol (COL) selectivity was achieved with nearly complete CAL conversion. The acidity of ZnO activated the C=O group of CAL, the basicity of CN facilitated the adsorption of FA, and the decorated Ru assisted the FA to H₂ formation leading to the selective production of COL. A FT-IR study confirmed the effective adsorption of CAL through C=O, yielding the selective formation of COL. In contrast, under photochemical conditions, hydrocinnamaldehyde (HCAL) was the selective hydrogenation product that was formed due to the efficient migration of charge carriers at the interface of the Z-scheme heterojunction of CN and ZnO. The synergistic effects at the interface were crucial for the charge transfer mechanism, enhancing the charge carriers' lifetime and enabling excellent charge separation under photocatalytic conditions. Detailed characterization and control reactions were performed to establish the structure–activity relationship and to conclude the plausible reaction mechanism under both conditions.</p> 
186.	<p>Thermodynamic and kinetic aspect of solid state reduction of electric arc furnace slag through coke: An experimental study SS Chandel, NS Randhawa, PK Singh - Materials Today: Proceedings, 2023</p> <p>Abstract Steel slag is one of the major wastes produced during the steelmaking process. In the present scenario, the world's utilization rate of steel slag is comparatively very low and primarily used for landfills only. The untreated slag used for the dumping will affect the environment adversely and causes loss to the economy as well. In the present study, we are concentrating on steel slag through the latter. The mineralogy of primary slag ensures the presence of various constituent ranges, Fe₂O₃/FeO (18–30%), CaO (23–48%), SiO₂ (2–6%), MgO (4–17%), and Al₂O₃ (2–15%), mainly depends on the quality of raw material as well as processing relies on the quality of raw material as well as processing. One of the significant components of steel slag with a large variety of ranges is iron oxides. Iron Oxide is present in the steel slag in the form of FeO, Fe₂O₃, and FeO.SiO₂. This study analyzed the reduction kinetics of steel slag based on the Coats-Redfern method and explained the reduction mechanism of Fayalite for different slag basicity. The investigation involves a temperature</p>

	<p>range of 960–1478 K with a carbon-to-oxygen ratio of C/O-1. The non-isothermal experiment covers the solid reduction of EAF slag. The TG curve shows the reduction reaction of steel slag and coke from 0.5 to 1.5 is 7.31% to 10.88%. During the investigation, the activation energy of iron reduction process will get decrease with increased slag basicity.</p>
187.	<p>To live with the artificial or to live as the artificial?: the essential human and the art of life R Kour, S Jayadevan - <i>Inscriptions</i>, 2023</p> <p>Abstract Human beings are at the crossroads where technology can be used to transcend the limits of nature. In our search for who we essentially are, there are two possibilities at the ends of a spectrum: one, the technologicus, a complete technological being ideated by Kevin Warwick; the other, the aestheticus, a higher liberated being implied by Goethe available in the works of Herbert Marcuse. Should we find our essential nature by being more human or blend in with technology? We show that the current trend in philosophy of technology is predictively and politically inadequate to handle this question. Interestingly, Schirmacher crosses the traditional boundary between the subject and the object, and posits the generator that is quintessentially artificial. If we are artificial at our core, is achieving the aestheticus any more significant? We weigh both the technologicus and the aestheticus with the generator, and contemplate the possibilities towards finality.</p>
188.	<p>Trajectory and resource allocation for UAV replacement to provide uninterrupted service N Gupta, S Agarwal, D Mishra, B Kumbhani - <i>IEEE Transactions on Communications</i>, 2023</p> <p>Abstract Unmanned aerial vehicles (UAVs) have emerged as a specular technology that can assist the terrestrial base stations. However, the battery limitation of UAV inhibits the system performance by decreasing the overall lifespan of coverage provided by the UAV, driving the necessity of replacement and recharging. Thus, the energy-depleted UAV must be returned to a charging station and be replaced by a fully charged UAV to increase the service span. Therefore, this paper presents a novel framework of UAV replacement to maintain coverage continuity in a UAV-assisted wireless communication system when a serving UAV runs out of energy. Our objective during this replacement process is to maximize the minimum achievable throughput to the UAV-served ground users by jointly optimizing the three-dimensional (3D) multi-UAV trajectory and resources allocated to the users from the individual UAVs. The formulated problem is non-convex for which an efficient algorithm based on successive convex approximation and alternating optimization is proposed. Numerical results provide insights into the UAV trajectories and the effectiveness of the proposed scheme compared to the existing benchmark schemes.</p>
189.	<p>Transition metal dichalcogenides and hybrids for electrochemical sensing SP Kaur, V Mishra, B Chakraborty, <i>2D Materials-Based Electrochemical Sensors</i>, 2023</p> <p>Abstract Transition metal dichalcogenides are useful for both industrial materials and scientific research. This chapter emphasizes the theoretical and experimental methods that can be applied to sensing applications. The sensing characteristics of the TMDCs are influenced by sensing parameters such as adsorption configuration, adsorption site, charge transfer, etc. The sensing behavior of TMDCs is governed by the influence of energy cut-off values, k-points, and exchange-correlation functional. The sensing properties of TMDCs are computationally expensive and can be computed using highly advanced theoretical methods to obtain correct results. The use of high-speed, large-memory supercomputers will be beneficial in the future to obtain precise TMD sensing properties. The remarkable experimental electrochemical performance of TMDCs led to its incorporation in second-generation glucose biosensors.</p>
190.	<p>Transitioning from conventional to organic smallholder farming among Indian farmers: a</p>

	<p>psychological perspective P Singh, P Satpathy, V Vaishnav – The Journal of Agricultural Education and Extension, 2023</p> <p>Abstract Purpose: Despite hazardous consequences, the use of fertilizers and pesticides has been exceptionally high, mainly to increase crop yield. Socio-economic factors have been explored to understand the inability to curb its overuse; however, literature on psychological factors affecting farmers' decision-making is very scarce. Psychological factors are important to understand as these factors mediate the effects of external socio-economic factors on one's behaviour. The present study focused on farmers' intentions to convert their farming practices from conventional to organic. Design/methodology/approach: The data was collected from 389 participants, mainly using semi-structured face-to-face interviews. The observations were analysed through regression and structural equation modelling. Findings: A significant association has been observed between attitudes, subjective norms, perceived behavioural control, awareness and farmers' intention to switch to organic farming practices. Practical implications: As the observed factors are significantly associated with conversion intentions and malleable by nature, the study serves as a confirmatory node to proceed with the interventional plan based on the belief system restructuring module to educate farmers about sustainable farming practices. Theoretical implications: The study verified the applicability of the theory of planned behaviour in the Indian context and highlighted the factors to be targeted to convert the intentions of conventional farmers to organic farming. Originality/value: In order to curb the overuse of chemicals in agriculture, policymakers can plan suitable interventions and use the relevant psychological measures to target the factors identified in the present study.</p>
191.	<p>TRASH: traffic aware hybrid-CRAN scheme for V2I connectivity enhancement SK Singh, R Singh, B Kumbhani - IEEE Transactions on Vehicular Technology, 2023</p> <p>Abstract Cloud Radio Access Network (CRAN) is the most preferred cellular architecture to support milli-meter wave (mm-Wave) transmission. It fulfills the requisites of mm-Wave communication by enabling Coordinated Multi Point (CoMP) framework. However, the potential of CRAN is not exploited to its maximum, especially from the perspective of high mobility scenarios, e.g., vehicular transmission. This is because; CoMP-enabled framework requires exceptional pre-transmission processing, which may soon outdate for high mobility scenarios, the network is usually designed to support peak hour traffic and hence mostly remains under-utilized during sparse traffic conditions. To mitigate such issues, this work proposes a modified RAN with Traffic Aware Hybrid CRAN Scheme (TRASH) aiming two-fold advantages; micro-Wave and mm-Wave are jointly utilized to enhance reliability of fast moving scenario, a sub-RAN architecture is introduced to support traffic fluctuations. Moreover, through simulation results, it is shown that TRASH provides significant performance enhancement against traditional CRAN based transmission.</p>
192.	<p>Traversing ruins: Kristen Radtke's post-apocalyptic dark tours in <i>Imagine Wanting Only This</i> N Soman, S Krishna - Journal of Graphic Novels and Comics, 2023</p> <p>Abstract Kristen Radtke's graphic memoir <i>Imagine Wanting Only This</i> (2017) visually chronicles the author's journeys through post-apocalyptic sites including abandoned cities, derelict landscapes, and architectural ruins in order to process the grief over the loss of her uncle and to confront her recurrent thoughts on mortality. Diagnosed with a fatal heart condition that catapults her into reflections on the transience of human existence, Radtke seeks answers by engaging in a series of dark tours to find physical manifestations of her inner turmoil amidst deserted cities and modern ruins. This essay examines how Radtke treads complex subjects of loss, angst, and death through nuanced visual storytelling while associating her vulnerable body with the dilapidated structures</p>

	<p>she explores. It further investigates how ruins as transitional spaces that simultaneously evoke recollections of a catastrophic past as well as the hope of human endurance offers avenues of self-reflection for the grieving protagonist, aiding her to successfully navigate her grief and overcome her anxieties.</p>
193.	<p>Triggering of electro-elastic anti-superhydrophobicity during non-Newtonian droplet collision G VVS Vara Prasad, P Dhar, D Samanta - Proceedings of the Royal Society A, 2023</p> <p>Abstract</p> <p>The present article discusses the electrohydro-dynamics of impacting non-Newtonian dielectric droplets on superhydrophobic (SH) surfaces. The role of important parameters like electric Eotvos number (Eoe), Weber number (We), dielectric particle concentration (TiO₂) and polymer concentration (PEG-400) were elucidated in this experimental study. Due to the interplay of non-Newtonian effects and electric field, we had observed the suppression of drop rebound on SH surfaces at much lower Eoe compared to its Newtonian counterpart. It has been observed that with an increase in both polymer concentration or dielectric particle concentration, the suppression of drop rebounds was observed at lower Eoe. In order to encapsulate the combined effects of electric field and non-Newtonian dynamics on drop rebound suppression, we have introduced the ‘electro-elastic effect’. Contrary to the common observations of drop rebound on SH surfaces, this electro-elastic effect induces inhibition of drop rebound, thereby resulting in anti-superhydrophobicity. Subsequently, we also established a scaling relationship to show that the rebound suppression is observed as a manifestation of the onset of electro-elastic instability, when a proposed electric Weissenberg number (Wie) exceeds unity. Finally, we demarcated the rebound and rebound suppression regimes of droplet dynamics through a detailed phase map.</p>
194.	<p>Two-dimensional (2D) MT₂ (M = Ba, Hf, Si, Sr and T = F, O) monolayers for possible electronic and optoelectronic applications V Kumar, H Jeon, P Kumar...R Ahuja... - Optical and Quantum Electronics, 2023</p> <p>Abstract</p> <p>The present work shed light on the structural, electronic, dielectric, and optical properties of MT₂ (M = Ba, Hf, Si, Sr and T = F, O) two-dimensional (2D) monolayers using density functional theory. The investigated electronic properties indicate that these 2D monolayer materials exhibit insulating properties. The complex dielectric function is calculated to investigate the optical functions of these monolayer materials. The dielectric and optical calculations are performed for the electric field vectors’ orientation parallel (E x, i.e., in-plane direction) and perpendicular (E z, i.e., out-of-plane direction) to the plane of these 2D monolayer materials in the energy range 0–60 eV. It is noticed that the dielectric and optical responses of BaF₂, HfO₂, and SrF₂ are shifted toward the lower energy in the ultraviolet (UV) region compared to SiO₂. It may be attributed to their larger ionic radii. Due to a similar chemical environment, the studied properties show similar behavior in BaF₂ and SrF₂. These 2D materials offer high absorption of incident light in a wide energy range of UV region, hence the higher extinction coefficient. The obtained reflection and transmission coefficients in the vacuum ultraviolet (VUV) wavelength region suggest the potential candidature of these materials for VUV optical coatings, such as reflection, bandpass, absorption edge filters, and avoiding solar heating. BaF₂ and SrF₂ can combine to make low–high refractive index pair material with high refractive index HfO₂. The present results indicate that these 2D monolayer materials may be potential candidates for designing optical, photonic, and optoelectronic devices.</p>
195.	<p>Type-I to Type-II non-Masing behavior of 304L SS under low cycle fatigue: Material's internal changes SS Yadav, SC Roy, J Veerababu... - International Journal of Fatigue, 2023</p>

	<p>Abstract: This study investigates the Type-I and Type-II non-Masing behavior of 304L austenitic stainless steel fatigue tested at room temperature for strain amplitudes ranging from $\pm 0.25\%$ to $\pm 1.0\%$ at a strain rate of $1 \times 10^{-3} \text{ s}^{-1}$. The material exhibited Type-I non-Masing behavior at lower life fractions ($\leq 10\%$) and Type-II non-Masing behavior at higher life fractions ($> 10\%$). Type-I indicates that the master curve construction is possible, but in Type-II, the master curve can not be constructed. Further, low cycle fatigue tests conducted at $\pm 0.25\%$, $\pm 0.6\%$, and $\pm 1.0\%$ of strain amplitude were interrupted at life fractions of 8%, 30%, and 50% to investigate the internal material changes. At $\pm 0.6\%$ and $\pm 1.0\%$ of strain amplitude, the martensite content, dislocation density, and local misorientation increased with increasing life fraction, whereas the twins fraction decreased. Low martensite content and internal defects observed at low life fraction (8%) cause a minimal change in the strain-hardening rate behavior at different strain amplitudes, thereby, the Type-I non-Masing behavior. However, at higher life fractions (30% and 50%), high martensite content, high dislocation density, stacking faults, deformation twins, shear bands, dislocation walls, and cells have caused a significant change in the strain-hardening rate behavior, and thus, the Type-II non-Masing behavior.</p>
196.	<p>Understanding the captured CO₂ utilisation potential of various cementitious materials through review and analytical modelling SK Saikia, AS Rajput - Magazine of Concrete Research, 2023</p> <p>Abstract Carbon dioxide sequestration in cement-based materials has emerged as a promising avenue for utilising captured carbon dioxide (CO₂) and reducing the carbon dioxide footprint of the concrete industry. This article presents a comprehensive review of various studies conducted in this domain with a particular emphasis on factors affecting the carbon dioxide uptake potential of various concrete types and the effect of carbonation on the critical properties of concretes. Studies conducted on the micro-mechanical analysis of carbon sequestered concrete show that carbonation significantly improved the microhardness of the concrete samples, thereby increasing the strength and reducing the cement intake requirement. Further, keeping two parameters, namely water/solid (w/s) ratio and carbonation reaction time, in focus, the carbon dioxide uptake capacity in concrete slurry waste (CSW) was evaluated using non-linear regression analysis. It was observed that CSW paste had a maximum carbon dioxide uptake with an intermediate w/s ratio of 0.2 due to carbon dioxide reaction hindrances during diffusion at a higher w/s ratio and lack of hydration at a lower w/s ratio. On the contrary, for belite-rich cement, a higher w/s ratio led to higher carbon dioxide uptake owing to belite phase consumption leading to increased calcite production. Additionally, comparing the maximum carbon dioxide uptake capacity of CSW at a particular condition with various other cement-based materials, it was observed that belite-rich cement had the ability to sequester the maximum amount of carbon dioxide compared to the other cement-based materials considered in this study.</p>
197.	<p>Unraveling instabilities and mixing behavior in two-layered flows: A quest for the optimum viscosity ratio P Banga, SN Maharana, M Mishra - Physics of Fluids, 2023</p> <p>Abstract A two-layer miscible displacement of density-matched but viscosity-contrasted fluids through a channel is numerically investigated in a nonlinear regime. The flow is governed by Navier–Stokes equations, which are coupled to a convection-diffusion equation via viscosity dependent concentration. Instabilities in the form of roll-ups or ligament waves are observed when a less viscous fluid is sheared over a more viscous fluid. Through interfacial length calculations, we demonstrate that the temporal evolution of the interface can be divided into three regimes: the initial diffusion-dominated regime, the intermediate convection-dominated regime, and the final diffusion-dominated regime. With the unstable roll-up growth only in a convection-dominated regime, the growth of instability delays at later times in diffusion dominated regime. Moreover,</p>

	onset time t_{on} vs R plots for each Reynolds number (Re), Péclet number (Pe), initial interface location (h), and thickness of initial mixing zone (q) depict that the instability originates early for intermediate viscosity ratios (R) than larger R . In contrast to earlier studies in the linear regime, we showed that if the viscosity ratio between two fluids is very large or small, the instability doesn't trigger in the nonlinear regime. The analysis of the concentration's global variance-based degree of mixing allows us to find optimum parameters for maximum mixing. We show that the optimal mixing is obtained at an intermediate value of R (optimum R). Furthermore, the degree of mixing is found to increase for increasing Re and decreasing Pe .
198.	<p>Women and the precarity of war: Reading women militants and activists in Sharmila Seyyid's Ummath A Nandha - Journal of International Women's Studies, 2023</p> <p>Abstract</p> <p>Ummath, written by Sharmila Seyyid, navigates the sensitive topic of the precarious lives of three separate women amid the chaos of war-torn Sri Lanka. The stories of main characters Yoga and Theivanai demonstrate women's challenges in and out of militancy. Their struggles led them to Thawakkul, a Muslim social worker devoted to the cause of rehabilitating disabled and widowed women who once served the LTTE (Liberation Tigers of Tamil Elam). Ummath provides a powerful social critique of the conditions that aggravated the separatist conflict, the stigmatization of women who become part of the LTTE, the inexorable violence perpetrated by all sides in a chaotic and prolonged internal conflict, and the failure of rehabilitating the militants into the community. The present article investigates the precarity faced by women in the anarchic context of civil violence and internal conflicts. The article discusses the disruption of education, militancy experience, the social stigma of being an ex-militant, and the challenges faced by reformers working to build peace in post-war society. The study employs Judith Butler's theory on precarity to investigate the social life of women militants and activists in the separatist war. Butler's concept of precarity addresses how people's vulnerability is politically induced, and hence different groups of people are exposed in different degrees to violence and death. In Butler's work, she argues that those who are not considered living in the first place, or whose lives are precarious and are not ascribed great value, are not mourned when they pass away. This article analyzes the problems that women militants and social workers face as well as the social ostracization they encounter daily through the focal points of Yoga, Theivanai, and Thawakkul's lives as narrated in Ummath. The exploration of the microcosmic experiences of the three women's lives highlights the need to study women's issues in the unstable context of a social uprising and the vulnerabilities they are exposed to in the context of human rights.</p>

Disclaimer: This publication digest may not contain all the papers published. Library has compiled the publication data as per the alerts received from Scopus and Google Scholar for the affiliation "Indian Institute of Technology Ropar" for the months of June, July and August, 2023. The author(s) are requested to share their missing paper(s) details if any, for the inclusion in the next publication digest.